AMERICAN UNIVERSITY OF BEIRUT

INTERACTION OF POLY LACTIC-CO-GLYCOLIC ACID (PLGA) WITH CURCUMIN: PLGA BASED NANOCAPSULES FOR CURCUMIN DELIVERY AND BIOMEDICAL APPLICATION

by
HANINE BACHIR ZAKARIA

A thesis
submitted in partial fulfillment of the requirements
for the degree of Master of Science
to the Department of Chemistry
of the Faculty of Arts and Sciences
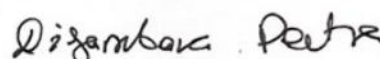at the American University of Beirut

Beirut, Lebanon
January 2021

AMERICAN UNIVERSITY OF BEIRUT

INTERACTION OF POLY LACTIC-CO-GLYCOLIC ACID (PLGA)
WITH CURCUMIN: PLGA BASED NANOCAPSULES FOR
CURCUMIN DELIVERY AND BIOMEDICAL APPLICATION

by
HANINE BACHIR ZAKARIA

Approved by:

_____   _____
Dr. Digambara Patra, Professor   Advisor
Chemistry

_____   _____
Dr. Lara Halaoui, Professor   Member of Committee
Chemistry

_____   _____
Dr. Tarek Ghaddar, Professor   Member of Committee
Chemistry

Date of thesis defense: January 13, 2022

AMERICAN UNIVERSITY OF BEIRUT

THESIS RELEASE FORM

Student Name: _ Zakaria _____ Hanine _____ Bachir _____
            Last   First   Middle

I authorize the American University of Beirut, to: (a) reproduce hard or electronic copies of my thesis; (b) include such copies in the archives and digital repositories of the University; and (c) make freely available such copies to third parties for research or educational purposes:

☐ As of the date of submission

☒ One year from the date of submission of my thesis.

☐ Two years from the date of submission of my thesis.

☐ Three years from the date of submission of my thesis.

___Hanine_____February 1, 2022_____

Signature   Date

(This form is signed & dated when submitting the thesis to the University Libraries ScholarWorks)

ACKNOWLEDGMENTS

My sincere gratitude goes to Professor Digambara Patra, my thesis supervisor, for his invaluable advice, continuous support, and patience. His wealth of knowledge and experience have encouraged me in all the time of my academic research.

Sincere appreciation is also expressed to my committee members, Professor Lara Halaoui and Professor Tarek Ghaddar, for their insightful comments,valuable time, and suggestions to improve my research.

I wish to show my sincere appreciation to the best research assistant, Miss Riham El Kurdi, who was an incredible guide and listener. Without her assistance and encouragement, this journey was to be tougher.

I wish to show a special thanks to my best friend and my unbiological sister, Fatima Al Ahmad who was always there listening to my naggings and wishing me all the best in everything. In this regards, let me express my gratitude to my amazing friend and partner Justine Dagher, who supported me all throughout this journey and made the most valuable and unforgettable memories.

I have to thank my family for their continuous love, help and support throughout my life. My wholehearted thanks to my father, our hero that we'll always need. I am grateful to my sisters for always being there for me as friends. I am forever indebted to my mother for everything, my academic journey would not have been possible without her, and I dedicate this work to her.

Finally, I wish to thank the members of the core lab; Kamal A. Shair Central Research Laboratory (KAS,CRSL) especially Miss Rania Shatila, for their technical support.

ABSTRACT
OF THE THESIS OF

Hanine Bachir Zakaria   for   Master of Science

Major: Chemistry

TITLE: Interaction of Poly lactic-co-glycolic acid (PLGA) with Curcumin: PLGA Based Nanocapsules for Curcumin Delivery and Biomedical Application

Nanotechnology is a promising developing field presenting a potential tools for the loading of curcumin in order to enhance its various applications. Several types of nanoparticles have arisen one of them is polymeric nanocapsules. In the present work curcumin (Cur) loaded Poly lactic-co-glycolic acid (PLGA) nanocapsules were synthesized using solid-in-oil-in water (s/o/w) emulsion technique. The prepared nanocapsules were coated by poly (diallyldimethylammonium) chloride (PDDA) polymer in order to increase the entrapement of curcumin into the core of PLGA polymer.

PLGA-Cur-PDDA nanocapsules were characterized using spectroscopic and microscopic techniques such as fluorescence spectroscopy, UV-Visible spectroscopy, thermogravimetric analysis (TGA), X-Ray diffraction technqiue (XRD), scanning electron microscopy (SEM), and Zeta potential analysis. The formed PLGA-CUR-PDDA NCs were established as nanoprobe for the detection of dopamine molecule. The selectivity and specificity of nanocapsules toward dopamine was achieved by measuring the fluorescence emission spectra of the NCs in the presence of other interference molecules such as tryptophan, melamine, adenine, etc. It was noticed that increasing the concentration of the different molecules had no significant change in the fluorescence signal of the nanocapsules. These results confirm the strong quenching between dopamine and curcumin in the nanocapsules. Hence, fluorescence emission technique was found to be selective, easy and fast with low cost for the determination of dopamine in a concentration range up to 5 mM with a detection limit equal to 23 μM. Additionally, the antiviral activity of these nanocapsules was investigated against the influenza A virus. Cytotoxicity assessment of the nanocapsules was performed. MTT results revealed that up to a concentration of 20 μM of the curcumin nanocapsules is well tolerated by A549 cells with cell death< 20 %. Then, using plaque reduction assay, antiviral activity against influenza A virus propagated in the A549 cell culture was evaluated. Results showed that a reduction in the plaque size was obtained upon treating infected PR8 cells with 10 μM of nanocapsules. Also, the EC50 was estimated to be 20 μM.

Besides, multilayered polymeric nanocapsules were prepared in three different compositions, using PLGA, PDDA polymer and silica nanoparticles. These nanocapsules were characterized using different techniques. The effect of additive layer was established; where it was found that silica nanoparticles and PDDA polymer increase the stability of the encapsulated curcumin. Drug release profile was examined

for PLGA-Cur-PDDA nanocapsules at three different pHs (4, 6 and 7). Highest release of curcumin was obtained at pH 4. Thus to control curcumin release at this pH, effect of multilayers addition was studied. Results showed a lower release of curcumin with the addition of multilayers where high encapsulation efficiency equal to 98.21% was obtained.

Moreover, the interaction between PLGA, PDDA and Curcumin was investigated by fluorescence spectroscopy. The modified Stern-Volmer equation was used to estimate the value of the binding constant K_a and the van't Hoff equation was used to estimate the corresponding thermodynamic parameters (ΔH^o, ΔS^o, and ΔG^o). The obtained results showed that the binding constant between PLGA and Curcumin is due to the formation of hydrogen bonds and van der Waals forces. However, PDDA interacts with curcumin through hydrophobic interactions. Moreover, zeta potential measurements were obtained for these polymers and the surface charge was compared in presence and absence of the negatively charged curcumin molecules. It was found that the results obtained by zeta potential measurements are in agreement with those obtained by fluorescence spectroscopy. It is also found that binding of curcumin with PDDA is further encouraged in the presence of PLGA.

Furthermore, the physical properties of Poly(lactic-co-glycolic acid) (PLGA polymer) are studied for the first time in solution using emission fluorescence technique and curcumin as a molecular probe. On the first hand, curcumin at a concentration of 2 μM was added to different concentrations of PLGA. In this case, the fluorescence of curcumin has been tracked. It was found that the critical micellar concentration (CMC) was equal to 0.31 g/L and the critical micellar temperature (CMT) was obtained at 25°C respectively. Furthermore, an insight on the effect of NaCl salt on the CMC value of PLGA is assessed through curcumin probing. Therefore, a decrease in the CMC has been observed with the increase in the concentration of NaCl. Moreover, in order to understand the aggregation behavior of PLGA in different solutions, CMC experiments were investigated using chloroform as a solvent. Results showed that the solvent does not affect the CMC value of the polymer; however, it only affects the shape of the obtained micelle. Finally, fluorescence quenching of curcumin with hydrophobic cetyl-pyridinium bromide CPB and hydrophilic KI quenchers was established, where it was proved that curcumin is located near the hydrophobic pocket of Stern-layer of PLGA micelle.

TABLE OF CONTENTS

CURCUMIN-PLGA BASED NANOCAPSULE FOR SPECTROSCOPIC DETECTION OF DOPAMINE 69

ASSESS ANTIVIRAL POTENTIAL OF CURCUMIN NANOPARTICLES AGAINST INFLUENZA A INFECTION. 84

ILLUSTRATIONS

TABLES

LIST OF ABBREVIATIONS

CMC: Critical Micelle Concentration

CMT: Critical Micelle Temperature

CPB: Cetylpyridinium bromide

CUR: Curcumin

PLGA- CUR NCs: Curcumin loaded PLGA nanocapsules

DL: Drug loading

EE: encapsulation efficiency

KI: Potassium iodide

Ksv: Stern-Volmer constant

PDDA: Poly diallyl dimethyl ammonium Chloride

PLGA: Poly lactic-co-glycolic acid

SEM: Scanning Electron Microscopy

TGA: Thermogravimetric analysis

XRD: X-Ray Diffraction

CHAPTER I

INTRODUCTION

A. Nanocapsules

Nanocapsules are characteristic class of nanoparticles made up of two or more active material representing the core and a protective matrix acting as a shell[1]. Nanocapsules gained a great interest due to their protective coating that is usually pyrophoric oxidizes easily[2]. Nanocapsules exist in a size ranges between 10 and 1000 nm[2].

Due to their sizes, Nanocapsules exhibit wide range of applications with high efficient reproducibility[2]. They are used in the dermatological and cosmetic field, and this was investigated as early as in 1990s[3]. Also, Drug Delivery has been one of the frequently studied applications for nanocapsules.

Many reasons stand behind the importance of nanocapsules in the medical application. The unique features that nanocapsules possess such as large surface to mass ratio make it very attractive for medical application[4]. This feature allow the nanoparticles to bind, adsorb and carry other materials like drugs and protein[4].

The usage of nanocapsules in drug delivery carries many advantages including[5]:

- Improved efficacy that results from the improved biodistribution and pharmacokinetics.

- Improved stability for hydrophobic drugs.

- Reduced toxicity through the usage of biocompatible nanomaterial.

- Reduced side effects for some drugs by accumulating it at targeted sites.

1. Types of nanocapsules

Nanocapsules can be present and formed as polymeric nanocapasules, and liposomes.

a. Polymeric nanocapsules

By definition, polymeric nanocapsules are vesicular particles with an oily core enveloped by thin polymeric wall. These particles have size smaller than 1 μm. Polymeric nanoparticles are stabilized by steric agents or by surfactants or by using both of them[6]. Polymeric nanoparticles are well studied in the pharmaceutical filed as drug delivery vehicles[7]. Many polymers had been used to formulate polymeric nanocapsules. These are classified as synthetic and natural polymers[8]. Polysaccharides and chitosan are the most commonly used natural polymers[9]. However, the mostly used synthetic polymers are the polyesters including poly (lactic acid) (PLA), poly (lactic -co-glycolic acid) (PLGA), and poly(ε-caprolactone) (PCL)[9]. These polymers share common features that make them compatible for the application of nanocapsules as drug delivery system. Biocompatibility, biodegradability and tunable properties are some of the most important features that the above mentioned polymers have[9].

b. Liposomes

Liposomes are spherical vesicles made up of one or more phospholipid bilayer [10]. They consist of hydrophilic inner core that can encapsulate hydrophilic compounds[11] and hydrophobic membrane that entrap insoluble agents[12]. Due to their biocompatibility, biodegradability, low toxicity and due their ability to encapsulate both hydrophilic and hydrophobic compounds, liposomes known to be good drug carriers[13].

In addition to the usage of liposomes in drug delivery, they are used in therapeutic and diagnostic applications[10]. Despite these various applications, liposomes exhibit some limitation due their low drug loading capacity and due to their low stability upon storage [14]. In term of their mode of action and their mechanism of intracellular delivery, liposomes are classified into five categories [15]:

    a.   Conventional liposomes

    b.   pH sensitive liposomes

    c.   Long circulating liposomes

    d.   Cationic liposomes

    e.   Immune liposomes

2. Preparation methods of polymeric nanocapsules

Different methods had been reported for the preparation of polymeric nanocapsules where the polymer is being dispersed[16]. These methods are divided into two; some are based on pre-formed polymer including solvent evaporation, nanoprecipitation, salting-out, dialysis and supercritical fluid technology. And others depend on direct polymerization of monomers using different techniques such as micro-emulsion, mini-emulsion, interfacial polymerization and surfactant-free emulsion[16-17].

a. Solvent evaporation

Solvent evaporation is the first and the most used technique to develop nanoparticles from preformed polymers[17]. It has been used in the preparation of nanoparticles using biodegradable polymers for drug delivery[16]. In this method,

polymer solution is prepared in volatile solvents like chloroform, dichloroform, and ethyl acetate[17].

The formulated emulsion is converted into nanoparticles suspension upon evaporation of the solvent[17]. For the formulation of emulsions two main strategies are being used. First one is the single emulsion which is known as oil-in-water (o/w), and the second one is the double emulsion or water-in-oil-in-water (w/o/w)[16]. Ultra-sonication is done, followed by the evaporation of the solvent, then the nanoparticles are obtained by ultracentrifugation, and finally lyophilized[17].

b. Nanoprecipitation

Nanoprecipitation method is also known as solvent displacement or interfacial deposition method[18] . This technique has advantages over other techniques, it is a one-step method, fast, does not involve much expenses, requires low electrical power and no precursor emulsion is needed in this method. It produces particles with a size ranging between 50 and 300 nm, hence a greater surface area will be available[19]. The preformed polymer is dissolved in an organic solution and it is added to an aqueous solution in presence or absence of surfactant. The deposited polymer on the interface due to the fast diffusion of the solvent causes instant formation of the colloidal suspension[20].

c. Salting-out

Another method for the preparation of nanoparticles is the salting out method. It includes the usage of salting-out agent like magnesium chloride and calcium chloride[21].

The oily phase consists of polymer dissolved in an organic solvent, and the aqueous phase consists of surfactant with an electrolyte that is not soluble in the organic solvent[18]. An emulsion is formed by emulsifying the oily phase in the aqueous phase under a high mechanical stirring [18]. This method differs from other methods in the fact that diffusion of the solvent step is not taking place due to the presence of the salting-out agent which is removed by centrifugation [18]. Nanoparticles are obtained by the migration of the hydrophilic organic solvent into the aqueous phase [18].

d. Dialysis

This method is considered as a simple and effective method to prepare small and narrow distributed polymeric nanoparticles[18]. After dissolving the drug and the polymer in a water soluble organic solvent, the solution is placed in a dialysis tube with proper molecular weight cut off [22]. The dialysis process is done against the aqueous phase causing a decrease in the interfacial tension[22]. After the displacement of the solvent inside the membrane, the polymer aggregate progressively due to the loss of its solubility and thus the homogenous suspension of nanoparticles is formed[18, 22].

e. Supercritical fluid technology

This method is considered environmentally safe since it does not require the use of organic solvents as in the above mentioned methods[23]. Supercritical fluid (SCF) is solvent that stays as a single phase at a temperature greater than its critical temperature and regardless of pressure[23]. Due to its nontoxicity, non-flammability, low price and due to its mild critical conditions, supercritical CO_2 is the most used Supercritical fluid[23]. The two most commonly applied techniques are supercritical anti-

solvent (SAS) and rapid expansion of critical solution (RESS)[23]. SAS requires a

complete miscibility between the supercritical fluid and the liquid solvent containing the

solute, but the solute must be insoluble in the SCF [24]. As a result, when they get in

contact, the solution is formed and supersaturation and precipitation of the solute are

formed. However, The process of RESS requires the saturation of the SCF with solid

substrate followed by depressurization and fast release of solute in gaseous state that

leads to the production of very small particles [24].

3. *Applications of Nanocapsules*

Since the development of nanotechnology field is increasing, the applications

of the nanoparticles are increasing as well. Due to their attractive characteristics

especially when it comes to their size, nanocapsules made it possible to have a wide

range of applications. The fields of application of the nanoparticles depend on the type

and the nature of the used nanoparticles[25]. Some of the applications are discussed

below.

a. Biomedical applications

i. *Drug Delivery*

The hollow cavity of the nanocapsules made it possible to use them as drug

vehicles. As a drug delivery systems, nanocapsules are capable to improve the

fundamental properties of the free drugs like solubility, stability pharmacokinetics, and

biodistribution[26]. Many aspects must be taken into account when using nanocapsules

as drug delivery system such as the route of administration whether oral or parenteral ,

toxicity, clearance from body, etc[27]. The modification of the surface of the nanocapsules

by polymers or inorganic metals allows for further functionalization and makes them biocompatible [28]. The release of the drug is done through the decomposition of the capsule either by chemical or physical decomposition [29].

ii. Bioimaging and Biosensing

Nanocapsules are used in bioimaging where they are considered as a good candidates for the loading of fluorescent dye for imaging due to their high surface area to volume ratio[27]. Moreover, different nanocapsules are studied in the biosensing domain where nanocapsules are capable to increase the sensitivity and to lower the detection limit to an individual molecule[30].

b. Environmental application

Nanocapsules have less application in the environmental domain than in the biomedical field. The use of nanoparticles in the detection and monitoring of microbes was successfully done, and it is further used to immobilize microbial cells that is capable to biorecover or degrade some chemicals[31]. Also, nanoparticles can be utilized as biocatalysts in reductive dechlorination [31]. Nanoparticles can increase the bioavailability of the hydrophobic organic contaminants in bioremediation in soil environment[31]. Besides, nanocapsules such as zerovalent metal nanoparticles, metal oxide nanoparticles, carbon nanotubes, and quantum dots are highly in use and provide an indispensable tool in wastewater treatment. [32]

c. Dermatological and cosmetology applications

Different applications of nanotechnology in dermatology and cosmetics are available. Some nanoparticles had been used in sunscreens formulation where they act

as penetration enhancer[33]. Nanoemulsions (oil/water) had been introduce in moisturizer where their size add more favorable properties[33]. Also, Nanoparticles are introduced in the phototherapy as well as in the field of antiseptics[33]. Nanoparticles had been used in cosmetic formulation where they enhance their quality and cosmetic elegance[33]. They introduced in the production of shampoos, perfume, after shave commodities, eye shadow, antiperspirant, and lipsticks [33] .

B. Curcumin

1. Brief Background

Curcumin longa is a member of ginger family. The underground horizontal stems of this plant are known as Rhizomes[34]. Turmeric which is derived from this rhizomes contains three constituents which are Curcumin, desmethoxycurumin, and bisdemethoxycurcumin[34-35]. These are related to the same family which is the curcuminoid family and they only differ by the methoxy substituent found on the aromatic ring[35].

Curcumin comprises 2-5% of turmeric[36]. The yellow color of turmeric is due to the phytochemical Curcumin which is responsible for the therapeutic benefits of turmeric[36].

2. Structure

The chemical nomenclature of Curcumin is (*E,E*)-1,7-bis(4-hydroxy-3-methoxy-phenyl)-1,6-heptadiene-3,5-ione as shown in figure 1[37]. It has to aryl groups that are connected by seven carbon chain which is given the name diarlyheptanoid[38]. Curcumin gains exciting photochemical and photophysical properties because of the conjugation of the aryl groups via the β-diketone moiety conveys tautomerisim[39]. The keto-enol tautomer's are found in equilibrium, but the enol form which acts as electron

donor is dominant in alkaline medium and the keto form which acts as hydrogen donor is dominant in acidic and neutral medium[40-41]. Other factors affect the ratio of the two tautomers such as polarity of the solvent, temperature, and the substituents found on aryl rings [41].
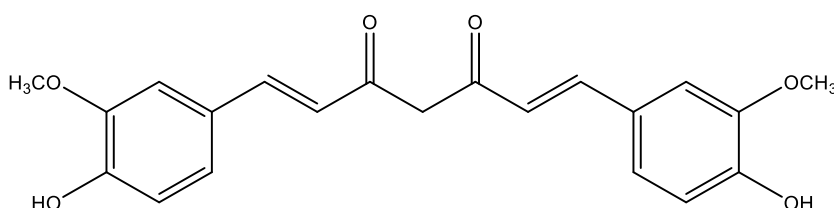
Figure 1 Structure of curcumin

3. *Photophysical properties*

Curcumin exhibits an exciting photo-physical property. Because of its yellow color, Curcumin shows a strong absorption in the UV-VIS region[42]. It exhibits an absorption maximum ranging between 408 and 432 nm[42]. The assigned strong band in the range 410-430 nm was related to the π-π* transition[42]. Studies showed that the absorption maximum has a strong dependency on the solvent being used. A red shift in the absorption maxima is observed with the increase in the polarity of the solvent[43]. The enol and the diketo forms of Curcumin exhibit different absorption maxima. Calculations by DFT methods predict a wavelength of 389 nm and 419 nm for the diketo and enol form respectively[42]. Similarly, the steady state fluorescence spectra showed a strong dependency on solvent polarity[44]. A significant variations in stokes' shift were obtained while changing the nature of the solvent[42]. Such dependency of the fluorescence properties on the solvent indicates that the nature of the excited state is intramolecular charge transfer[42]. Also, a large change in the dipole moment of the excited state was obtained and it led to the conclusion that the excited state of Curcumin

is more polar than the ground state[42]. This is due to the presence of the o-methoxyphenyl group that donates electron to the carbonyl groups of the diketo[42]. Curcumin is classified as a weak fluorescence molecules and to study its fluorescence decay properties in different solvents could be fitted to a double exponential decay function[43].

4. *Stability of curcumin*

a. Aqueous stability

Studies showed that the stability of Curcumin in aqueous medium is pH dependent. In buffer solutions with neutral and basic pH condition, Curcumin was unstable and 90% of it was decomposed rapidly. However, a significant increase in the stability was observed in acidic medium. The latter case is due to the conjugated diene structure[45]. This pH dependency is accompanied with a change in the color of Curcumin. A red color was obtained at pH < 1 due to the protonated form. A yellow color is obtained at pH ranging between 1 and 7 where most of the molecules exist in neutral form. And at pH greater than 7.5, an orange red color was observed[46].

b. Thermal stability

A study about the thermal behavior of Curcumin was done by Fujita et al in 2012. The TG-DTA curve of Curcumin showed a thermal degradation happening in two consecutive step, the first occurs between 205-441 ºC and the second between 441-630 ºC[47]. Also, it was possible to infer the thermal stability of Curcumin from TG curve which is 205 ºC[47]. Boiling Curcumin for 15 and 20 min caused a partial loss of

Curcumin by 27% and 32% respectively. Also, a 53% loss of Curcumin was obtained by processing turmeric in pressure cooker at 15 psi for 10 min[46].

5. *Biomedical activities of curcumin*

Curcumin possess multiple pharmacological activities some of them will be discussed below including anti-cancer, anti- bacterial, anti-viral and antioxidant activities.

a. Anti-cancer effect

Recently, it was found that curcumin exerts anti-cancer activities via its effect on a range of biological pathways involved in mutagenesis, oncogene expression, cell cycle regulation, apoptosis, tumorigenesis and metastasis[48]. The main mechanisms of action by which curcumin shows its unique anticancer activity comprise inducing apoptosis and constraining proliferation and invasion of tumors by suppressing a variety of cellular signaling pathways[49]. Numerous studies reported curcumin's antitumor activity on breast, lung, and prostate cancer, head and neck squamous cell carcinoma, and brain tumors[50].

An in vitro study done by Maniandan et al on human cancer cell lines showed that Curcumin exhibits anticancer effect. The used cell lines includes human colon adenocarcinoma HCT 15, HCT 116, and human larynx carcinoma Hep G-2 cell lines. Results showed that curcumin inhibits the growth of the above cell lines. The anticancer activity shown was related to cytotoxicity, nuclear fragmentation as well as condensation, and DNA fragmentation associated with the appearance of apoptosis[51].

b. Anti-bacterial effect

     Gunes et al evaluated the anti-bacterial activity of Curcumin against methicillin-sensitive Staphylococcus aureus (MSSA), methicillin-resistant Staphylococcus aureus (MRSA), Enterococcus faecalis, Bacillus subtilis, Pseudomonas aeruginosa, Escherichia coli and Klebsiella pneumonie using the macrodilution broth susceptibility test method. Results showed that when Curcumin is used in high concentration it shows a strong antibacterial activity[52].

c. Antiviral effect

     Curcumin has showed an exceptional antiviral activity against several deseases[53].

     The first proposal that curcumin has antiviral properties arose in the 1990s with the finding that curcumin could constrain the human immunodeficiency virus (HIV) viral protease in vitro, with a median inhibitory concentration (IC_{50}) of 100 μM[54]. Curcumin exerts antiviral activity against various types of enveloped viruses, by different mechanisms including direct interaction with viral membrane proteins; disruption of the viral envelope; inhibition of viral proteases; induce host antiviral responses[55]. Additionally, Curcumin shows an antiviral activity against coronaviruses including SARS-CoV, MERS-CoV, and SARS-CoV2[56]. It protects from lethal pneumonia and ARDS via targeting NF-κB, IL-6 trans signal, inflammasome and HMGB1 pathways[55].

d. Anti-oxidant effect

During natural cellular processes like cellular respiration, reactive oxygen species (ROS) are normally formed such as superoxide radical ($O^{\bullet-}_2$), hydroxyl radicals ($OH^{\bullet}$), singlet oxygen ($O^{\bullet}$) and H_2O_2[57]. The overproduction of ROS results in the oxidation of the components of cells thus causing damage in the affected tissues such damage can be reduced by the human body's antioxidant defense systems[58]. Curcumin is considered as an extremely potent lipid soluble antioxidant and has been proposed to act through its pro-oxidant/antioxidant effects, since formation of ROS by curcumin and curcuminoids correlates with their apoptotic activity on tumor cells[59].

6. Limitations

Although Curcumin consumption is tested to be safe, the therapeutic usage of curcmin is considered limited because of its low bioavailability. Thus, its free levels in plasma and tissues are very little. This was elucidated by the fact that curcumin has a high-rate conjugation through glucuronidation and sulfation which causes its low absorption[60].

Its poor bioavailability is related to its chemical instability rapid metabolism and rapid systemic elimination [61]. To overcome this limitation and to improve its delivery, different approaches have been studied such as encapsulation of Curcumin into polymeric nanoparticles[62], liposomes and phospholipids[63], polyethylene glycol[64], surfactants[65], and cyclodextrin complexation[66].

C. Poly-lactic-co-glycolic acid (PLGA)

1. Background

PLGA is a copolymer; it is made up of poly lactic acid (PLA) and poly glycolic acid (PGA) as shown in figure 2[67]. It has an asymmetric α-carbon which possess two stereochemical forms D or L[67]. Generally, PLGA stands for poly D, L-lactic-co-glycolic acid on which the D- and L-lactic acid forms are present in an equal ratio [68].
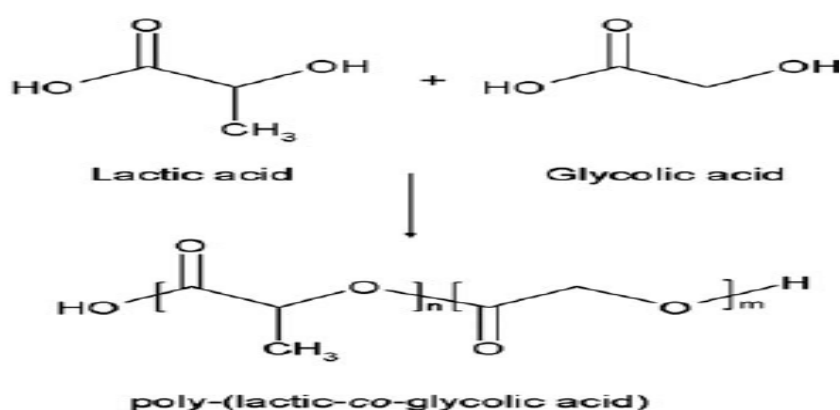
Figure 2 Structure of PLGA

2. Synthesis

PLGA is synthesized through a random ring opening copolymerization of the glycolic and lactic acid monomers in presence of a catalyst[68]. Some of the catalysts that had been used are tin (II) 2-ethylhexanote, aluminium isoproxide and tin (II) alkoxides[68]. During polymerization, the monomeric units are connected together via an ester linkage forming a linear, amorphous aliphatic PLGA polymer[69]. Depending on the ratio of the used monomers, different PLGA forms are obtained. For example, PLGA 50:50 comprises a copolymer that is made of 50 % lactic acid and 50 % glycolic acid[68-69].

3. Application

PLGA has been used in a wide range of application. Some of them will be discussed below including its usage in scaffolds, drug delivery, vaccines, and contrast agent for ultrasound.

a. PLGA-based scaffolds

PLGA based scaffolds is not only used as pure PLGA but also as a combination with other materials such as polymers or ceramics in order to make PLGA scaffolds biocompatible and to modify its degradability[70]. PLGA scaffolds have been utilized to regenerate damaged tissues, for example, in bone formation or in regenerative dentistry, along with stem cell-based therapy[71]. Using PLGA carriers incorporated with autogenous bone graft or different bone promoting substances such as bone morphogenetic protein-2 BMP-2 or simvastatin , bone formation was attained [71]. Besides, PLGA has been used in coating different materials including ceramics, metals, natural polymers, and bone allografts[72]. Moreover, PLGA has been used as fibers for bone tissues engineering purposes[72].

b. Drug Delivery

PLGA spheres that exit as microsphere and nanospheres are utilized for drug delivery purposes[73]. A review done by Su et al stated that PLGA including anticancer drugs, proteins or peptides and plasmid DNA [74]. A biodistribution studies revealed that PLGA nanoparticle delivery improves accumulation of diagnostic or therapeutic agents by the enhanced permeability and retention effect[75]. For instance, using a fluorometric assay method, PLGA NPs was used to deliver indocyanine green in healthy mice.

Results showed that the NPs led to higher indocyanine green deposit in organs as well as in blood compared with free solution, indicating the massive potential of PLGA NPs as a delivery system [76].

c. Vaccines

Moreover, PLGA microspheres have been utilized in developing vaccines. For a single-administration human immunodeficiency virus (HIV) vaccine using the gp120 subunit, PLGA microspheres showed an initial burst release and their delivery vehicle are designed in a way to produce a second delayed burst instead of a continuous release. The usage of such microspheres is Ideal in vaccination situations where a follow-up visit to a physician is not possible, where the initial burst release of gp120 acts as the priming vaccination and the second release act as the booster[77].

d. Contrast agent for ultrasound

AI-700 is a gas-filled PLGA microparticle technology utilized as an ultrasound contrast agent for echocardiography and has been taken through Phase III clinical trials. Due to its biocompatibility, PLGA is considered an attractive candidate for this application. These microparticles are designed using an emulsion and spray-drying method. To give the microparticles a porous, honeycomb-like structure, the inner aqueous phase was constituted with Ammonium bicarbonate. Results showed that these microparticles were not destroyed even under extreme ultrasound conditions, this means that PLGA microparticles are more stable than many commonly used ultrasound contrast agents[78].

D. Aims

General information about the three important components; Nanocapsules Curcumin and PLGA; that are used in our research work, were introduced in Chapter I. Our concentration will be on understanding the interaction between Curcumin and PLGA and on the synthesis of Curcumin loaded PLGA nanocapsules and further establishing their properties and applications.

The interaction between Curcumin and PLGA and Curcumin with PDDA was study using fluorescence spectroscopy technique as described in Chapter III.

In chapter IV of this work, our aim is to study self-assembly behavior of PLGA copolymer in solution, using fluorescence probing technique where Curcumin was used as a fluorescent probe. The CMC and CMT values of PLGA were obtained. Also the effect of NaCl and solvent on the aggregation behavior of PLGA was studied. Finally, position of curcumin inside the PLGA micelles will be determined through fluorescence quenching, using two different qunechers; CPB and KI.

The synthesis of Curcumin loaded PLGA nanocapsules is performed using solid in oil in water emulsion technique as it is described in Chapter V. These Nanocapsules will be coated by PDDA polymer. Different characterization techniques will be used in order to determine the different properties of the synthesized nanocapsules. Sensing of dopamine molecule will be established using these nanocapsules based on fluorescence emission intensity.

The anti-viral activity of the synthesized nanocapsules was evaluated in chapter VI. In this chapter the effect of our nanocapsules is investigated on Influenza A virus.
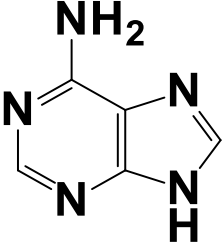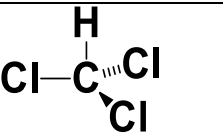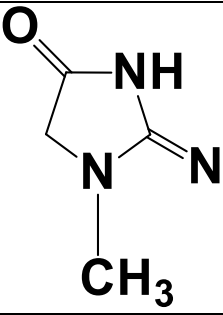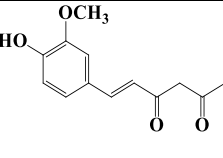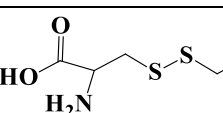
In Chapter VII, the effect of different pHs (4,6, and 7) on the release of Curcumin from nanocapsules synthesized in chapter IV will be studied. Additional silica and PDDA layers will be added to these nanocapsules in order to study their effect on drug release. The final form of these nanocapsules will be denoted as N2 (PLGA-CUR-PDDA-Si-PDDA) and N3 (PLGA-CUR--PDDA-Si-PDDA-Si-PDDA).
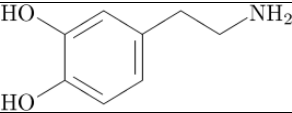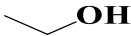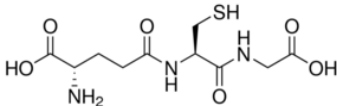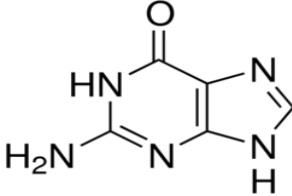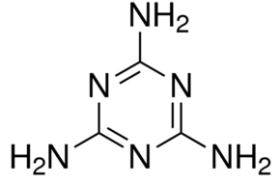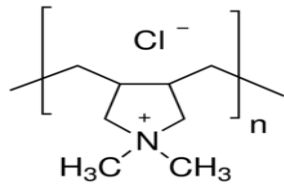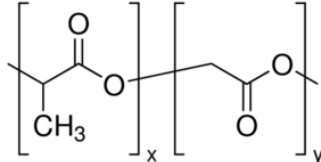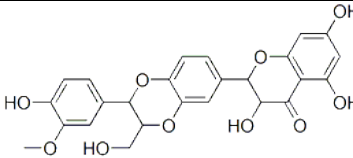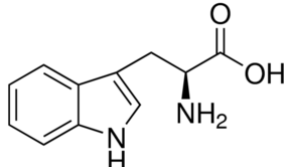
CHAPTER II

MATERIALS AND METHODS

A. Materials

All the chemicals that were used in this research work are presented in Table 1 with their corresponding chemical formula, chemical structure, purity and source.

Nomenclature	Chemical formula	Chemical structure	Purity (%)	Source
Adenine	$C_5H_5N_5$		99	Sigma Aldrich
Chloroform	$CHCl_3$		98	Merck
Creatinine	$C_4H_7N_3O$		97	Merck
Curcumin	$C_{21}H_{20}O_6$		99	Sigma Aldrich
Collodial Silica	SiO_2		99.8	Sigma Aldrich
Cystine	$C_6H_{12}N_2O_4S_2$		98	Merck

Cytosine	$C_4H_5N_3O$		98	Sigma Aldrich
Dopamine	$C_8H_{11}NO_2$		99	Acros
Ethanol	CH_3CH_2OH		99	Sigma Aldrich
Glutathione	$C_{10}H_{17}N_3O_6S$		99	Sigma Aldrich
Guanine	$C_5H_5N_5O$		98	Sigma Aldrich
Melamine	$C_3H_6N_6$		98	Sigma Aldrich
poly diallyl dimethyl ammonium chloride	$(C_8H_{16}ClN)n$		99	Sigma Aldrich
Poly lactic-co-glycolic acid (PLGA)	$(C_3H_4O_2)x(C_2H_2O_2)y$		98	Sigma Aldrich
Silymarin	$C_{25}H_{22}O_{10}$		98	Acros
Sodium Chloride	NaCl	NaCl		Sigma Aldrich
Tryptophan	$C_{11}H_{12}N_2O_2$		99	Acros
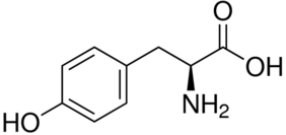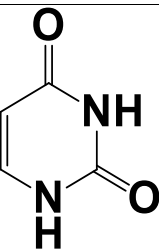
Tyrosine	C₉H₁₁NO₃		99	Acros
Uracil	C₄H₄N₂O₂		99	Sigma Aldrich

Table 1 List of chemicals used

B. Sample preparation

Briefly, the nanocapsules were prepared using solid-in-oil-in water (s/o/w) emulsion technique (See figure 3). Breifly, 45 mg of PLGA was socked in 1.5 mL chloroform for 24 hours. Later on, 5 mg of curcumin was added to the mixture and sonicated using probe sonicator for 1 minute. The obtained emulsion was added to 20 mL of polydiallyldimethyl ammonium chloride (1% w/v) followed by 2 minutes sonication.

To evaporate the solvent, the mixture was stirred for 3 hours at 500 rpm. The obtained emulsion was centrifuged at 15000 rpm for 10 minutes to precipitate the nanocapsules. The obtained nanocapsules were washed twice with deionized water. Finally, nanocapsules are freeze dried in order to obtain PLGA-Cur-PDDA nanocapsules in form of powder.
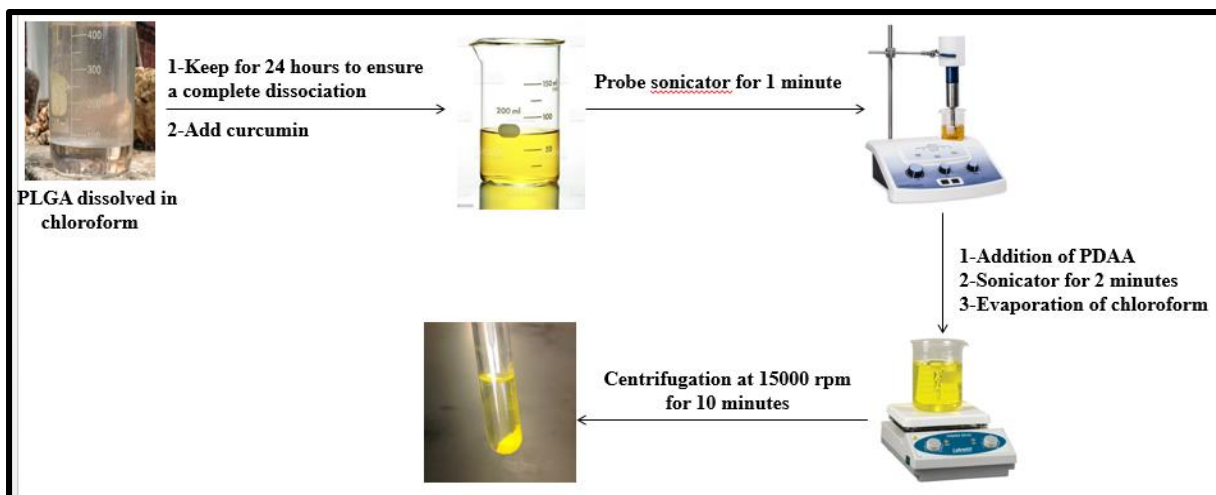
Figure 3 Schematic illustration of the nanocapsules's preparation.

C. Instrumentation

JASCO V-570 UV-VIS-NIR spectrophotometer was used to record the absorption spectra at room temperature in a wavelenght range of 200- 800 nm in a 3 mL cuvette.

Scanning electron microscopy (SEM) analysis was done using a Tescan, Vega 3 LMU with an Oxford EDX detector (Inca XmaW20) at 5 kV accelarating voltage. Briefly, few drops of suspended NCs were deposited on an aluminum stub and coated with carbon conductive adhesive tape.

The X-ray diffraction (XRD) analysis was obtained using a Bruker D8 discover X-ray diffractometer equipped with Cu-Ka radiation ($\lambda = 1.5405$ Å). The monochromator used was a Johansson type monochromator. The X-ray scans were done for 2θ between $10°$ and $45°$.

Zeta potential and dynamic light scattering value were measured using Particulate systems, NanoPlus Zeta Potential/Nano Particle analyzer.

Fluorescence spectra were measured using a Jobin-Yvon-Horiba Fluorolog III fluorometer and the FluorEssence program. The excitation source was a 100 W Xenon lamp, and the detector used was an R-928 instrument. The excitation and emission slits width were kept at 5 nm. Temperature was controlled by a thermostat which is coupled to the fluorometer sample holder. An external thermometer was used for measuring the temperature.

Thermo gravimetric analysis (TGA) was accomplished using a Netzsch TGA 209 in the temperature range of 30 to 1000 °C with an increase of 10 °C. min^{-1} under N_2 atmosphere.

D. Photophysical properties of PLGA polymer using curcumin as a fluorescent probe

Micellization is an important property of polymers. The aggregation behavior of PLGA polymer will be studied. The CMC and CMT values will be determined using Curcumin as a fluorescence probe. The effect of different factors on the aggregation of PLGA will be studied this includes:

- o   Effect of NaCl salts

- o   Effect of Solvent

- o   Effect of two Quenchers ; CPB and KI

The preparation of samples for each application is indicated in its specific chapter.

E. Application of Curcumin loaded PLGA nanocapsules

Curcumin loaded PLGA nanocapsules have taken much importance in the biomedical field. These nanocapsules have been used basically in sensing applications and in drug delivery, anti-cancer agent, anti-viral agent, and anti-inflammatory, etc. In our research work, three main applications were implemented to examine the efficiency and suitability of the synthesized nanocapsules. These 3 applications are:

o   The use of curcumin loaded PLGA nanocapsules as a nanoprobe for the detection of dopamine

o   The study of curcumin release from these nanocapsules

o   The elaboration of curcumin's effect as antiviral agent against Influenza.

It is worth to mention that for each application, the procedure followed for sample preparation is indicated in its specific chapter.

CHAPTER III

A BINDING STUDY OF THE INTERACTION BETWEEN CURCUMIN AND POLY LACTIC-CO-GLYCOLIC ACID AND POLY DIALLYLDIMETHYLAMMONIUM CHLORIDE

A. Introduction

In supramolecular chemistry, typically the first query that a researcher might need to ask is: "how strong is this complex or interaction?". Binding constants are a distinct case of equilibrium constants. It helps to extent the bonding affinity amongst two or more molecules at equilibrium. In supramolecular chemistry, binding constants for either host–guest complexation or host–host aggregation (e.g., dimerization) are typically the topic of concern. The determination of binding constants is an essential step in understanding and describing molecular interactions[79]. The binding constant can be measured using specialized techniques as the analytical methods such as solubility methods, potentiometric, and mass spectrometry were also used for this purpose[80]. In addition, other techniques were investigated as NMR[81], UV–vis[82], fluorescence[83], and calorimetric titrations[84]. It is possibly safe to say that above 90% of all experimentally calculated binding constants in supramolecular chemistry are recently determined using the last fore cited techniques. Thus, nowadays researchers are focusing on the efficiency of fluorescence spectroscopy technique for the determination of binding constant. In fact, this technique has arisen as a common method because it is quick, very sensitive, and easy to perform[85].

In this study, fluorescence spectroscopy was utilized in order to study and compare the interaction between curcumin and both polymers PLGA and PDDA

respectively. Also, thermodynamic parameters, binding constants, binding sites and the type of present interaction forces were explored.

B. Materials and methods

1. *Fluorescence Studies*

The emission spectra of samples in the absence and presence of various concentrations of PLGA and PDDA were recorded over a wavelength range 440-700 nm at three different temperatures (25, 35, and 45 °C). The temperature was controlled by a thermostat which is coupled to the fluorometer sample holder. An external thermometer was used in order to fix the sample temperature. The width of the used cuvette was 1 cm.

2. *Sample preparation*

In order to study the interaction of curcumin with PLGA in solution, fluorescence measurements for 11 samples of different PLGA concentrations in the range of 0-0.290 g/L were conducted. Briefly, PLGA was first dissolved in chloroform then evaporated using rotatory evaporator. Later on, double distilled water was added and the sample was sonicated for final use.

Likewise, to study the interaction of curcumin with PDDA in solution, 9 samples with different PDDA concentrations in the range of 0-5.6 µg/L were prepared. Curcumin's concentration was maintained constant at 2 µM in all samples.

To check the emission intensity of PLGA and PDDA alone, a sample containing 290 µg/L of PLGA and 3.5 µg/L of PDDA were prepared respectively.

C. Results and Discussion

The interaction of curcumin with PLGA and PDDA was estimated in order to find the binding constant for PLGA and PDDA.

1. Binding constant of PLGA

Curcumin's concentration was fixed at 2 μM, while the concentration of PLGA was increased from 0 to 0.29 g/L. It was found that the emission intensity of curcumin is proportional to the increase of PLGA's concentration (See Figure 4). The enhancement of the intensity was also accompanied with a blue shift from ~542 nm to ~507 nm. This blue shift is due to the fact that curcumin experiences a more nonpolar environment in PLGA, meaning that Curcumin is being incorporated in the hydrophobic core of the polymers.
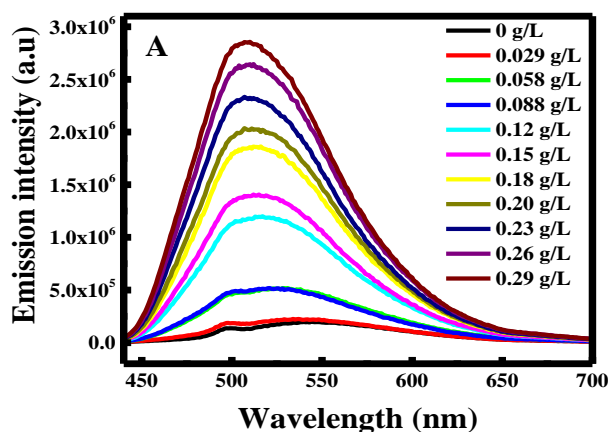
Figure 4 Fluorescence emission spectra of curcumin at different concentrations of PLGA excited at λ=425 nm

To find the binding constant and thermodynamic parameters of the interaction of PLGA with curcumin, the plot of log [(F-F0)/F0] vs the logarithim of polymer concentration was established according to the modified Stern-Volmer equation:

$$\log(F-F_0)/F_0 = \log K_a + n\log[P] \qquad\qquad \text{equation (1)}$$

Where n is the number of sites and Ka is the binding constant[86].

Based on the curve obtained in Figure 5, the binding constant (Ka) value of curcumin with PLGA was found to be equal to 119.89 L/g. Hence, the linear fit equation was set as y= 1.7557x+2.0788. These results showed that curcumin possessed two binding site to PLGA polymer at ambient temperature.
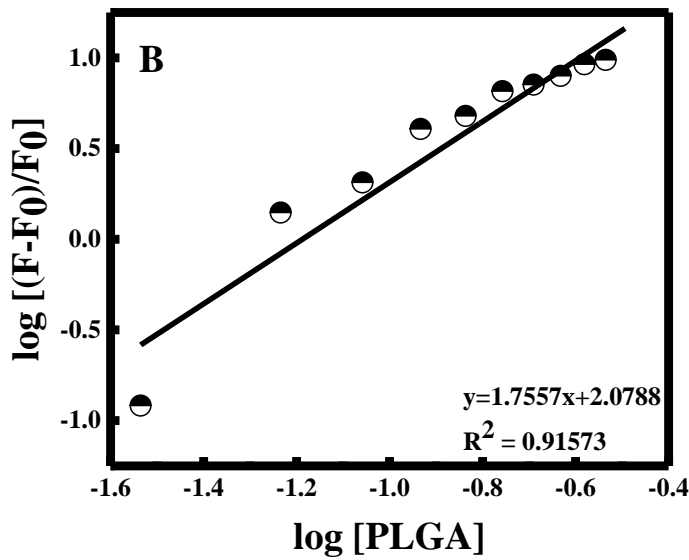
Figure 5 Modified Stern-Volmer plot for PLGA.

To have a better understanding of the thermodynamics of the reaction between Curcumin and PLGA, the binding constant was evaluated at three different temperatures; 298.15 °K, 308.15 °K, and 318.15 °K. Thereby, the standard enthalpy change (ΔH^o) and the entropy change (ΔS^o) were determined by using the van't Hoff equation (equation 2) and the standard free energy change (ΔG^o) was estimated using the thermodynamics equation (equation 3)[87].

$$\text{Log (Ka)} = \Delta S^o/R - \Delta H^o/RT \qquad\qquad \text{equation (2)}$$

$$\Delta G^o = \Delta H^o - T\Delta S^o \qquad\qquad \text{equation (3)}$$

As shown in Figure 6A, the emission intensity of curcumin decreases with the increase of the temperature. This variation is due to the change of the PLGA environment while the temperature increases.

Modified Stern-Volmer plot for PLGA at 3 temperatures and van't Hoff plot were depicted in Figure 6B&C.
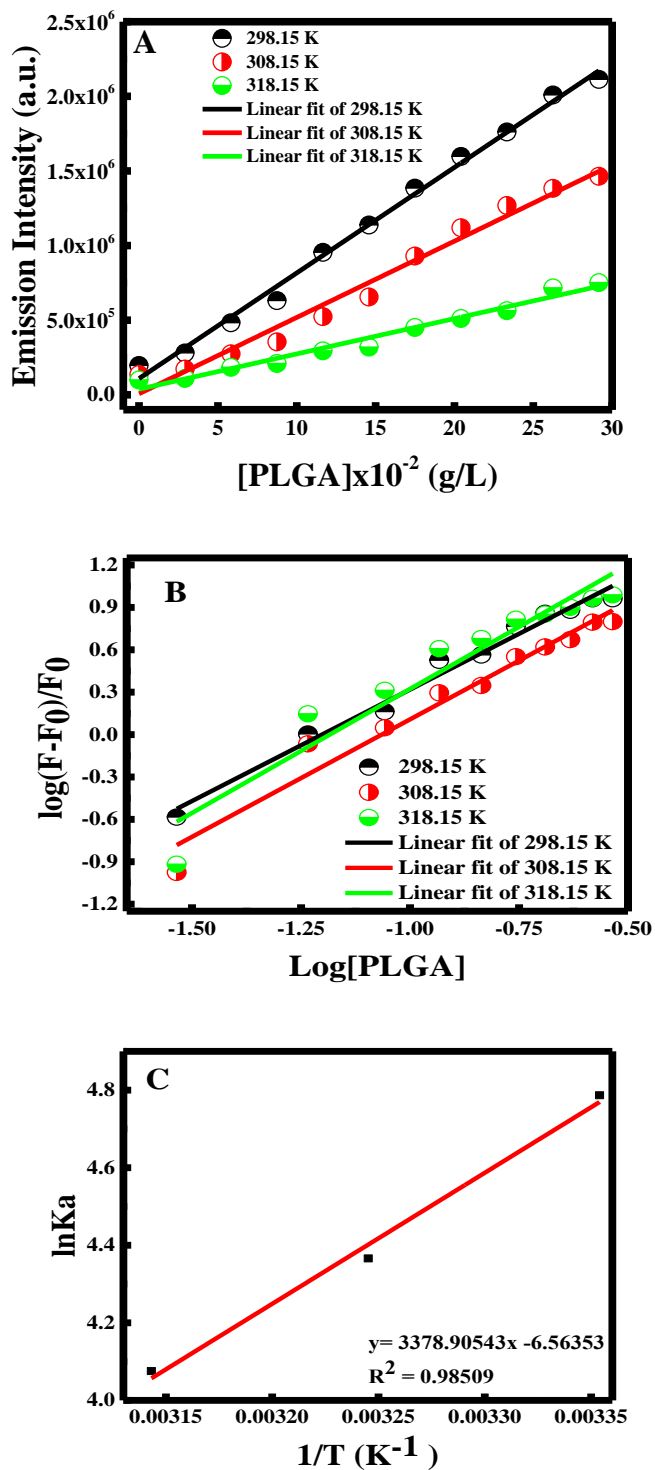
Figure 6 (A) Effect of the temperature on the emission intensity of curcumin in the presence of different PLGA concententration; (B) Modified Stern-Volmer plot for PLGA at 3 temperatures and (C) van't Hoff plot.

The thermodynamics parameters (ΔH^o, ΔS^o and ΔG^o) were calculated and tabulated in Table 2.

Temperature (°K)	n	Ka (L/g)	ΔS (J.mol^{-1}.K^{-1})	ΔG (KJ.mol^{-1})	ΔH (KJ.mol^{-1})
298.15	1.76	119.67		-11.82	
308.15	1.57	78.72	-54.57	-11.28	-28.10
318.15	1.66	58.75		-10.73	

Table 2 Binding and thermodynamic parameters for curcumin-PLGA interaction at different temperatures

Generally, based on the values of standard enthalpy changes (ΔH^o) and standard entropy changes (ΔS^o), there are three different types of interaction between drug and biomolecules that can exists [87-88]:

a) If both ΔH^o and ΔS^o are positive, then hydrophobic interaction exists.

b) If both ΔH^o and ΔS^o are negative, then van der Waals interactions and hydrogen bonds occur.

c) If ΔH^o negative and ΔS^o positive, then electrostatic interactions are present.

Henceforth, the negative ΔH^o and negative ΔS^o calculated, confirm the presence of van der Waals interaction and hydrogen bonding with curcumin. Moreover, the negative value of ΔG^o indicates that the interaction of PLGA with curcumin was due to a spontaneous process.

2. Binding constant of PDDA

Similarly, the binding constant of PDDA was conducted by varying its concentration from 0-55.47 μg/L. As observed in Figure 7 the increase in PDDA concentration, boost the intensity of curcumin with a blue shift from ~550 nm till ~499 nm. Hence, these results were identical to the results obtain with PLGA polymer, where

curcumin experiences also a more nonpolar environment in PDDA micelles, indicating

that curcumin is being incorporated in the hydrophobic core of the PDDA polymer.
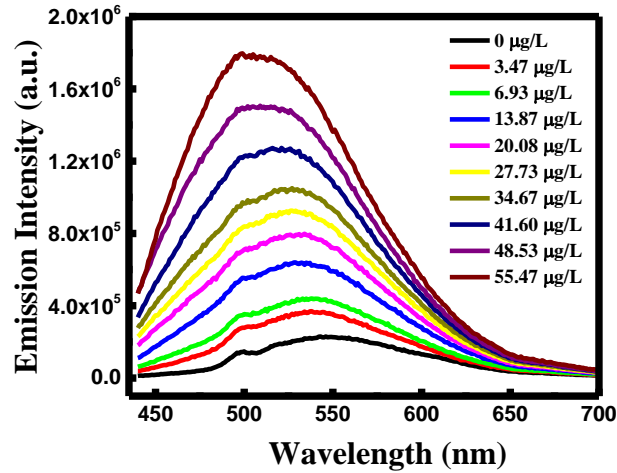
Figure 7 Fluorescence emission spectra of curcumin at different concentrations of
PDDA excited at λ=425 nm and

The binding constant (Ka) was calculated after analyzing the binding curve in

Figure 8. Ka value of curcumin with PDDA was found to be equal to 30.38 L/g.

Interestingly, the main difference between PLGA and PDDA polymer is that curcumin

possessed one binding site to PDDA based on the linear equation y=0.6879x+1.4826.
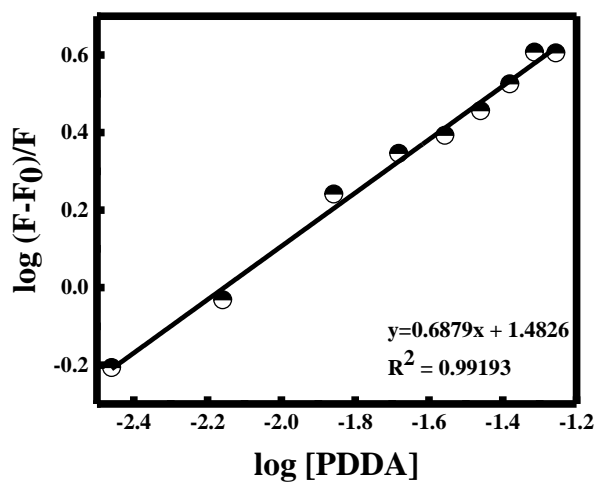
Figure 8 Modified Stern-Volmer plot for PDDA.

Afterwards, the binding constant was evaluated at three different temperatures; 298.15 °K, 308.15 °K, and 318.15 °K. As shown in Figure 9A, the emission intensity decreases with the increase of the temperature. This can be due to the increase of the PDDA viscosity, inhibiting the entrapment of curcumin into the micelles.

Furthermore, Modified Stern-Volmer plot for PDDA at 3 temperatures and van't Hoff plot were presented in Figure 9B&C respectively.
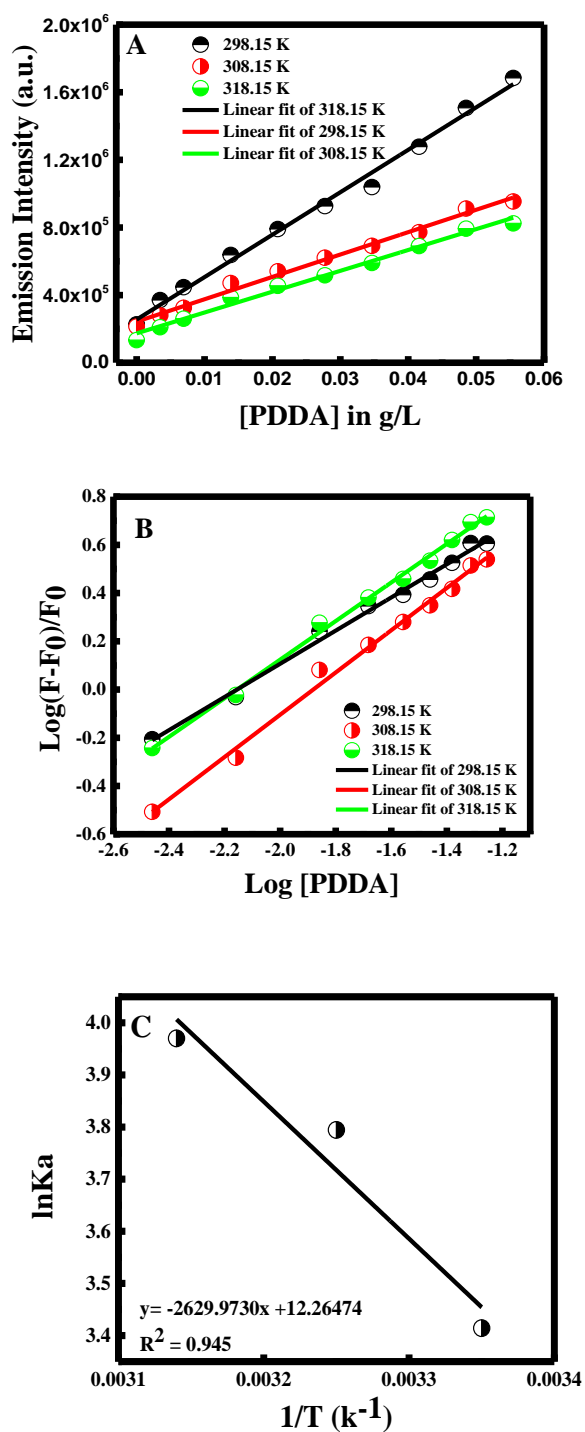
Figure 9 (A) Effect of the temperature on the emission intensity of curcumin in the presence of different PDDA concententration; (B) Modified Stern-Volmer plot for PDDA at 3 temperatures and (C) van't Hoff plot.

The thermodynamics parameters (ΔH^o, ΔS^o and ΔG^o) were calculated and supplied in Table 3.

Based on the calculated values, the positive ΔH^o and positive ΔS^o values suggest that the dominant interaction between Curcumin and PDDA is hydrophobic interaction. Besides, the negative value of ΔG^o indicates that the interaction of PDDA with curcumin was based on a spontaneous process.

Temperature (°K)	n	Ka (L/g)	ΔS (J.mol^{-1}.K^{-1})	ΔG (KJ.mol^{-1})	ΔH (KJ.mol^{-1})
298.15	0.69	30.39		-8.54	
308.15	0.88	44.45	101.97	-9.56	21.87
318.15	0.80	52.98		-10.58	

Table 3 Binding and thermodynamic parameters for curcumin-PDDA interaction at different temperatures

3. *Binding constant of PDDA in the presence of PLGA*

To study the effect of PLGA on the interaction of curcumin with PDDA, 9 samples were prepared where PDDA concentration was increased in the range of 6.9 g/L to 56 g/L, PLGA and curcumin concentrations were fixed at 20 µg/L and 2 µM respectively.

As can be seen in Figure 10A the emission intensity of curcumin increased in the presence of PLGA. But, in the presence of PLGA the intensity decreased by ~3 fold compared to the results obtained in the absence of PLGA. This diminution in the emission intenisty can be due to the fact that more particles are present in the solution and thus more collisions are generated inducing radiation-less decay. These radiation-

less decay cause a loss of energy as heat that in turn lead to the decrease in the
fluorescence intensity. The Stern Volmer plot at 3 different temperatures is depicted in
Figure 10B.
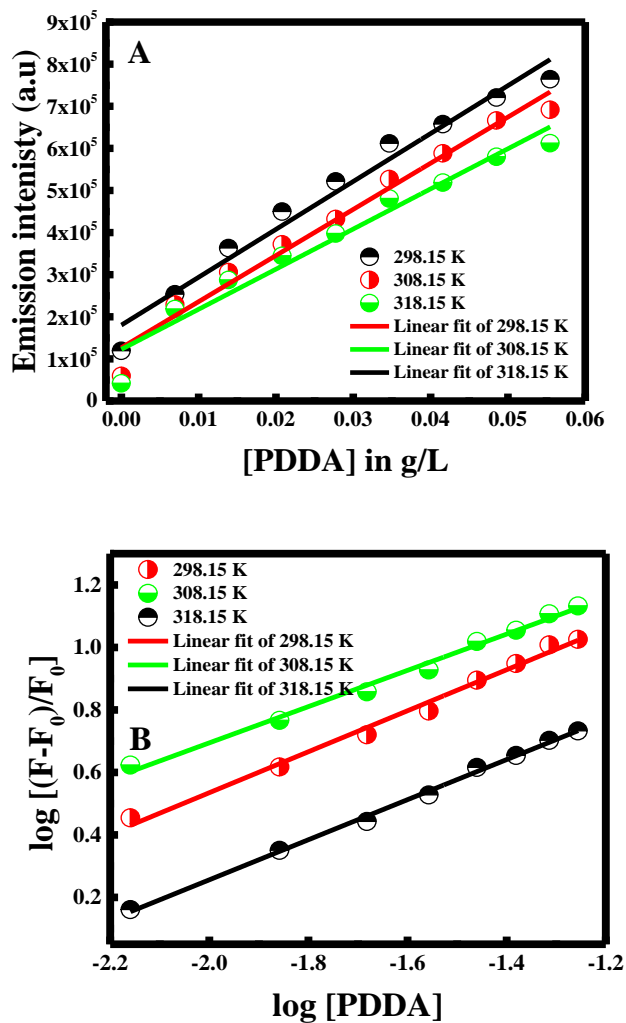
Figure 10 (A) Fluorescence intensity of curcumin versus concentration of PDDA in
presence of PLGA at different temperatures and (B) Modified Stern-Volmer plot for
PDDA in presence of PLGA at 3 temperatures.

The binding constants were calculated and formulated in Table 4. Comparing Ka
values in the presence of PLGA values to K_a values in absence of PLGA, we can see
that the binding affinity has increased in presence of PLGA. This is because PLGA is
forcing curcumin in water phase and pushing it toward the PDDA polymer.

Temperature (°K)	K_a in presence of PLGA (g/L)	K_a in absence of PLGA (g/L)
298.15	34.59	30.39
308.15	70.28	44.45
318.15	71.58	52.98

Table 4 comparison of K_a values for the interaction of PDDA in presence and absence of PLGA

4. *Zeta potential measurements*

To further understand the interaction between Curcumin, PLGA and PDDA, zeta potential measurement was performed using Particulate systems, NanoPlus Zeta Potential/Nano Particle analyzer.

By measuring the zeta-potential, it is possible to probe a characteristic colloidal property in a mixture of particles, making it a useful technique to elucidate their behavior[88]. The zeta-potential is generated between the interfacial double layer of the dispersed particle versus the continuous phase away from the interface[89].

Thus, the biomaterial's zeta-potential reveals the electric surface properties. Zeta potential was obtained in the first place for curcumin, PLGA, and PDDA alone. Then, it was also measured for the mixture of curcumin-PLGA, curcumin-PDDA, and curcumin-PLGA-PDDA. PLGA and Curcumin exhibit a negative surface charge equal to -26.59 mV and -4.98 mV respectively.

Interestingly, upon mixing these two together a positive zeta potential was obtained. Considering the negative charge of both compounds, we would expect an increase in the total negative charge. Thus, a positive surface charge was obtained confirming the formation of hydrogen bond upon binding curcumin with PLGA molecules (See Figure 11A).
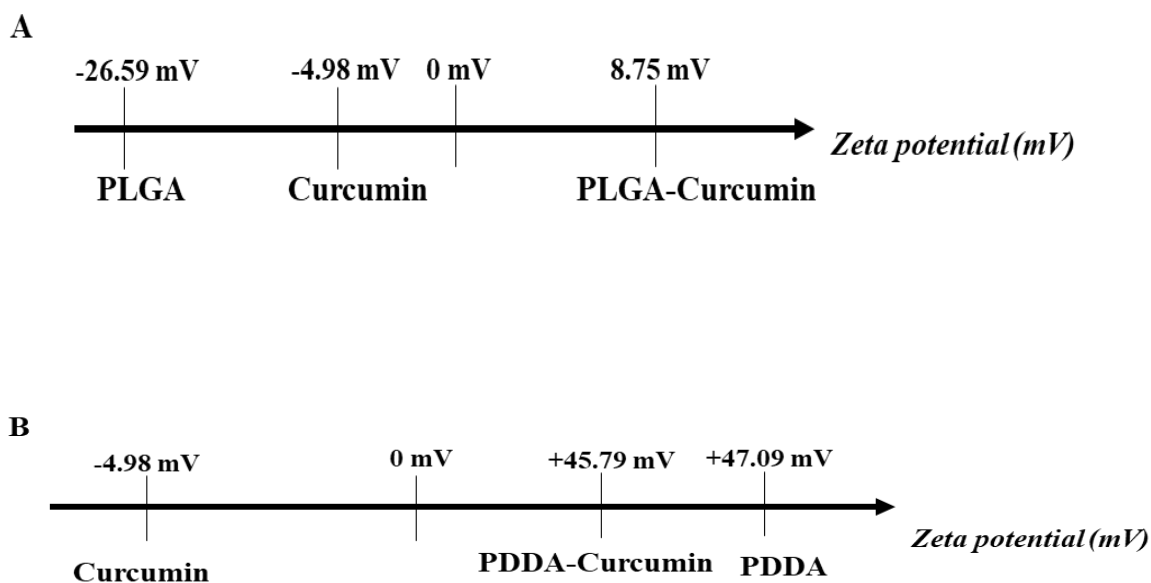
Figure 11 zeta potential values for Curcumin, PLGA, and PDDA and their mixture.

Similar results was obtained by Meesaragandla et al, where the mixture of the negatively charge humane serum albumin with the negatively charged PEG-NH$_2$ coated NPs results in an increase in the overall positive potential. Such unexpected behavior was related to the formation of hydrogen bonding between these molecules[90].

With respect to PDDA polymer which is positively charged (+47.09 mV), a decrease in its charge was obtained upon mixing it with curcumin (See Figure 11B). This decrease in the surface charge confirms the hydrophobic interaction between these molecules.

D. Conclusion

In summary, different sample with varying PLGA and PDDA concentration were prepared in presence of fixed curcumin concentration. The emission spectra were obtained for these samples at three different temperatures (298.15, 308.15, and 318.15 °K) at 425 nm excitation wavelength.

Starting from these data the Modified Stern-Volmer plot was obtained at room temperature and the binding constant of PLGA and PDDA with Curcumin was estimated to be 119.67 and 30.39 g/L respectively.

Thermodynamic parameters were calculated using Van't Hoff equation. Based on the obtained values, it was concluded that curcumin binds to PLGA through hydrogen bonding and van der waals interaction, while PDDA interacts with curcumin through hydrophobic interactions.

Moreover, binding of curcumin with PDDA is further encouraged in the presence of PLGA.

CHAPTER IV

A NOVEL STUDY ON THE SELF-ASSEMBLY BEHAVIOR OF POLY (LACTIC-CO-GLYCOLIC ACID) PROBED BY CURCUMIN FLUORESCENCE

A. Introduction

Micellization can occur above a certain concentration of polymer known as critical micellar concentration and above a certain temperature known as critical micellar temperature[91-92]. When in aqueous solution, the associate hydrophobic group and the hydrophilic group are left exposed to the solvent, the structure is known in this case as "normal" micelle[93].

However, in nonpolar solvent, the hydrophilic group is poorly solvated. This results in the formation of the interior of the aggregate, and the hydrophobic group surrounds therefore the formed polar core which is responsible of the solubility of the aggregate. Thereby, the formed structure is denoted as a "Reverse Micelles"[93]. Indeed, in non-polar solvents, the CMC value is not well defined as in aqueous medium because the aggregation number of reverse micelles is small which make its determination difficult[93].

In this manner, different methods were established in the literature for the aim of studying the CMC and CMT changes in block copolymers. Some of these methods comprise Fourier-transform infrared spectroscopy technique (FTIR)[94], surface tension measurements[95], DPH solubilization method[96], surface plasmon resonance[97], and fluorescence probing[98]. In the latter method, pyrene molecules were always used and have proved to be a powerful tool as a fluorescence probe. In fact,

pyrene is lethal to the kidneys and liver. It is also known that pyrene molecule affects numerous existing functions in fish and algae. Thus, it was the need to find relative fluorescence molecule having less toxic effects[99]. For this purpose, curcumin is being developed to be used as fluorescence probe for the determination of the polymer's physical properties.

Hence, in this study, curcumin was utilized as an external fluorescence probe in order to understand the self-assembly behavior of PLGA. To the best of our knowledge, till present the physical properties of PLGA are not well studied and published.

B. Materials and methods

1. *Sample Preparation*

a. CMC sample preparation

A stock solution of PLGA (1.8 mg/mL) was prepared in acetone-water mixture. Likewise, a stock solution of 1 mM curcumin (m=1.105 mg) was dissolved in methanol. Subsequently, dilutions were made as desired. The CMC study was investigated by substituting the acetone-water mixture with chloroform, and the effect of sodium chloride salt was also established.

For this purpose, fluorescence measurements for 10 samples of different PLGA's concentration in the range of 0-0.54 g/L were conducted. Curcumin's concentration was maintained constant at 2 μM in all the samples.

To study the effect of salt on the CMC of PLGA, sodium chloride's concentration was increased from 10 to 50 and then 150 mM.

To prove the effectiveness of curcumin as fluorescence probe the CMC study was conducted using pyrene as a fluorescence probe instead of curcumin.

b. CMT sample preparation

For the CMT study, one sample was prepared where the PLGA and curcumin concentrations were maintained fixed at 0.48g/L and 2 µM respectively.

Fluorescence measurements for this sample were done by varying the temperature from 10°C to 80°C with 5°C increments.

c. Quenching study

For quenching experiment, PLGA and curcumin concentrations were kept constant at 0.48 g/L and 2µM respectively.

As for using KI as quencher the concentrations used were 0, 0.2, 0.4, 0.6 and 1 M. As for CPB, the concentration used were as follow; 0, 50, 100, 200, 500, 800 and 1000 µM.

C. Results and discussion

The CMC and CMT experiments, in addition to the quenching study, were established by measuring the emission intensity of curcumin at $\lambda_{ex} = 425$ nm in the emission range 440-700 nm.

1. Self-assembly and critical micelle concentration

Even though micellization is a spontaneous process, it only begins above a certain concentration of the polymer known as the critical micellar concentration (CMC), at a fixed temperature. To determine this concentration, several physical

properties such as surface tension, electrical conductivity, or osmotic pressure can be tracked as a function of polymer concentration[100]. To examine the CMC of PLGA, curcumin was used as a fluorescence probe to study the aggregation behavior of PLGA.

The emission intensity of curcumin in the presence of different PLGA concentrations was measured at room temperature, excited at λ_{ex}=425 nm in the emission range of 440-700 nm. It is commendable to note that the fluorescence emission intensity for a sample containing only PLGA polymer was measured and found to be negligible. It was found that the error is within 10%, meaning that the fluorescence is only due to curcumin's presence.

As shown in Figure 12A, the emission spectra of curcumin showed a peak at ~498 nm after excitation at 425 nm. A blue shift from ~ 545 nm (in absence of polymer) to ~ 496 nm was observed at higher concentrations of PLGA. The change in the fluorescence intensity at 498 nm with increase in PLGA concentration is shown in Figure 12B. It is obvious that the emission intensity of curcumin increases in two different ways. In the beginning, the emission intensity increases rapidly to a certain concentration, where it continued to increase; thus with smaller slope. Such break in the fluorescence intensity vs the PLGA concentration can be attributed to the aggregation/micellization of PLGA.

Therefore, it resembles the CMC value which is estimated to be ~0.31±0.01 g/L. The observed blue shift and the increase in the fluorescence intensity indicate that curcumin experiences a more nonpolar environment in the formed PLGA micelles. This signifies the incorporation of curcumin into the hydrophobic core of PLGA micelles.
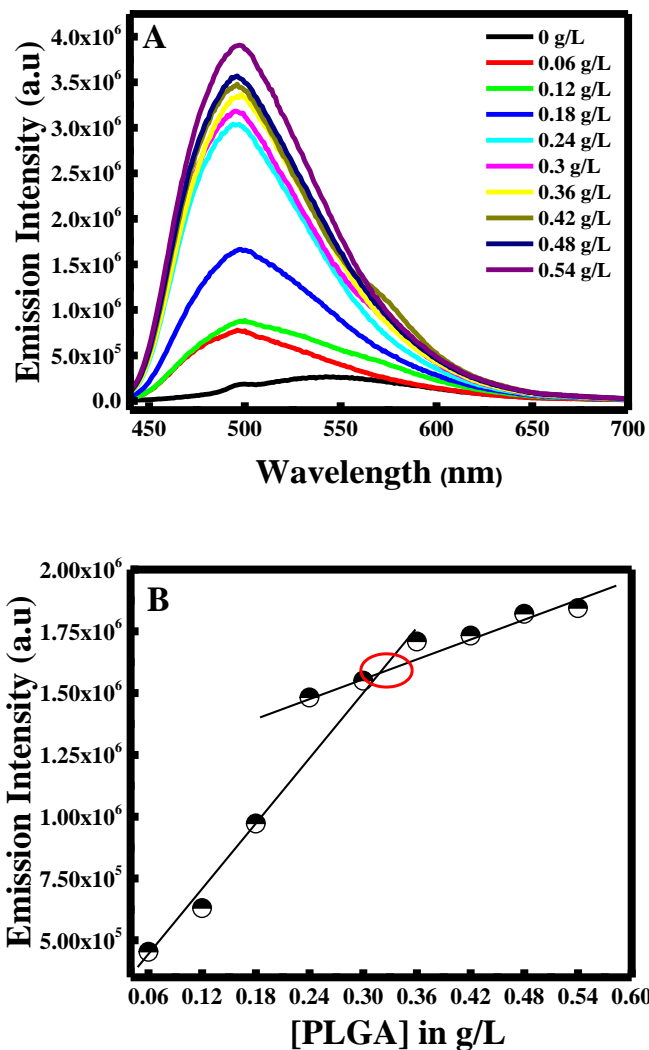
Figure 12 Fluorescence emission spectra of curcumin at different concentrations of PLGA (B) Fluorescence intensity of curcumin at $\lambda_{em} = 498$ nm versus concentration of PLGA

To prove the efficiency of curcumin as a fluorescence probe in the determination of the CMC value, same experiment was carried out using pyrene as a fluorescence probe. The results are depicted in figure 13. It is clear, that the increase in the emission intensity of pyrene was similar to the enhancement of the fluorescence intensity of curcumin. Hence, when using pyrene the CMC value was equal to 0.33±0.01 g/L. This value is almost equivalent to the CMC value obtained using curcumin. These results

prove the efficiency of curcumin as a fluorescent probe in the determination of the polymer's physical properties.
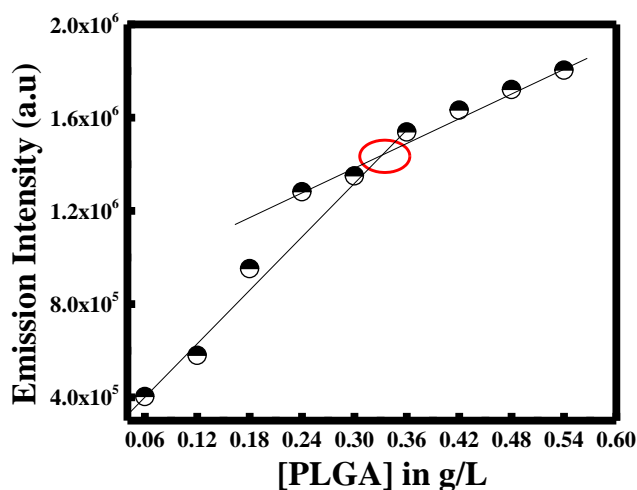
Figure 13 Fluorescence emission spectra of pyrene at different concentrations of PLGA.

2. Self-assembly and critical micelle temperature

Due to the strong dependence of the CMC on temperature, the concept of the CMT has been extensively used[101]. Temperature induces a crucial effect on the micellization process, thus we decided to evaluate the CMT of PLGA at a concentration (0.48 g/L) that exceeded the CMC value of PLGA (0.31 g/L) obtained in above mentioned CMC experiment.

The representative fluorescence spectra of the PLGA solution at a concentration of 0.48 g/L were recorded at different temperatures over the range 10-80°C. As shown in Figure 14A the emission intensity decreases with the increase of the temperature. The maximum of the emission intensity at 482 vs the temperature is depicted in Figure 14 B. In fact, at low temperature two essential aspects were present. On the first hand, PLGA

did not associate in aqueous solution and on the other hand curcumin was not

solubilized in a hydrophobic environment.
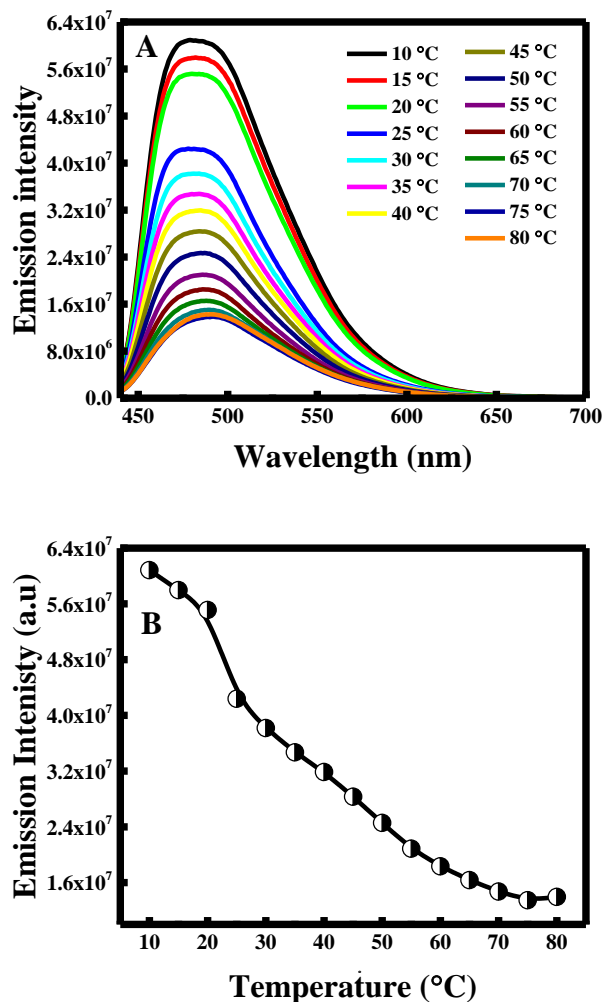
Figure 14 (A) Fluorescence spectra of PLGA solution C = 0.48 g/L at various temperatures in the range of 10-80 °C and (B) Plot of maximum fluorescence intensity vs the temperature.

Therefore, the fluorescence intensity was strong. Thus, at high temperature, the

formation of micelles is encouraged inducing the solubilization of curcumin in the

hydrophobic micelle interior. Hence, the entrapment of curcumin in the hydrophobic

core of the PLGA polymer, diminish the emission intensity of curcumin. Therefore, we

can say that there is a distinct temperature at which fluorescence intensity decline

dramatically indicating the aggregation of PLGA into micelles. This break point can therefore be allocated   as CMT. In this case, it was obtained at 25 ° C.

3. *Effect of NaCl salt on the CMC of PLGA.*

To study the effect of ionic strength on the interaction of curcumin with PLGA, different concentrations of NaCl were used. The examined concentrations were 10, 50, 150 mM. The fluorescence intensity of curcumin was monitored at 498 nm for each NaCl concentration in the presence of different PLGA concentrations as shown in Figure 15A-C.

In the absence of NaCl the CMC value was equal to 0.31 g/L. Hence, the CMC value was lowered by around two folds from 0.31 to 0.14 g/L as the NaCl concentration reaches 150 mM (See Figure 12D).

Certainly, this change in the CMC value was expected, as it is widely found in earlier comparable studies that NaCl drops the CMC value of the polymer. Hence, a study conducted by Desai et al. showed similar results when using pluronic polymer. In fact, the presence of sodium chloride had boosted the hydrophobicity in PPO moiety and thereby lowered the hydrophilicity of PEO moiety, leading to the formation of micelles at low concentration[95].

Consequently, the reduction in the CMC value in the presence of NaCl salt induces the enhancement of micelles formation. Hence, in our case NaCl is pushing out the PLGA polymer from the aqueous phase, thus improving the micelle formation. This latter effect of NaCl salt is known as salting-out effect[100].
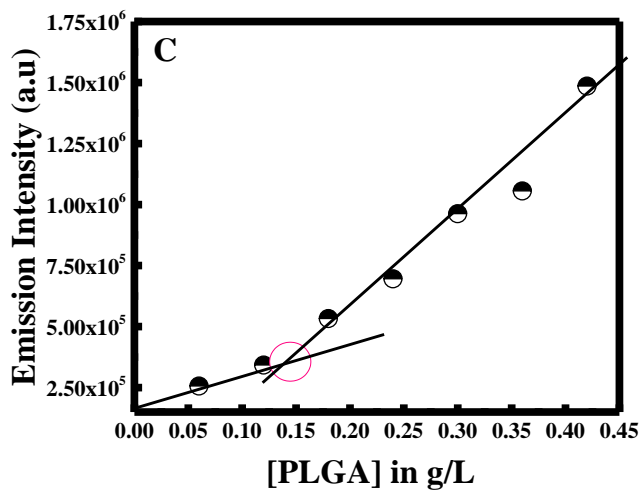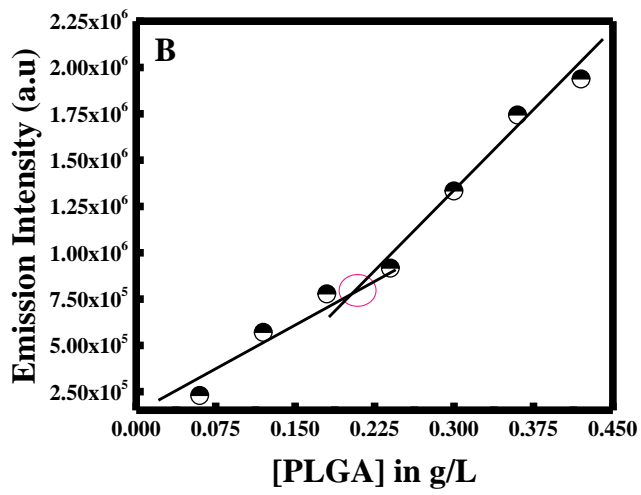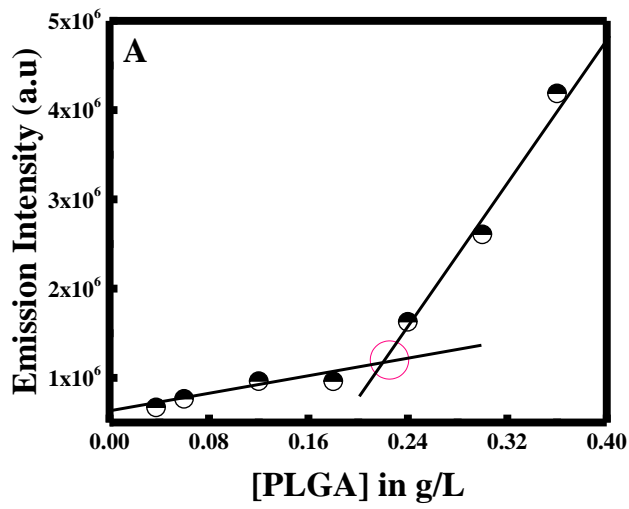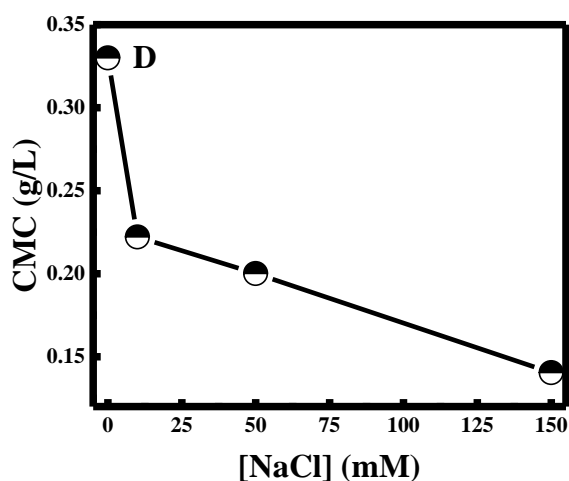
Figure 15 Fluorescence intensity of curcumin at λem =498 nm plotted versus concentration of PLGA in the presence of (A) 10 mM; (B) 50 mM; (C) 150mM NaCl and (D) Change in CMC value with increased concentration of NaCl.

4. Solvent effect on CMC values

To study the effect of solvent on the micellization of the polymer, this experiment was repeated while dissolving PLGA in an organic non-polar solvent which is chloroform.

To understand the interaction of PLGA with curcumin in the presence of chloroform, various concentrations of PLGA were prepared in the range of 0-0.54 g/L, where curcumin's concentration was remained constant at 2 μM.

As shown in Figure 16, the emission intensity of curcumin increased proportionally within the increase in the PLGA concentration until it reaches a maximum at 0.33 g/L, then it starts to decrease gradually. This maximum concentration is related to the CMC value that was equal to 0.33 g/L. The CMC value found in the presence of chloroform was almost equal to the CMC value obtained when dissolving the PLGA in water-acetone mixture. Thus, the main difference was in the change in the

62

emission intensity, where a decrease in emission intensity was observed above the CMC

value when using chloroform.
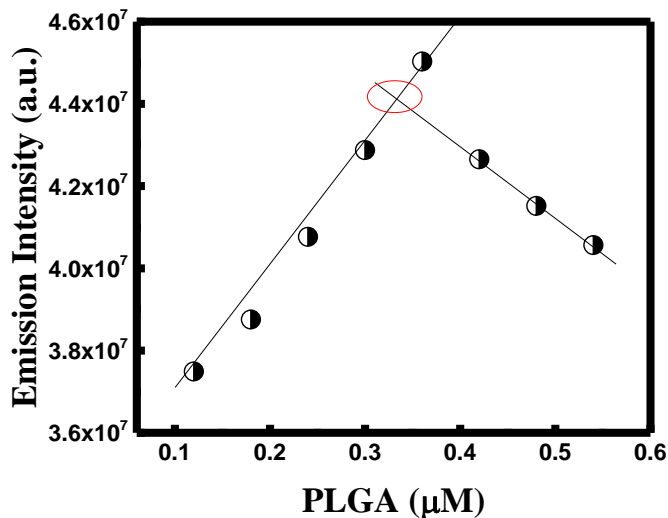
Figure 16 Fluorescence emission spectra of curcumin at different concentrations of
PLGA in the presence of chloroform

Indeed, as PLGA concentration increases a greater number of PLGA molecules

start coming together and bind to curcumin in solution. Such assembly process helps the

hydrophobic long chain group to associate with curcumin and improves its

fluorescence. And so, the fluorescence intensity continued to increase with the increase

of the polymer concentration until 0.33 g/L and start to decrease for $C > 0.33$ g/L. This

change in the emission intensity reveals that the assembly of PLGA ultimately creates

aggregation or a structure similar to reversed micelle. However, here we talk about an

aggregated form where the solvent enhances the formation of a reversed micelle,

meaning that the outside environment is highly hydrophobic, and the core is being

hydrophilic or less non-polar (See Figure 17A&B).
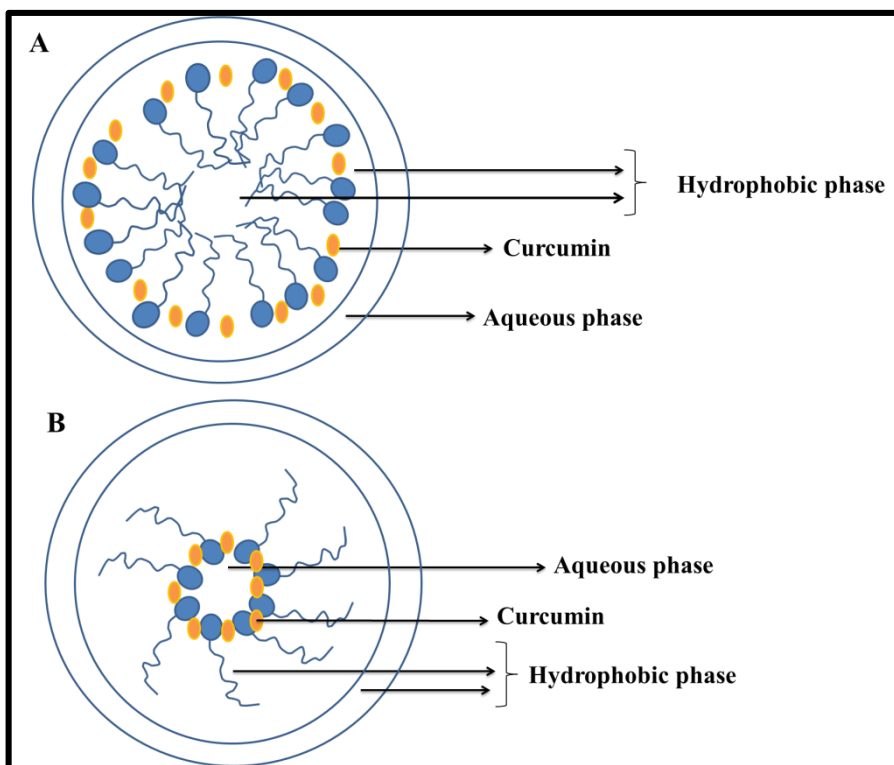
Figure 17 (A) normal structure of micelle and (B) reverse micelle structure.

In fact, due to the presence of phenolic and enolic groups in curcumin molecule, curcumin prefers an environment of a regular micelle (hydrophobic core). Hence, the increase in the hydrophilicity of the micelles core diminishes the fluorescence. This is due to the fact that the fluorescence of curcumin is decreased in polar medium compared to non-polar medium. Nonetheless, this kind of interaction is not observed in aqueous environment when water is used as a solvent for PLGA.

5. *Quenching study*

To gain an insight about the accessibility of curcumin into the PLGA micelle, fluorescence quenching experiments were conducted.

For this purpose, KI and CPB quenchers were used. In fact, CPB is a hydrophobic quencher, its ion (cetryl pyridinium ion (CPy+) is an electron acceptor which quenches the fluorescence of probe molecules by electron transfer mechanism [102]. Thus, KI is a hydrophilic quencher, due to its negatively I$^-$ that prefers to stay in the aqueous phase[100, 103].

Hence, the fluorescence intensity of curcumin was measured at different concentration of both quenchers. The fluorescence quenching of curcumin was measured using Stern-Volmer relationship under steady state conditions [104] :

$F_0/F = 1 + Ksv[Q]$

where I_0 and I are the fluorescent intensity in the absence and present of the quencher molecule, respectively, and Ksv is the Stern-Volmer quenching constant.

As shown, in Figure 18A&B the fluorescence intensity of curcumin decreases as the concentration of KI and CPB quenchers increases and the maximuim emission wavelength was almost unaltered. Actually, when using CPB, curcumin acts as an electron donor, where electron in the excited state is transferred from its aromatic ring to electron deficient N+-atom of CPB [104].
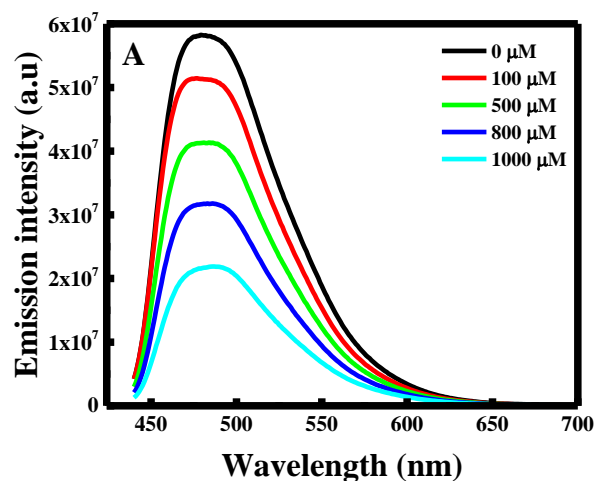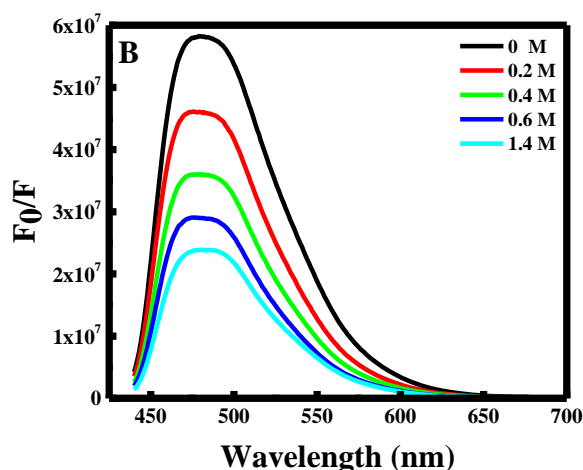
Figure 18 Fluorescence emission spectra of curcumin in PLGA polymer at (A) various CPB concentrations; (B) various KI concentrations

Therefore, the CPB tail intercalates into the hydrophobic part of PLGA micelles and remains at the Stern layer with its charged moiety exposed at the surface. Thus, if curcumin that is present in PLGA micelle is aligned parallel to the hydrophobic part of CPB, the interaction between curcumin and pyridinium ion will be favored. This is in agreement to what is reported earlier when curcumin is encapsulated in liposomes[105-106]. Hence, when the electron transfer process occurs, curcumin leaks the hydrophobic pocket of PLGA into the aqueous phase, thus leading to the decrease in the intensity of Curcumin.

Stern-volmer plots in the presence of CPB and KI are depicted in Figure 19 A&B respectively. The Stern-Volmer quenching constant of curcumin by CPB was found to be 0.00125 μM^{-1} and it is similar to the value obtained when curcumin is quenched by CPB in F108 polymers [100].
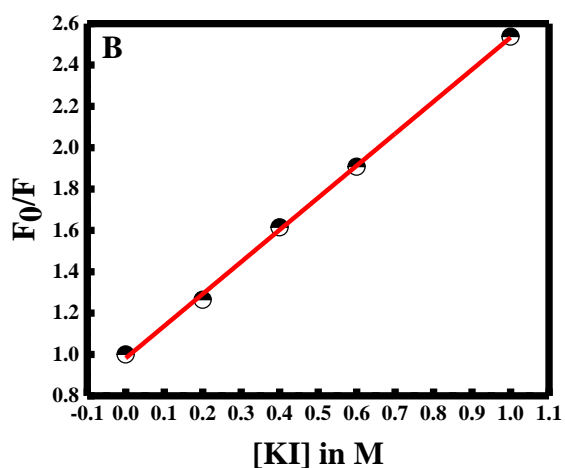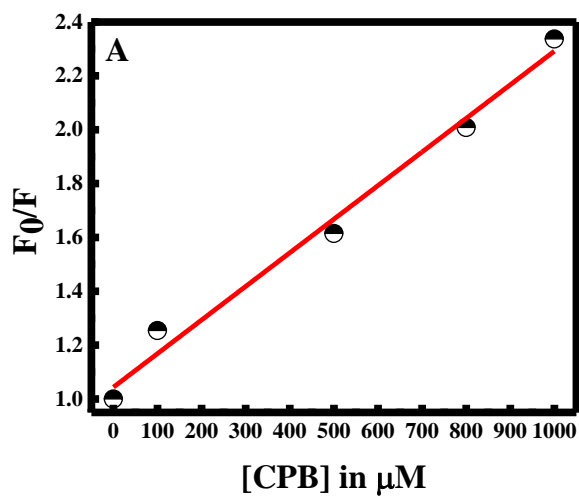
Figure 19 (A) Stern−Volmer plot at various concentrations of CPB; (B) Stern−Volmer plot at various concentrations of KI

Similarly, curcumin was quenched by KI, but the Stern-Volmer constant was equal to 1.55608×10^{-6} μM^{-1}, smaller than that of CPB. This interaction with iodide may results from the hydrogen bonding present between PLGA and Curcumin. Also, this interaction may be due to a reductive quenching where electron transfer from Iodide ion to the excited state of curcumin is taking place, thus forming radical anion.Therefore, curcumin encapsulated inside the PLGA micelle is greatly quenched by the hydrophobic

quencher CPB compared with the iodide quencher. This also confirms that curcumin is positioned in the hydrophobic pocket of the micelle at the stern layer (See Figure 20).
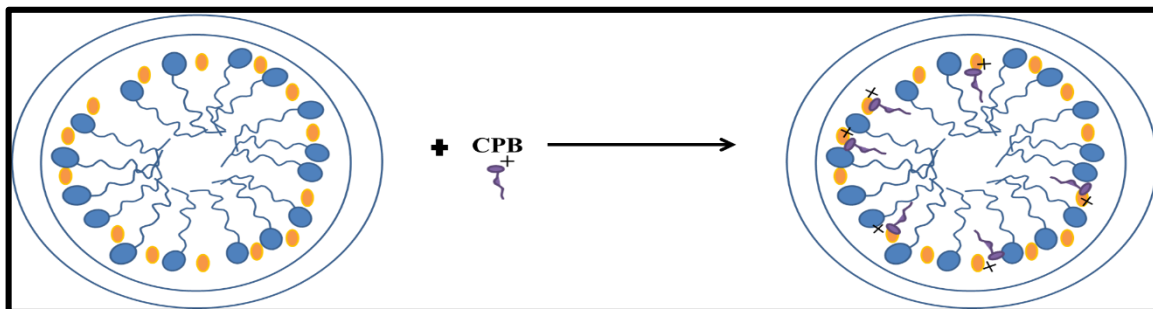
Figure 20 schematic representation of curcumin quenching in the presence of CPB.

D. Conclusion

To sum up, curcumin was utilized as a fluorescence probe to determine the CMC and CMT of PLGA, which were found to be 0.33 g/L and 25 °C, respectively. Curcumin was also used to study the effect of adding NaCl salt to the CMC value. It was found that the increase in NaCl concentrations reduced the CMC by around two folds from 0.25 to 0.14 g/L as the NaCl concentration reaches 150 mM. This is due to the salting out effect. The effect of solvent on the aggregation behavior of the PLGA polymer was studied using chloroform, it was found that the polymer aggregate at similar concentration as in acetone-water mixture. However, the main difference was in aggregation behavior where reverse micelles are obtained in chloroform instead of normal micelles. Finally, in order to determine the position of curcumin in PLGA micelles, fluorescence quenching experiment was conducted using two quenchers; KI and CPB. Based on the obtained results, it was concluded that curcumin is located near the hydrophobic pocket of Stern-layer of PLGA micelle.

CHAPTER V

CURCUMIN-PLGA BASED NANOCAPSULE FOR SPECTROSCOPIC DETECTION OF DOPAMINE

A. Introduction

The aim of nanocapsules formation is to ensure the entrapment of a specific drug into the membrane of phospholipids, or micelles. The drug encapsulation will help the drug to get through the exact target. Curcumin is being combined to nanomaterials to design effective nanosensors for the detection of specific analytes. For example, liposomal curcumin nanocapsules in the presence of PDDA polymer were used to detect ATP molecule [107]. In addition, a study conducted by Beshnak et al. has proven the efficiency of curcumin/F-108 polymeric nanocapsules in the detection of nucleic acid [108].

Many researches had been done on the incorporation of curcumin into PLGA based nanocapsules. Studies showed that PLGA- CUR nanocapsules have a spherical shape[109]. Hence, it was confirmed that the loading of curcumin in PLGA could increase the bioavailability of curcumin[110]. Due to the biodegradable nature of PLGA, it enhances the biocompatibility of curcumin[111]. Also, the solubility of curcumin is greatly enhanced upon encapsulation[111].The antioxidant properties do not alter with long term storage of PLGA- CUR nanocapsules[112].

Dopamine is a catecholamine neurotransmitter in nervous, cardiovascular and hormonal systems, plays an important role as an extracellular chemical messenger [113-114]. Many diseases result from disorder in the level of dopamine. Low level of dopamine causes sleeping disorders, schizophrenia, Huntington's and Parkinson's diseases [114].

Whereas, high dopamine level leads to cardiotoxicity which is accompanied with hypertension, drug addiction, increased heart rate and heart failure [115]. Developing techniques for the detection of dopamine play a significant role in increasing the efficiency of finding suitable treatments. Many methods have been developed for the determination of dopamine including surface plasmon resonance, fluorescence, chemiluminescence, photoelectrochemical sensor, high-performance, liquid chromatography, in addition to electrochemical methods [113, 116]. These methods suffer from low selectivity, the necessity of big amount of samples, long time manipulation, etc. For this reason, it was necessary to find a simple method to detect dopamine with high selectivity and sensitivity.

In this work, curcumin molecules were entrapped into PLGA polymer, and coated with poly diallyl dimethyl ammonium chloride (PDDA) polymer in order to increase its stability and bioactivity. Hence, the produced nanocapsules will be utilized as fluorescent probe for sensitive and selective detection of dopamine.

B. Methods of preparation

1. Sample preparation for dopamine detection

A stock solution of 10 mM of dopamine was prepared by dissolving 15.3 mg in 10 mL of double distilled water. Several solutions were prepared with concentrations in the range of 0 to 5 mM. As per investigating the interference, several concentrations of tryptophan, adenine, uracil, guanine, cytosine, melamine, glutathione, cystine, kreatinine, tyrosine, silymarin were measured at a concentration equal to 5 mM. All the experiments were done by keeping the concentration of PLGA-Cur-PDDA NCs constant in a total volume of 3 mL.

C. Results and Discussion

1. Characterization of PLGA CUR--PDDA NCs

Curcumin loaded PLGA nanocapsules were successfully synthesized by solid-in-oil-in water (s/o/w) emulsion technique. This method relays on the fact that the active ingredient (curcumin) is encapsulated as a solid and added to an oil phase (PLGA in chloroform), which formed a solid-oil dispersion. Therefore, in order to enhance the drug absorption, the dispersion is mixed with water to form a continuous phase [117]. In the beginning, the formed NCs were characterized using SEM and compared with free curcumin. As depicted in Figure 21A, the nanocapsules were present in spherical shape. However, CUR alone (aggregated solid form) has a rod-like structure (See Figure 21B). Thus the change in morphology from rod-like to spherical shape indicates and ensures the formation of nanocapsules.
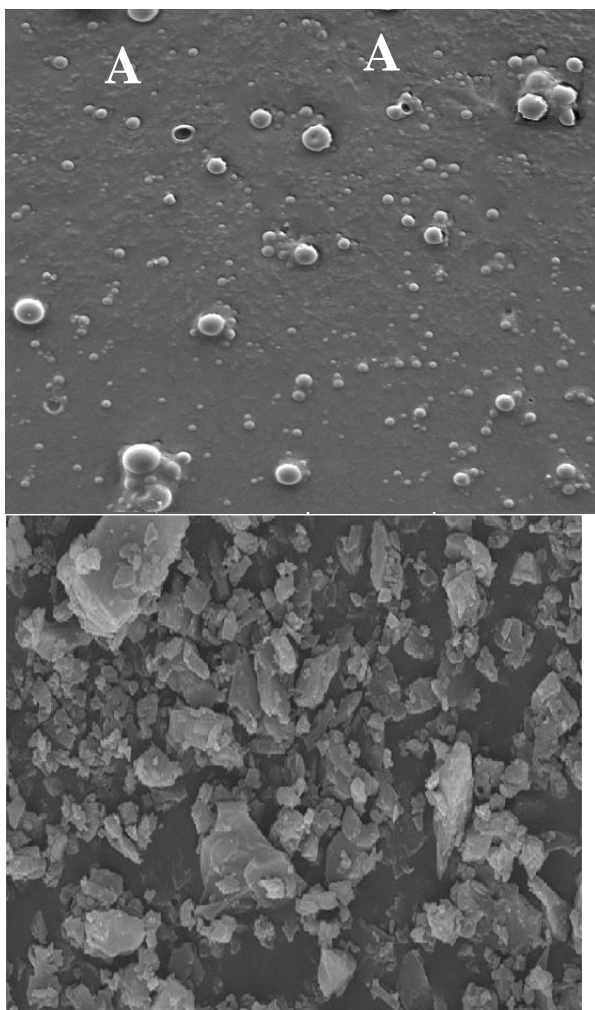
Figure 21 SEM image of (A) PLGA-CUR--PDDA NCs and (B) pure curcumin

Furthermore, the surface charge of PLGA- CUR-PDDA nanocapsule was investigated through zeta potential analysis. Interistingly, the formed nanocapsules were positively charged with a value equal to + 10.07 mV (See Figure 22). This is mainly due to the presence of ammonium NH4+ in the PDDA molecules which was adsorbed on the outer layer of the PLGA-CUR NCs causing their stabilization and thus leading to the production of positively charged PLGA- CUR-PDDA NCs.
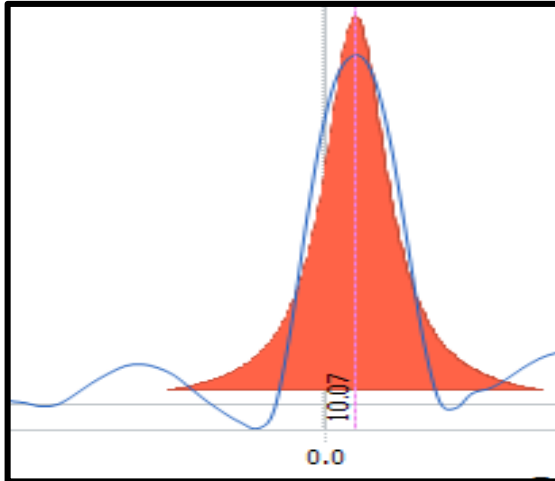
Figure 22 Zeta potential analysis of PLGA- CUR-PDDA NCs

Moreover, the UV-Visible spectrum was established for curcumin and the produced nanocapsules as shown in Figure 23. Curcumin absorbs prominently in the UV-visible region around 426 nm ($S_0{\rightarrow}S_1$ transition). However, absorption of PLGA-CUR-PDDA NCs appears at ~469 nm. Thus, the identification of absorption ~469 nm makes it easier for establishing the formation of PLGA- CUR-PDDA NCs in the solution. In addition, it is remarkable that a sharp and strong absorption peak was obtained for PLGA- CUR-PDDA NCs. Meaning that, all the curcumin was encapsulated into the core shell of the PLGA polymer, thereby the absence of free curcumin in the formed NCs.
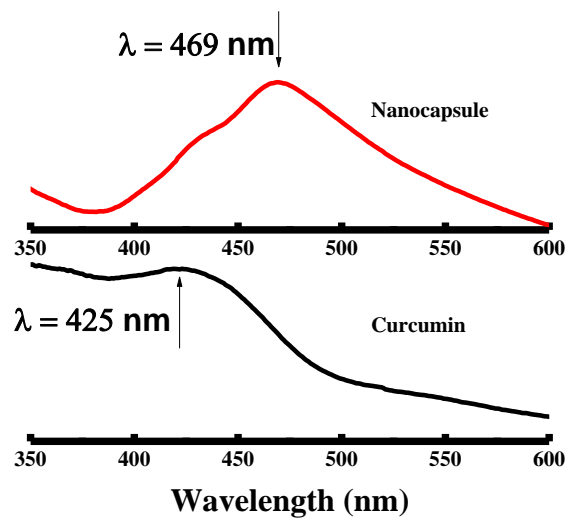
Figure 23 UV-Visible spectra of pure curcumin and PLGA-CUR-PDDA NCs

Furthermore, the successful production of nanocapsules was verified through the fluoresence emission spectra. As shown in Figure 24, a blue shift was occurred when curcumin is being entrapped in the core shell of the PLGA polymer. In fact, the nanocapsules emits at $\lambda= 510$ nm and NCs emits at $\lambda= 555$ nm. This shift is due to the incorporation of curcumin inside the PLGA forming smaller nanocapsules. Also, this can be related to the hydrophobic environment caused by the PLGA polymer. Is experiencing more non polar environment due to the hydrophobic part of plga oymer
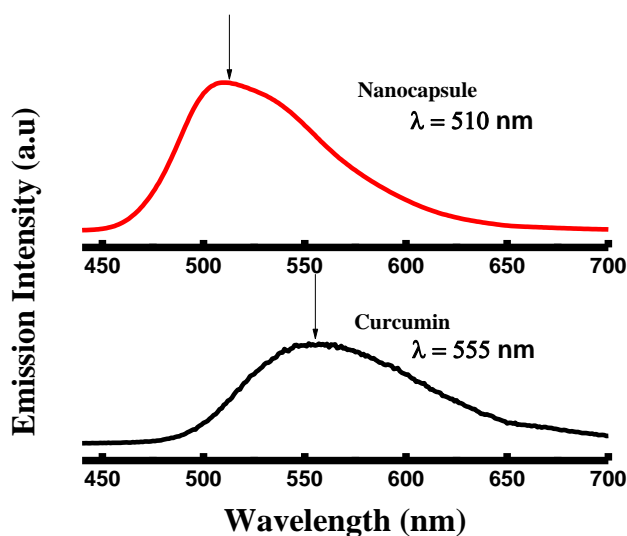
Figure 24 Fluorescence spectra of pure curcumin and PLGA- CUR-PDDA NCs.

To further establish the physical characteristic of the nanocapsules, PLGA-CUR-PDDA NCs and curcumin were analyzed by X-Ray Diffraction (XRD) technique. The diffractograms of curcumin and nanocapsules are illustrated in Figure 25. The main characteristic peaks of curcumin appeared at diffraction angles of 2Ө equal to 8.06°, 9.20°, 12.46°, 14.95°, 17.75°, 19.8°, 23.7°, 24.6°, and 26.5° revealing the crystalline form of curcmin [118]. Yet, as it is shown in the diffractogram of the nanocapsules, these peaks were completely absent. Hence, this confirms the encapsulation of curcumin inside the core shell of the PLGA polymer, inducing the formation of amorphous nanocapsules.
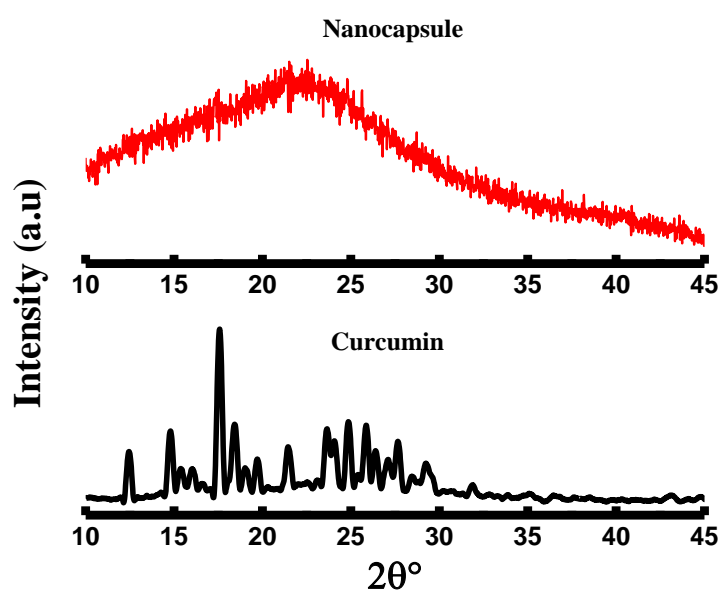
Figure 25 X-Ray diffractogram of pure curcumin and PLGA- CUR-PDDA NCs.

Finally, thermogravimetric analysis was performed to assess the stability of the prepared Nanocapsules. As shown in Figure 26, around 200°C the weight losss pattern of raw curcumin occurs, where it loses around 65 % of its mass between 200 and 560°C. Hence, a gradual decrease in the mass of curcumin was obtained within the increase of the temperature. Consequently, for PLGA- CUR-PDDA NCs no weight loss was observed around 100 °C, this assures that the synthesized NCs are dehydrated. However, the weight loss of PLGA- CUR-PDDA NCs was observed around 300°C, after which it shows a sharp weight loss that ends at ~400°C. In this temperature range, 86% weight loss was observed. This difference in the degradation pattern means that the temperature over which curcumin is stable has been increased. Therefore, curcumin gained extra stability when encapsulated inside the nanocapsules. Same degradation pattern of PLGA was obtained with Mathew et al. Accordingly, we can conclude that PLGA- CUR-PDDA NCs follows the same degradation pattern of PLGA.
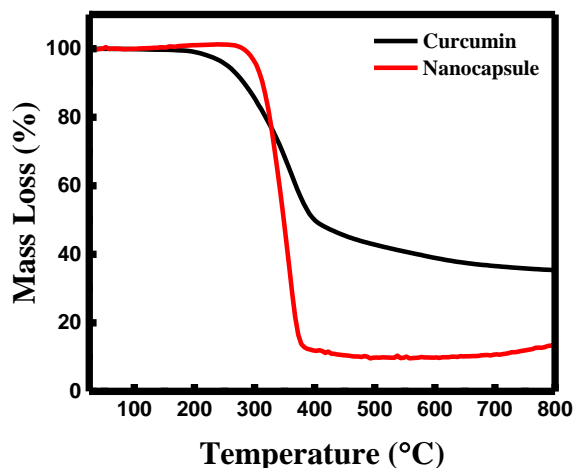
Figure 26 thermogravimetric analysis of pure curcumin and PLGA- CUR-PDDA NCs.

2. *Dopamine detection*

Nanomaterials are well recognized to own outstanding electrical, optical, thermal, catalytic properties and strong mechanical strength, which offer great chances to build nanomaterials-based probes [119]. Based on these facts, the formed PLGA- CUR-PDDA NCs were used as nanoprobe for the detection of dopamine.

First of all, PLGA- CUR-PDDA NCs were mixed with 1 mM of dopamine and the emission intensity of was measured. Interestingly, a remarkable decrease was noticed accompanied with a red shift (See Figure 27A). Based on this, several solutions were prepared with different dopamine's concentration in the range from 10 μM to 5 mM. As presented in Figure 27B, the emission intensity of the nanocapsules decreases within the increase in dopamine's concentration. However, at high concentration of dopamine, higher than 1 mM, a remarkable red shift occurred from 504 nm to 531 nm, meaning that curcumin is being presented in the polar region. Thus, when varying the concentration from 10-500 μM, the emission intensity decreases slightly. This decrease can be due to the binding of the negatively charged dopamine, to the positively charged

NCs. However, the enhancement of dopamine's concentration leads to an effective fluorescence quenching. Therefore, dopamine molecules are excluding curcumin from the core of the polymer to the aqueous solution.
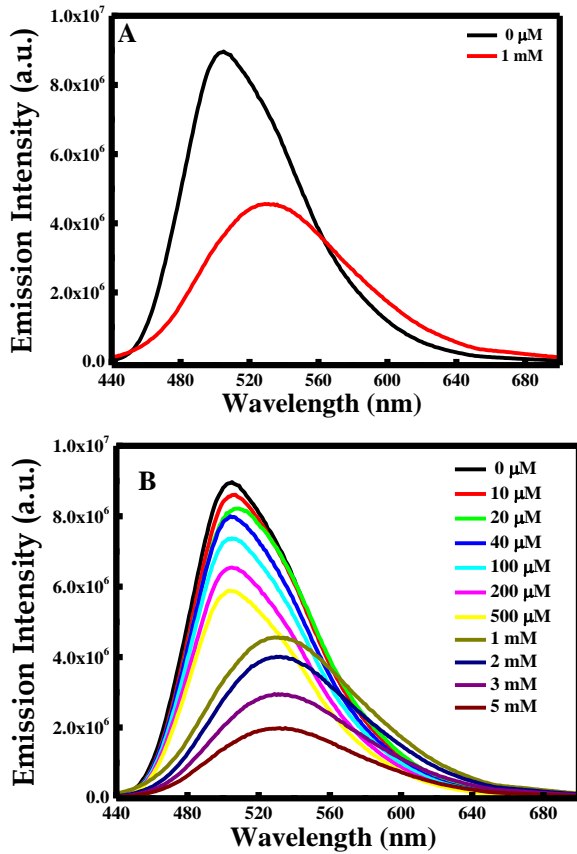
Figure 27 Emission intensity of PLGA- CUR-PDDA NCs in the presence of (A) 1 mM of dopamine and (B) several concentration of dopamine in the range of 10 μM to 5 mM.

During fluorescence intensity reduction, the quenching efficiency can be symbolized as $(I_0-I)/I_0$, where I_0 and I represent the fluorescence intensity of curcumin in the NCs in the absence and presence of dopamine. Hence, the Stern-Volmer quenching constant (K_{sv}) can be found using Stern-Volmer equation:

$I_0/I = K_{sv} \times C_{dopamine} + 1$

In this case, the plot between I_0/I and the concentration of dopamine showed a good linear relationship (with $R^2=0.9951$) in a wide concentration range from 0 to 5 mM (See Figure 28). Moreover, the Stern -Volmer equation can be fitted as: $I_0/I= 0.96441 \times C_{dopamine} +1$, while Ksv was found to be 0.96 mM^{-1}, equal to the slope value of the linear fit. Consequently, the Ksv value is considered large which confirms the binding between dopamine and curcumin.

Hence, the detection of dopamine was done in the range of 0.01 mM – 5 mM, with a limit of detection equal to 23 μM. The efficiency of the method was compared to previous study in the literature (See Table 5).
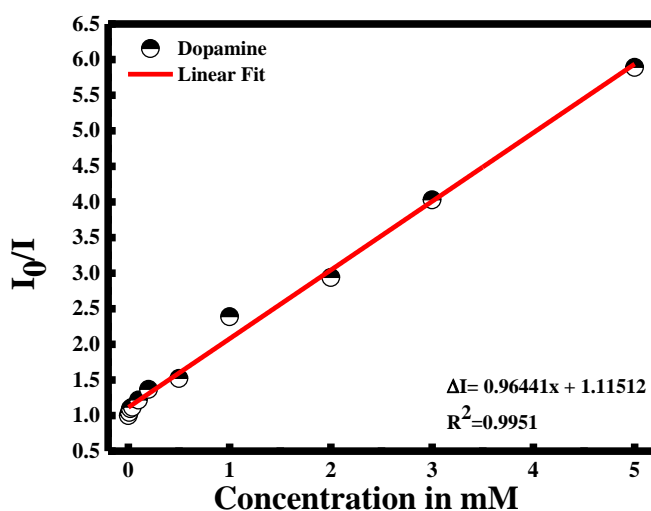
Figure 28 Linear correlation of I_0/I of PLGA- CUR-PDDA vs. concentration of dopamine.

Method used	Concentration range	LOD	Interference	Reference
FRET between acridine orange and CuO NPs	1-40 μM	40 nM	Ascorbic acid, uric acid, glucose, tryptophan and acetaminophen	[120]
A simple and convenient fluorescent strategy based on graphene quantum dots	0.5-120 μM	0.16 μM	NaCl, KCl, CaCl$_2$, glucose, cysteine, ascorbic acid, epinephrine	[121]
Calorimetric detection using microfluidic paper	0.5-4.75 μM	0.37 μM	Ascorbic acid, uric acid	[122]
Calorimetric detection using gold nanoparticles	0.5-10 μM	0.2 μM	Amino acids, glucose, ascorbic acid, uric acid	[122]
FRET between PLGA-Cur-PDDA	0.01-5 mM	23 μM	Tryptophan, adenine, uracil, guanine, cytosine, melamine, glutathione, cystine, Kreatinine, tyrosine, silymarin	Our work

Table 5 Method used to detect dopamine

To prove the efficiency and the role of the nanocapsule, a control experiment was handled in the presence of curcumin alone and dopamine in aqueous solution. Interestingly, I_0/I of curcumin remain constant in the presence of different dopamine's concentration (See Figure 29). These results reveal the role of the encapsulation of curcumin into the core of PLGA polymer in the presence of PDDA layer.
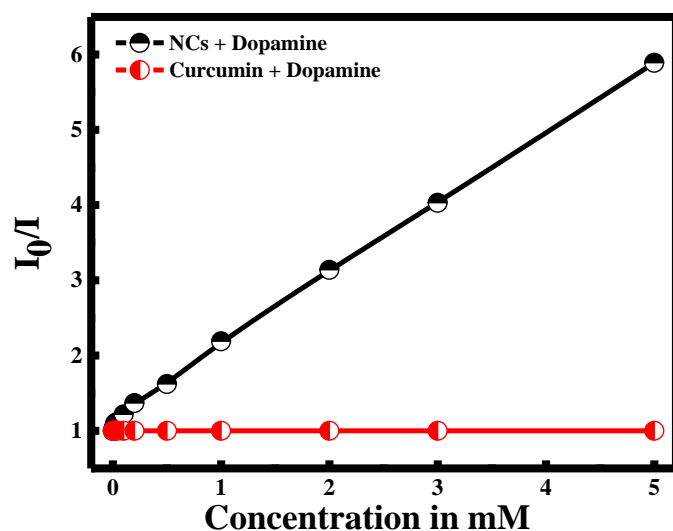
Figure 29 Selectivity of PLGA- CUR-PDDA NCs for the detection of dopamine compared to free curcumin.

Furthermore, the assessment of the selectivity and specificity of the PLGA-Cur-PDDA NCs toward dopamine detection was attained by measuring the fluorescence emission of the NCs in the presence of other interference molecules such as tryptophan, melamine, adenine, etc. These molecules were selected because they own comparable structures to that of dopamine, so they can typically interfere in dopamine detection. Thus, in Figure 30 it is obvious that increasing the concentration of the different molecules had no significant change in the fluorescence signal of the nanocapsules. These results confirm the strong quenching between dopamine and curcumin in the nanocapsules.
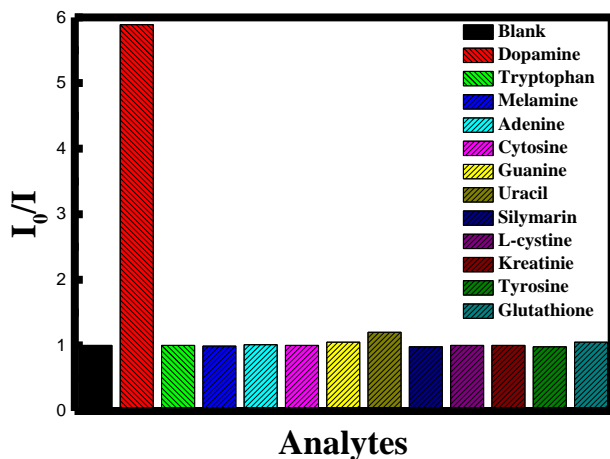
Figure 30 Ratio of emission intensity (I/I_0) of PLGA- CUR-PDDA NCs for different species.

Moreover, the stability of the proposed system was done by measuring the fluorescence emission intensity within 1 hour in the presence and absence of dopamine. Hence, within 1 hour I_0/I remain constant revealing the stability of the proposed nanoprobe in the detection of dopamine (See Figure 31).
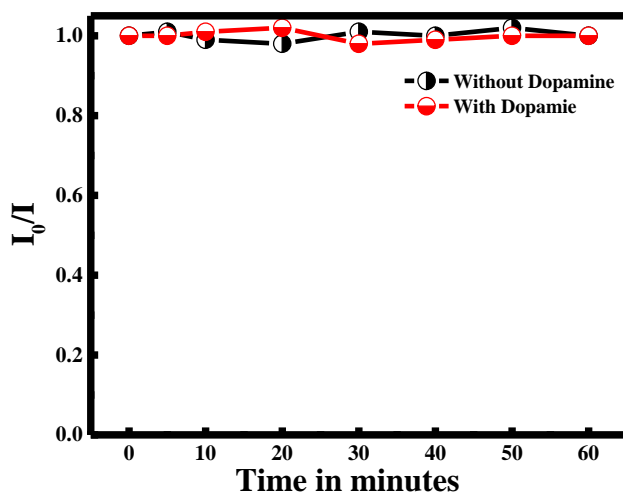
Figure 31 Plot of I/I_0 of PLGA- CUR-PDDA with time in the absence and presence of dopamine.

Finally, to test the applicability, the analytical recovery of three unknown samples was estimated by using the obtained fitted calibration curve. The obtained

results where summarized in Table 6. The percent of recovery of dopamine was obtained to be between 98.75 and 100.5 % (n=3).

	Theoretical concentration (mM)	Experimental concentration (mM)	Recovery (%)
Sample 1	0.03	0.0298	99.3
Sample 2	0.4	0.402	100.5
Sample 3	4	3.95	98.75

Table 6 Recovery percentage of the proposed method

D. Conclusion

In Summary, curcumin loaded PLGA nanocapsules were successfully coated by poly(diallyldimethylammonium)chloride (PDDA) polymer . The formed PLGA-Cur-PDDA NCs were used to develop a new nanosensing scheme for determination of dopamine. The binding constant was estimated using the stern-volmer equation to be around 0.96 mM. This value confirms the binding between dopamine and Curcumin, releaving the efficiency of the nanocapsule as nanoprobe to detect dopamine. Based on this method, no interference from other biological and chemical analogues was observed, confirming the selectivity of the proposed nanoprobe. Finally, the method gave a detection limit of 23 μM and works well in the concentration range up to 5 mM.

CHAPTER VI

ASSESS ANTIVIRAL POTENTIAL OF CURCUMIN NANOPARTICLES AGAINST INFLUENZA A INFECTION

A. Introduction

The advancement in nanotechnology has enabled the formulation of nanoparticles, and polymeric nanoparticles that can be utilized to encapsulate Curcumin[123]. This could overcome its limitation by improving its sustained release to target diseased cells, enhancing its bioavailability, avoiding it from degradation or metabolism, and increasing its therapeutic potential[124]. Polymeric nanoparticles are biocompatible and biodegradable and have been established as drug delivery vehicle and have important properties like better encapsulation of compounds to protect and deliver them efficiently [125]. One of the used polymer is Poly lactic-*co*-glycolic acid (PLGA).

In fact, Influenza A virus (IAV) is a major human respiratory pathogen causing annual epidemics as well as periodic pandemics[126]. Several medicines were synthesized to diminish the effect of IAV such as amantadine, oseltamivir, and zanamivir. Hence, these drugs are known to have several and severe side effect. Consequently, it was necessary to find an agent that quashes its ability to replicate and, henceforth, hinders its ability to proliferate with minimal side effects.

Curcumin has showed an exceptional antiviral activity against several deseases[53]. For this reason, curcumin was selected as a safer drug against Influenza A

virus. Hence, curcumin was encapsulated in the core of PLGA polymer and its antiviral activity was evaluated against IAV.

B. Material and Methods

1. Drug loading and encapsulation efficiency

After centrifugation, the absorbance of the obtained supernatant was measured using UV-Vis spectrophotometry at $\lambda = 428$ nm. The % encapsulation efficiency was calculated using the following formula[127]:

$$\% \text{ EE} = \frac{total\ mass\ of\ used\ curcumin - mass\ of\ free\ curcumin\ in\ supernatant}{total\ mass\ of\ used\ curcumin} \times 100$$

For the drug loading, the mass of the dried nanocapsules was measured after freeze drying the washed precipitate 24 hours and. The % Drug loading (DL) was calculated based on the following formula[127]:

$$\% \text{ DL} = \frac{total\ mass\ of\ entapped\ curcumin}{mass\ of\ obtained\ nanoparticles} \times 100$$

Finally, the % yield of the synthesized nanocapsules was calculated by the formula:

$$\% \text{ yield} = \frac{mass\ of\ obtained\ nanoparticles}{mass\ of\ curcumin + mass\ of\ PLGA\ used\ for\ the\ synthesis\ of\ NPs} \times 100$$

2. Culture of Influenza A virus cells

Madin-Darby canine kidney (MDCK, ATCC) and human lung adenocarcinoma epithelial cell line (A549, ATCC) were cultured in Dulbecco's Modified Eagle's Medium-high glucose supplemented with 10% fetal bovine serum (FBS) and 5% of 100 U/ml penicillin-streptomycin and maintained in 5% CO_2 at 37°C.

3. Cytotoxicity study by MTT Assay

To study the antiviral activity of Curcumin loaded into PLGA nanocapsules, small amounts of the latter have to be examined for cytotoxicity. For this purpose, the effect of C_6-ceramide and the drugs used to inhibit ceramide biosynthesis on the viability of A549 cells were assessed using the 3-(4,5-Dimethylthiazol-2-yl)-2,5-diphenyltetrazolium (MTT) assay. Briefly, A549 cells were treated with increasing concentrations of the nanocapsules (10, 16, 20, and 40 µM). All the cells were cultured in 96-well culture plates at a density of 2×10^4 cells/well. These Cells were treated with FB (50 µM) and/or Myr (0.1 µM) or with increasing concentrations of C_6-ceramide (10, 20, and 30 µM). After incubation (48 hrs), 20 µl of MTT reagent was added to each well and incubated for 2 h at 37°C. Then, the supernatant was eliminated and the purple formazan crystals obtained by the reduction of MTT by the viable cells were solubilized using 100 µl of isopropanol. Finally, the absorbance was recorded using spectrophotometer at a wavelength of 595 nm (259).

4. Plaque Reduction for virus titration

Virus titers were established using plaque assay in MDCK cells, as previously described[126]. Briefly, 10-fold serial dilutions of the virus were prepared. The homogeneously confluent monolayers of MDCK cells, seeded at 7×10^5 cells per well in 6-well tissue culture plates, were washed twice with PBS++ in the next day. Then, 10-fold serial dilutions of the virus were prepared. Each well were infected with 200 µl of the virus and incubated at 37°C for 1 h, with tender shaking every 15 min. Then, the virus was detached by aspirator, and the monolayers were shielded with a nutritive medium containing 0.5% of freshly prepared agarose and 1 µg/ml TPCK-trypsin. The

nutritive overlay was composed of VIM prepared at double concentration (2x) to which an equal volume of 1% agarose was added. The agarose was dissolved by heating in the microwave, cooled, then both agarose and 1 µg/ml TPCK-trypsin were added to the 2x media. After incubating the dishes at 37°C for 72 h, the agar overlay was removed, and the cells were stained with crystal violet solution. Finally, the plaques were counted.

C. Results and Discussion

1. Encapsulation efficiency and drug loading of PLGA- CUR-NCs

The absorbance of the decanted supernatent obtained after the centrifugation step in the synthesis of the nanocapsules was measured . Then, the mass of free curcumin was calculated. The %EE of synthesized nanoparticle was 90.21%. This encapsulation effeciency is considered high and compatible with other value found in the literature[128-129]. This result in such drug carrier particles can lead to a stronger therapeutic effect along with reduced side effect[130]. One of the important properties in nanomedicine is % DL of the entrapped drug which is curcumin in this case. The calculated %DL was 24.4%. Regarding the % yeild, it was found to be 40.04%.

2. MTT assay and Plaque reduction results

The MTT assay is a colorimetric assay used to measure cellular metabolic activity as an indicator of cell viability, proliferation and cytotoxicity. It is based on the ability of nicotinamide adenine dinucleotide phosphate (NADPH)-dependent cellular oxidoreductase enzymes to reduce the tetrazolium dye MTT to its insoluble formazan[131].

Thus MTT reflects the number of viable cells. Cytotoxicity assessments preceding the performance of antiviral evaluations are indispensable to determine the concentration limits to be used in the next step, that a useful substance should exhibit minimal toxicity against the host[132].

As shown in Figure 32, MTT result showed that up to a concentration of 20 µM of the Curcumin nanoparticles is well tolerated by A549 cells with cell death< 20 %.
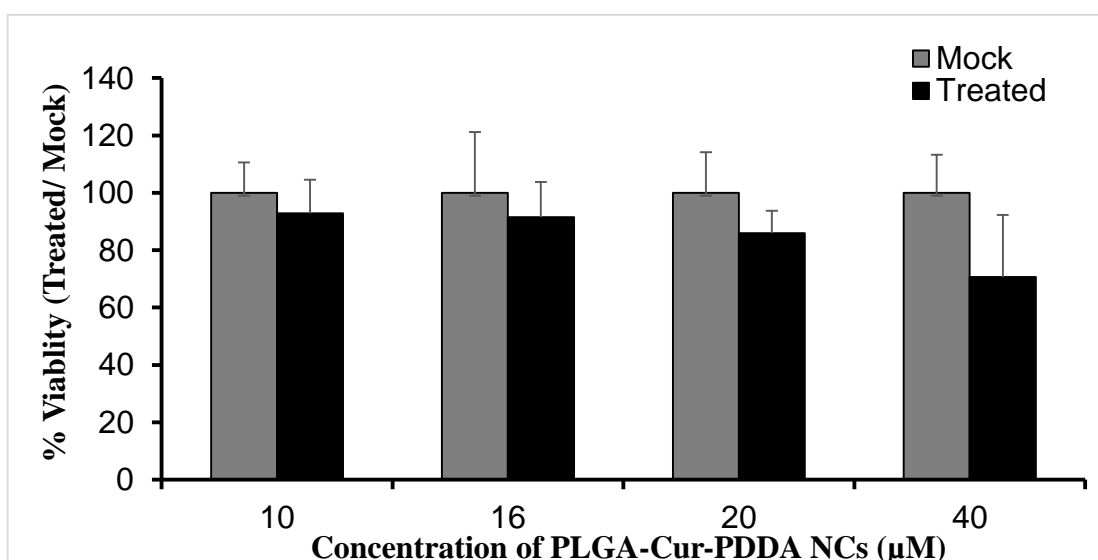
Figure 32 MTT assays of PLGA-Cur-PDDA NCs towards A549 cells

The antiviral activity against influenza A virus propagated in the A549 cell culture was evaluated through the use of plaque reduction assay. The concentrations of drug that reduce the number of virus-infected cells by 50% (EC50) was evaluated by using plaque reduction assay. Based on the results summarized in Figure 33, the EC50 is estimated to be 10 nM.
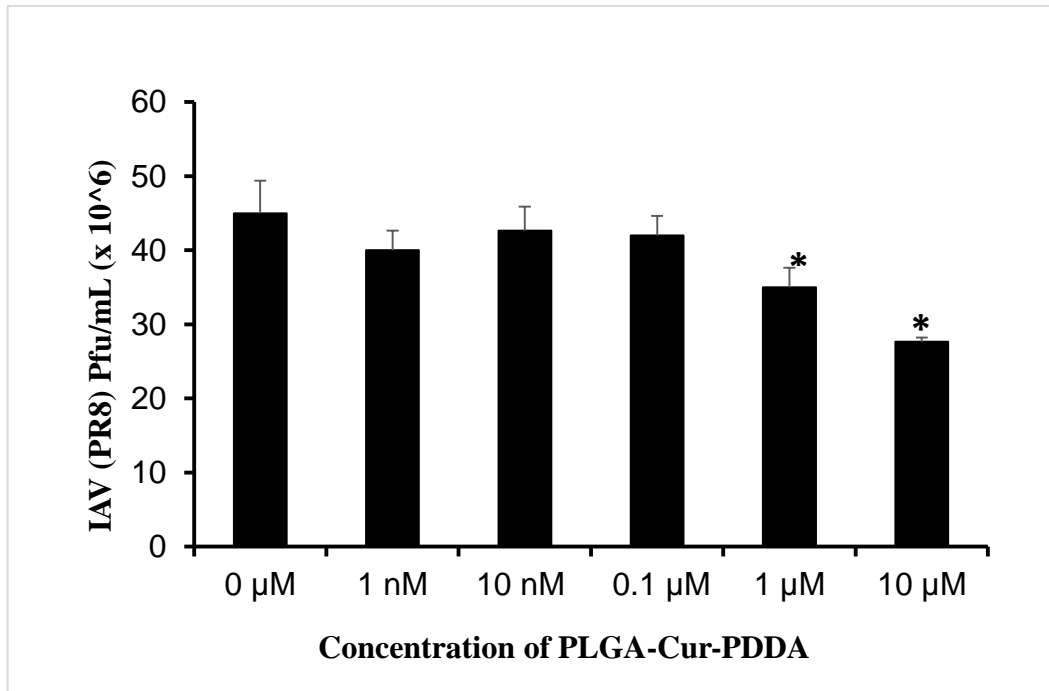
Figure 33 Plaque reduction of PLGA-Cur-PDDA NCs towards A549 cells

Treating infected PR8 cells with 10 µM curcumin nanoparticles lead to a reduction in the plaque size compared to infected non-treated PR8 cells as shown in Figure 34. This can be related to several reasons including Mutations in NA, low fitness clones, slower rate of increase during many cycles of infection, the slow increase could be accounted for by a delay in the formation of infectious virus in each cycle accompanied by a simultaneous delay in release, or retarded growth might be related to faulty assembly because of incompatibility of virus antigens.
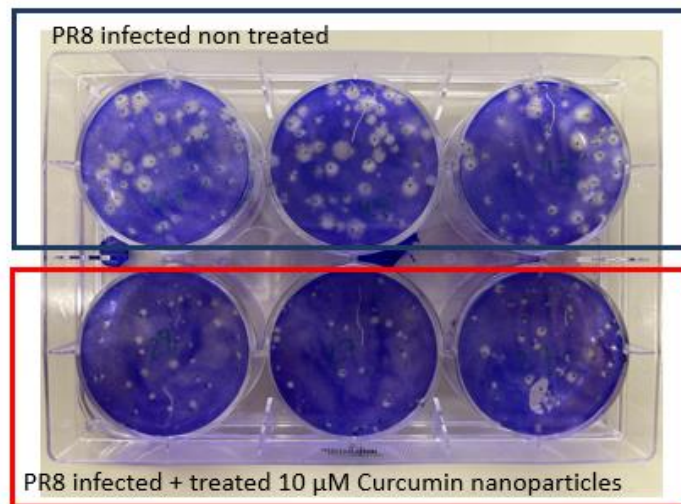
Figure 34 Microscopic study of PR8 infected non-treated and PR8 infected treated

D. Conclusion

In Summary, Curcumin was successfully encapsulated inside PLGA nanocapsules. The antiviral activity of Curcumin was examined against the influenza A virus. MTT results showed that Curcumin nanocapsules is well tolerated by A549 cells with cell death< 20 % up to a concentration of 20 μM. Results of plaque reduction assay showed that a reduction in the plaque size was obtained upon treating infected PR8 cells with 10 μM of Nanocapsules. Furthermore, the EC50 was estimated to be 20 μM.

CHAPTER VII

EFFECT OF pH AND ADDITION OF MULTILAYERS ON THE DRUG RELEASE OF CURCUMIN LOADED PLGA NANOCAPSULES

A. Introduction

As nanotechnology has been developed, nano-drug delivery systems has been utilized in biomedical applications, including anti-inflammatory, antibacterial, anti-cancer, and antioxidant applications[133].

In fact, nanoparticles drug delivery systems tend to be very useful for the reason of their drug controlled release, their higher intracellular uptake, their capability in enhancing the stability of active ingredients, and their ability to target specific sites[134-135]. Additional advantages are accompanied with these systems including their high encapsulation efficiency, small polymer content, protection of drugs from degradation factors such as pH and light[135]. Nanotechnology-based drug delivery systems have the prospective to improve the efficacy of poorly soluble drugs for systemic delivery[136]. Indeed, since the latter half of twentieth century, controlled drug release is one of the most looked properties, that the scientific community has been endeavor for [137].

In recent years, polymeric nanocapsules have gained great interest in drug delivery applications, owing their unique core-shell microstructure[138]. Actually, the encapsulation of drug inside the polymeric shell protect the drug from degradation or burst release prompted by the temperature change, pH variations, enzymes, etc[138]. Certainly, polyethylene glycol (PEG), poly(D,L-lactide) (PLA), poly(D,L-glycolide) (PLG), and their copolymers poly(lactide-co-glycolide) (PLGA) are among the most used biodegradable polymers for the synthesis of nanocapsules[139].

Above all, PLGA has been broadly considered for the development of devices for controlled delivery of small molecule drugs, proteins, and further macromolecules in research [67, 140].

For this purpose, several curcumin polymeric nanocapsules using PLGA polymers were prepared and established as a drug carrier for curcumin release.

B. Material and Methods

1. Preparation of PLGA-Curcumin nanocapsules

PLGA-Cur nanocapsules were prepared using solid-in-oil-in water (s/o/w) emulsion technique[141]. Breifly, in 1.5 mL chloroform, 45 mg of PLGA were socked for 24 hours. Then, 5 mg of curcumin was added to the obtained mixture and sonicated for 1 minute using probe sonicator. The obtained emulsion was added to 20 mL of polydiallyldimethylammonium chloride (1% w/v) and the mixture was sonicated for 2 minutes. In a later step, the solution was stirred for 3 hours at 5000 rpm in order to evaporate the chloroform. Finally, the solution was centrifuged at 15 000 rpm and the precipitate was washed twice with 10 mL of double distilled water (DDW) and then dissolved in 20 mL of DDW for final use. Hence, the precipitate containing the NCs was labeled in this case N1 (PLGA-Cur-PDDA).

On the other hand, other NCs were prepared with the incorporation of the silica nanoparticles between two layers of PDDA polymer. For this, 10 mL of LUDOX silica nanoparticles (2%) was added to 10 mL of the N1 NCs solution followed by 30 seconds sonication. Then the obtained mixture was added to 10 mL PDDA (1% w/v) and sonicated again for 30 seconds. Similarly, the solution was stirred and centrifuged at 15 000 rpm, and the precipitate was dissolved in 20 mL of DDW for final use. In this case,

the formed nanocapsules (N2) were consisted of one-layer PLGA, one-layer SiO_2 NPs and 2 PDDA layers (PLGA-Cur-PDDA-SiO_2NPs-PDDA).

Lastly, to prove the efficiency of the cumulative layers, another layer of SiO_2 NPs and PDDA were added. Certainly, to incorporate an additional silica layer, 10 mL of N2 solution was taken and mixed with 10 mL of LUDOX silica nanoparticles (2%), followed by 30 seconds sonication, and finally mixed with 10 mL PDDA (1% w/v) and sonicated again for 30 seconds. Similarly, the solution was stirred and centrifuged at 15 000 rpm, and the precipitate was dissolved in 20 mL of DDW for final use. In this case the obtained nanocapsules (N3) were formed as follow; PLGA-Cur-PDDA-SiO_2NPs-PDDA-SiO_2NPs-PDDA.

2. *Drug loading and encapsulation efficiency*

After centrifugation, the supernatant was collected, and its absorbance was measured using UV-Vis spectrophotometry at $\lambda = 428$ nm. The % encapsulation efficiency was calculated using the following formula[127]:

$$\% \text{ EE} = \frac{total\ mass\ of\ used\ curcumin - mass\ of\ free\ curcumin\ in\ supernatant}{total\ mass\ of\ used\ curcumin} \times 100$$

For the drug loading, the precipitate was freeze dried for 24 hours and the mass of the dried nanocapsules was measured. The % Drug loading (DL) was calculated based on the following formula[127]:

$$\% \text{ DL} = \frac{total\ mass\ of\ entapped\ curcumin}{mass\ of\ obtained\ nanoparticles} \times 100$$

C. Results and discussion

1. *Characterization of the synthesized nanocapsules*

Based on the technique used, primary reactant, surface modifications, etc., the nanocapsules can be produced either in different shapes, either in different sizes [140]. As described in section II.2, three different cases of nanocapsules were prepared by modifying their surface. In the 3 cases, the same concentration of curcumin and PLGA polymer was used. The main difference was the increase in the external layer of silica nanoparticles and PDDA polymer. Remarkably, the increase of layers number induces the color change of the NCs, where it turned from pale yellow to dark yellow (See Figure 35A-C).
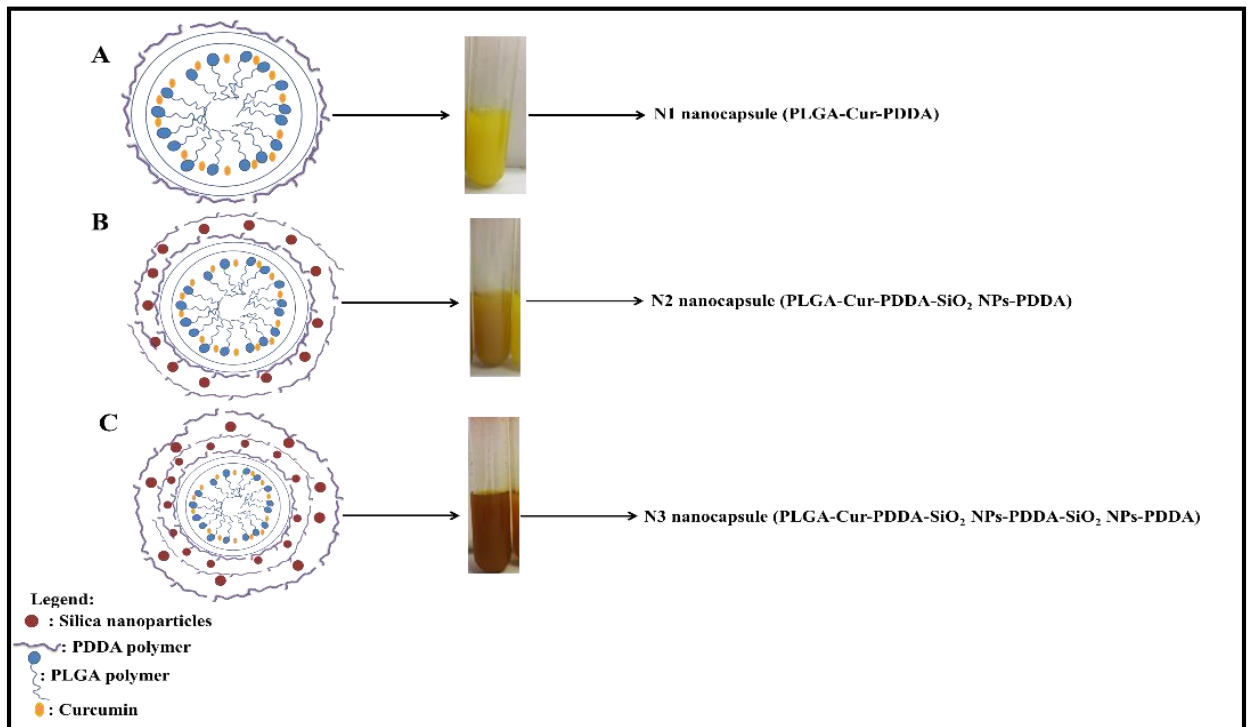
Figure 35 Preparation of three different nanocapsules (A) N1 nanocapsule (PLGA-Cur-PDDA); (B) N2 nanocapsule (PLGA-Cur-PDDA-SiO$_2$ NPs-PDDA); (C) N3 nanocapsule (PLGA-Cur-PDDA-SiO$_2$ NPs-PDDA-SiO$_2$ NPs-PDDA)

To check the difference between the 3 nanocapsules, scanning electron microscopy (SEM) was conducted in the first place. As shown in Figure 36A-C, the NCs were obtained in a spherical shape. Hence, the main difference was observed in the size where the size of the NCs decreases from 200 nm for N1 nanocapsules, to 100 nm for N2 nanocapsules to have at the end 50 nm NCs for N3. In fact, the enhancement of the additive layer boosts the formation of smaller and more uniform NCs. Indeed, the addition of layers on the surface tends to force the dispersion of curcumin molecules into the core of the nanocapsules and thus leading to the formation of smaller nanoparticles.
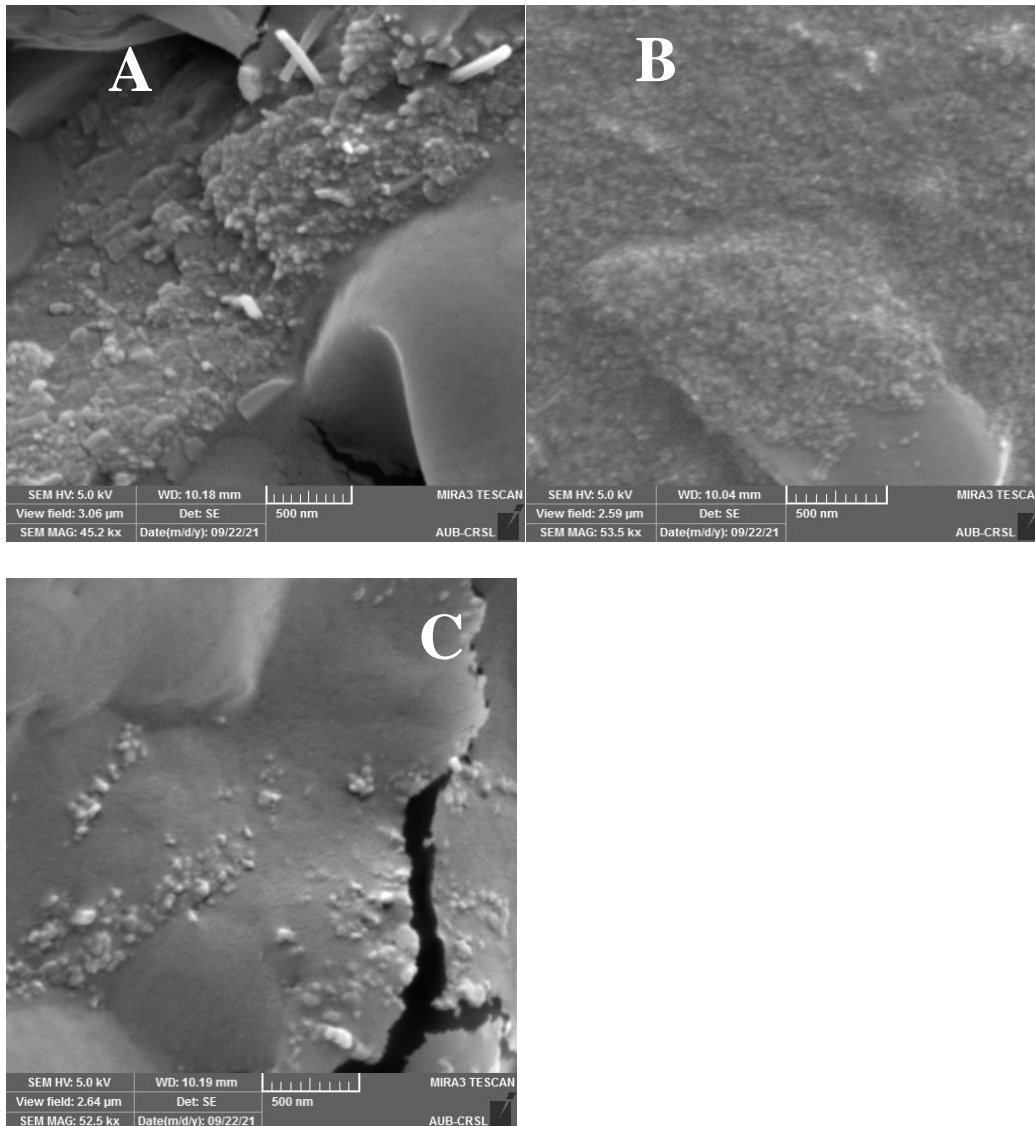
Figure 36 SEM images for the different polymeric nanocapsules (A) N1 nanocapsule (PLGA-Cur-PDDA); (B) N2 nanocapsule (PLGA-Cur-PDDA-SiO$_2$ NPs-PDDA); (C) N3 nanocapsule (PLGA-Cur-PDDA-SiO$_2$ NPs-PDDA-SiO$_2$ NPs-PDDA)

Furthermore, the deposition of SiO$_2$ NPs layer was confirmed by applying EDX analysis. Hence, the EDX spectrum had proved the presence of silica and oxygen as expected, revealing the presence of SiO$_2$ NPs (See Figure 37).
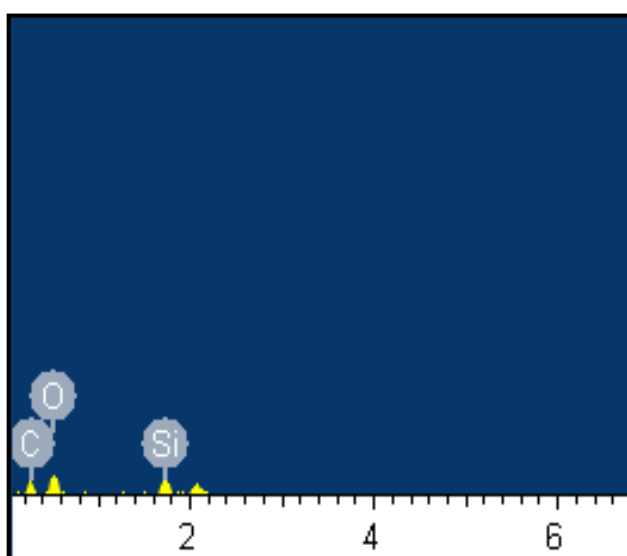
Figure 37 EDX analysis for N2 and N3 nanocapsule.

Besides, Dynamic Light Scattering (DLS) was used to analyze the size of the prepared nanocapsules. For this purpose, the three samples were diluted and sonicated to minimize the aggregations resulted from the presence of polymers. As shown in Figure 38A-C, the nanocapsules size was between 200 nm - 500 nm for N1 NCs, between 100 nm – 300 nm for N2 NCs and between 50 nm – 150 nm for N3 NCs.
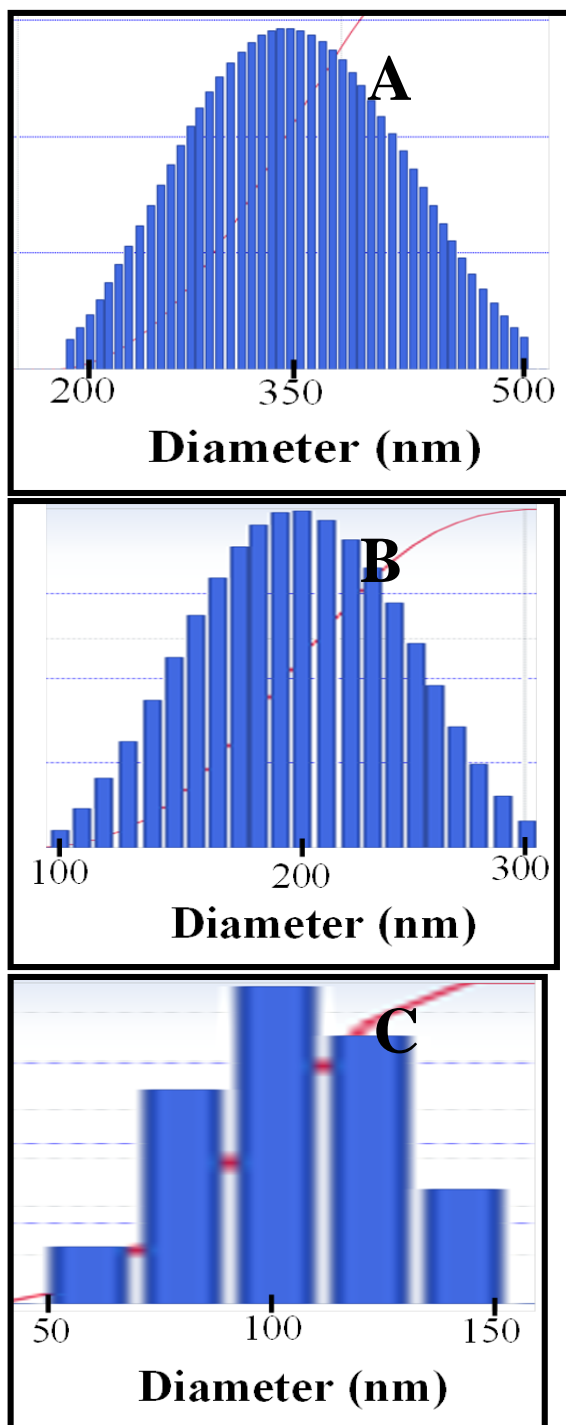
Figure 38 Dynamic light scattering analysis for the different polymeric nanocapsules (A) N1 nanocapsule (PLGA-Cur-PDDA); (B) N2 nanocapsule (PLGA-Cur-PDDA-SiO$_2$ NPs-PDDA); (C) N3 nanocapsule (PLGA-Cur-PDDA-SiO$_2$ NPs-PDDA-SiO$_2$ NPs-PDDA).

Moreover, to examine the crystallinity of encapsulated curcumin in the three different nanocapsules, X-ray diffraction (XRD) was performed. The diffractograms of

free curcumin, N1, N2 and N3 nanocapsules are illustrated in Figure 39. The main characteristic peaks of curcumin appeared at diffraction angles of 2θ equal to 8.06°, 9.20°, 12.46°, 14.95°, 17.75°, 19.8°, 23.7°, 24.6°, and 26.5 ° revealing the crystalline form of curcmin[142]. However, as it is revealed in the diffractogram of N1 nanocapsule, a broad peak was obtained at 2θ equal to 22.5°, where the others peak were absent. This shift in the peak, and the disappearance of most of curcumin peaks reveals the encapsulation of curcumin into the core of PLGA polymer and thereby the diminishment of curcumin's crystallinity. Otherwise, for N2 and N3 nanocapsules, the XRD diffractograms showed a complete amorphous structure, proving the total encapsulation of curcumin into the PLGA polymer, boosted by the SiO_2 NPs and PDDA layers.

Figure 39 XRD Patterns and of for pure curcumin; N1 nanocapsule (PLGA-Cur-PDDA); N2 nanocapsule (PLGA-Cur-PDDA-SiO_2 NPs-PDDA); N3 nanocapsule (PLGA-Cur-PDDA-SiO_2 NPs-PDDA-SiO_2 NPs-PDDA).

Furthermore, to study the thermal stability of the prepared nanocapsules, Thermogravimetric Analysis (TGA) was performed for pure curcumin, and the three nanocapsules. Hence, the results are depicted in Figure 40. In fact, pure curcumin shows thermal decomposition between $240°C–560°C$[143], where it loses around 70% of its total mass. Hence, same thermal decomposition was obtained for N1, N2 and N3 except that the encapsulation of curcumin into PLGA polymer increases its stability. Hence, for PLGA-Cur NCs (N1) the weight loss of curcumin was around 55% of its total curcumin mass. Thus, as for N2 and N3 the thermal stability increased remarkably where the weight loss obtained was around 25% and 10% respectively. Meaning that, SiO_2 NPs and PDDA layers, act as protective layers ensuring thereby the total entrapment of curcumin in the core of PLGA polymer. Interestingly, no mass loss was occurred below $100°C$, revealing that the NCs dried were dehydrated.
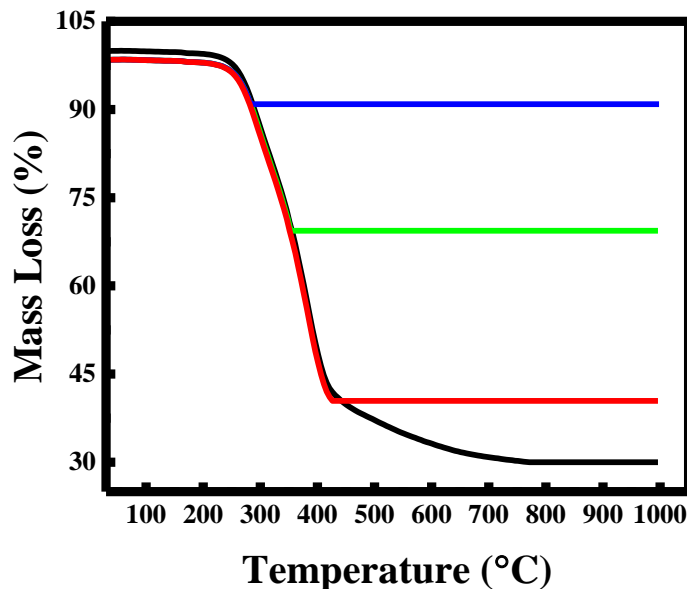
Figure 40 thermogravimetric analysis of for pure curcumin; N1 nanocapsule (PLGA-Cur-PDDA); N2 nanocapsule (PLGA-Cur-PDDA-SiO_2 NPs-PDDA); (C) N3 nanocapsule (PLGA-Cur-PDDA-SiO_2 NPs-PDDA-SiO_2 NPs-PDDA).

2. Spectroscopic analysis for N1, N2 and N3 nanocapsules

The fluorescence emission spectra were measured for curcumin, N1, N2, and N3 nanocapsules at two excitation wavelengths; 425 nm (for enol form of curcumin) and 350 nm (for enol form of curcumin)[144], in the emission range between 440 nm - 740 nm and 370 nm – 600 nm respectively (See Figure 41A&B). The emission intensity of curcumin dissolved in methanol exhibited a major peak at $\lambda = \sim$550 nm at both excitation wavelengths $\lambda_{ex} = 425$ nm and $\lambda_{ex} = 350$ nm. Hence, for both excitation wavelengths, a blue shift was occurred when curcumin is being entrapped in the core shell of the PLGA polymer.
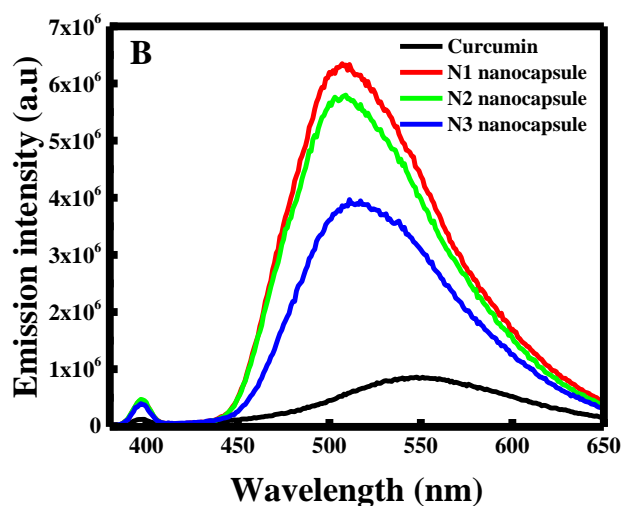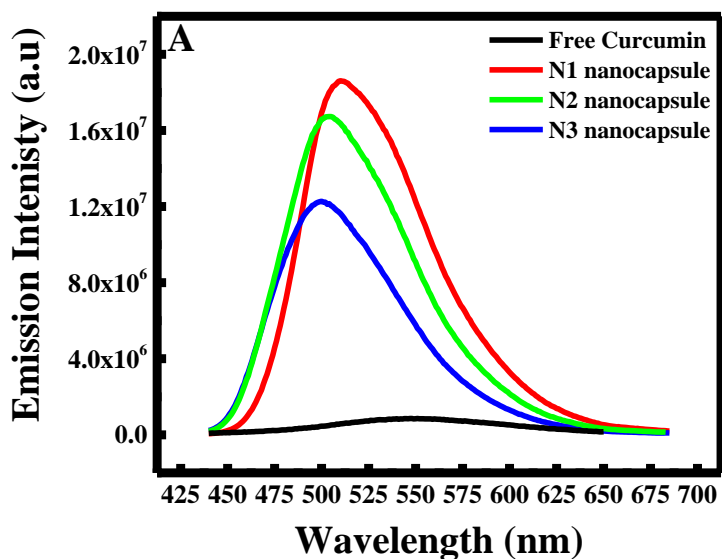
Figure 41 (A)Flurescence emission spectra excited at λ = 440 nm; (B) Flurescence emission spectra excited at λ = 350 nm; for pure curcumin; N1 nanocapsule (PLGA-Cur-PDDA); (B) N2 nanocapsule (PLGA-Cur-PDDA-SiO₂ NPs-PDDA); (C) N3 nanocapsule (PLGA-Cur-PDDA-SiO₂ NPs-PDDA-SiO₂ NPs-PDDA).

Henceforward, when exciting at 425 nm the emission wavelength is shifted from

550 nm (pure curcumin) to ∼510 nm for N1 NCs, ∼503 nm for N2 NCs, and ∼499 nm

for N3 NCs. Moreover, a blue shift to ∼510 nm was also noticed for the three different

nanocapsules capsules at λ_{ex} = 350 nm. In both emission spectra, the lowest emission intensity was obtained for N3 NCs. This difference in the emission wavelength is due to the incorporation of curcumin inside the PLGA forming smaller nanocapsules, proving that curcumin is forced from the aqueous phase of the PLGA polymer to its hydrophobic phase.

Furthermore, the UV-Visible absorption spectrum for free curcumin and the three NCs is depicted in Figure 42. Generally, curcumin absorbs in the UV-visible region at nearby 266 nm ($S_0{\rightarrow}S_2$ transition) and at around 426 nm ($S_0{\rightarrow}S_1$ transition)[145-146]. However, the entrapment of curcumin into the core shell of PLGA polymer is verified in the first place by the transformation of the sharp absorption peak obtained at 425 nm to a broad peak for N1. Additionally, UV-visible absorption of N2 and N3 appears at λ = 457 nm and λ = 469 nm indicated deprotonated form of curcumin (which is normally observed in basic medium above pH 9), thus, makes it easier to confirm the entrapment of curcumin into the core of PLGA polymer. Similarly, it was noticed that the absorbance of the three nanocapsules decreases going from N1 to N3 compared to free Curcumin, suggesting that curcumin is encapsulated more in N3 nanocapsules.

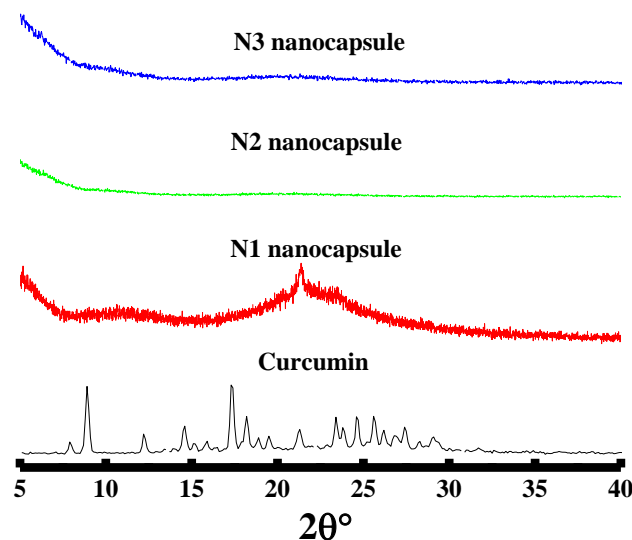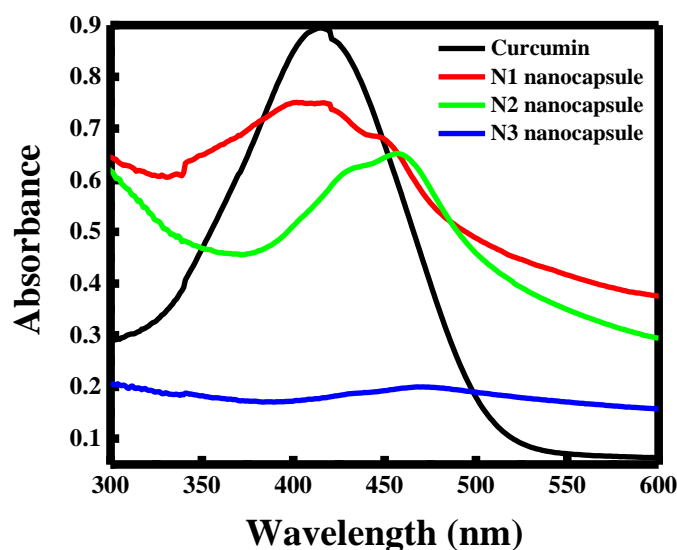Figure 42 UV-Visible spectra for pure curcumin; N1 nanocapsule (PLGA-Cur-PDDA); (B) N2 nanocapsule (PLGA-Cur-PDDA-SiO$_2$ NPs-PDDA); (C) N3 nanocapsule (PLGA-Cur-PDDA-SiO$_2$ NPs-PDDA-SiO$_2$ NPs-PDDA).

3. Drug loading and encapsulation efficiency

The absorbance of the decanted supernatent obtained after the centrifugation step in the synthesis of the nanocapsules was measured and the mass of free curcumin was calculated. The EE and DL percentage value are summarized in Table 7.

The encapsulation efficiency of N1, N2 and N3 was equal to 90.21%, 93.26% and 98.51 respectively. The enhancement of the EE percentage is due to the increase in the layer added, where it boosts the encapsulation of curcumin into the core of PLGA polymer. The high encapsulation effeciency value obtained in our case was similar to the EE value calculated by Gao et al[147]. One of the important properties in nanomedicine is drug loading percentage of the entrapped drug. The calculated % DL was equal to 24.10 %, 25.5 % and 28.30 % for N1, N2 and N3 NCs respectively. Hence, high encapsulation effeciency and high drug loading in such drug carrier particles can lead to stronger therapeutic effect along with reduced side effect [130].

Nanocapsules	N1	N2	N3
Encapsulation Efficiency (%)	90.21	93.26	98.51
Drug loading (%)	24.10	25.50	28.30

Table 7 Encapsulation Efficiency and drug delivery values for, N1 nanocapsule (PLGA-Cur-PDDA); N2 nanocapsule (PLGA-Cur-PDDA-SiO$_2$ NPs-PDDA); and N3 nanocapsule (PLGA-Cur-PDDA-SiO$_2$ NPs-PDDA-SiO$_2$ NPs-PDDA).

4. Effect of pH on the Drug Release Activity

To study the effect of pH on the release of curcumin from the synthesized nanocapsules (N1), UV-Visible measurement was obtained for the supernatant collected after centrifugation at 15000 rpm for 10 min in order to follow up the amount of released drug. The drug delivery profiles were obtained at T = 37°C at three different pHs 4, 6, and 7 as shown in Figure 43.
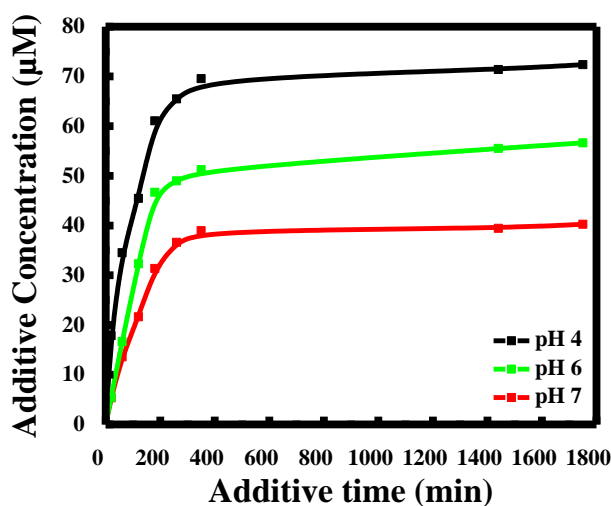
Figure 43 Drug release for N1 nanocapsule (PLGA-Cur-PDDA) at three different pHs (4, 6, and 7).

An important factor that affects the mode of release of the encapsulated drug is the surface charge[148]. As a result, Zeta-potential titration analysis was done for

curcumin and the nanocapsules at the studied pHs. Results showed that curcumin is

negatively charged at pH 6 and 7, while it is positively charged at pH 4. Also, Zeta

potential measurements of the nanocapsules showed that these nanocapsules are

positively charged at these pHs (See Table 8). It was revealed that at high acidic

conditions (pH 4), curcumin showed the highest release from the nanocarrier system,

since both curcumin and N£ NCs exhibit a positively surface charge at this pH; inhibit

thereby the entrapment of curcumin into the membrane of the nanocapsules.

Consequently, lower drug release was obtained at lower acidic medium (pH 6 and 7). In

fact, this is due to the attractive electrostatic interaction between two opposite charged

spices enhancing therefore the entrapment of curcumin and causing subsequently a

lower drug release. The higher drug release of curcumin at pH 6 compared to pH 7 is

related to the higher surface charge obtained at pH 7 for the prepared nanocapsules.

Zeta value (mV) pH	4	6	7
N1 nanocapsule	+17.34	+20.83	+25.74
Curcumin	+2.2	-2.2	-4.2

Table 8 Zeta potential value for N1 nanocapsule (PLGA-Cur-PDDA) and Curcumin at
three different pHs(4,6, and 7).

5. *Effect of additive multilayer on drug release*

In order to lower the release of the drug at pH 4, multilayered nanocaspsules (N2 and

N3) were prepared and the drug release profile was obtained at pH 4 as shown in Figure

44. It is clear that the release rate of curcumin decreases with the increase of the layer

number.
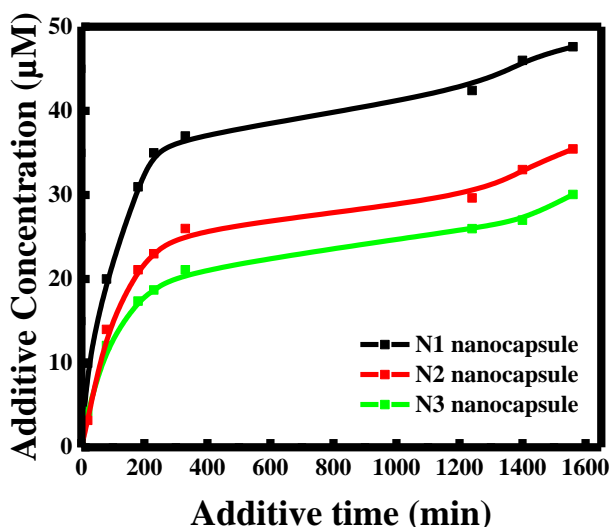
Figure 44 Effect of Additive layers on the release of Curcumin in N1 nanocapsule (PLGA-Cur-PDDA); N2 nanocapsule (PLGA-Cur-PDDA-SiO$_2$ NPs-PDDA); and N3 nanocapsule (PLGA-Cur-PDDA-SiO$_2$ NPs-PDDA-SiO$_2$ NPs-PDDA) at pH 4.

In this situation, it was expected that curcumin release will drop with the increase in the number of layers. This was confirmed by the obtained plot, where faster release of the drug is obtained when the nanocapsules surface was only coated by PDDA layer. However, the rate of release decreases by adding at first an additional silica nanoparticles layer and decreases more by adding a second silica layer. In all three cases, the drug release increased over the studied period reaching a maximum release for N1 and a minimum release for N3. Such layer by layer assembly improves the stability of the nanocapsules due to the electrostatic interaction between the oppositely charged polymer and silica nanoparticles[149]. Accordingly, the stability of the nanocapsule increases when more layers are added to its surface as our results explain.

Indeed, silica nanoparticles are negatively charged and PDDA polymer is positively charged, as a result; when silica is incorporated between two PDDA layers stronger electrostatic interaction will be present (See Table 9). Hence, the addition of

extra silica layer will enhance strangely the electrostatic interaction, and at the same time it will delay the release of curcumin encapsulated within the PLGA nanocapsules. Hence, the addition of multiple layers increase the diffusion distance and thus delay the contact between the drug and the release medium significantly for a longer time[150].

Nanocapsules	N1	N2	N3
Zeta Potential Value (mV)	+32.41	+35.67	+38.66

Table 9 Zeta potential value for N1 nanocapsule (PLGA-Cur-PDDA); N2 nanocapsule (PLGA-Cur-PDDA-SiO$_2$ NPs-PDDA); and N3 nanocapsule (PLGA-Cur-PDDA-SiO$_2$ NPs-PDDA-SiO$_2$ NPs-PDDA).

D. Conclusion

In Summary, the effect of three pHs (4, 6 and 7) on curcumin release from PLGA-Cur-PDDA nanocapsules was studied. It was revealed that the highest release of curcumin from the nanocapsules occur at pH 4. In order to lower curcumin release at the acidic medium, multilayered   nanocapsules were synthesized; N2 NCs (PLGA-Cur-PDDA-SiO$_2$ NPs-PDDA), and N3 NCs (PLGA-Cur-PDDA-SiO$_2$ NPs-PDDA-SiO$_2$ NPs-PDDA). Results showed that as the number of layers increases the release of curcumin was reduced.

CHAPTER VIII

CONCLUSION

In the present thesis, curcumin was highlighted to be a potential candidate for sensing dopamine as well as being a good agent for analytical and therapeutical applications. The interaction of Curcumin with PLGA and PDDA was studied and it was found that Curcumin interacts with PLGA through hydrogen bonding and van der Waals interaction and with PDDA through hydrophobic interaction.

Spectroscopic measurements such as fluorescence were conducted using Curcumin and pyrene as a fluorescence probe was conducted to determine the critical micelle concentration of PLGA which was found to be 0.31 g/L. Also, the critical micelle temperature was estimated and it was found to be 25 °C.

The effect of NaCl salt and solvent on the self-assembly behavior of PLGA polymer was studied. It was found that the increase in NaCl concentrations lowered the CMC by around two folds from 0.25 to 0.14 g/L as the NaCl concentration reaches 150 mM. Moreover, using chloroform, the effect of solvent on the aggregation behavior was studied, it was found that the polymer aggregate at similar concentration as in acetone-water mixture. But, the main difference was that a reverse micelles are obtained in case of chloroform instead of normal micelles.

Moving forward to determine the position of curcumin in the PLGA micelles, quenching experiment was conducted using two quenchers: hydrophilic KI and hydrophobic CPB. The results obtained confirmed the location of curcumin to be located near the hydrophobic pocket of Stern-layer of PLGA micelle.

Moreover, the encapsulation of Curcumin inside PLGA was successfully done using solid in oil in water emulsion technique. The nanocapsules was coated with PDDA polymer in order to stabilize the synthesized nanocapsules. The successful encapsulation of curcumin into the polymeric nanocapsules was verified using UV-Visible, fluorescence emission analysis, X-ray Diffraction (XRD), thermogravimetric analysis (TGA) and scanning electron microscopy (SEM). Moreover, the efficiency of PDDA as a protective layer was confirmed through zeta analysis.

Based on the high encapsulation efficiency obtained for the synthesized nanocapsules PLGA- CUR-PDDA NCs were used as a nanoprobe to detect dopamine, which was based on the fluorescence emission, a selective, easy, and a low cost technique. Several solutions were prepared with different dopamine's concentration in the range from 10 μM to 5 mM. From 10-500 μM, the emission intensity decreases slightly due to the binding of the negatively charged dopamine, to the positively charged NCs. However, the enhancement of dopamine's concentration causes an effective fluorescence quenching. The binding constant was estimated using the stern-volmer equation to be around 0.96 mM.

Besides, the antiviral activity of PLGA- CUR-PDDA NCs was examined against the influenza A virus. Based on the results of MTT assay, it was found that Curcumin nanocapsules is well tolerated by A549 cells with cell death< 20 % up to a concentration of 20 μM. And the results of plaque reduction assay showed that a reduction in the plaque size was found upon treating infected PR8 cells with 10 μM of Nanocapsules. Finally, the EC50 was estimated to be 20 μM.

As a future direction for this research work, the anti-cancer and anti-oxidant activity of PLGA-CUR-PDDA NCs will be evaluated.

REFERENCES

1.   Nilewar G, M. P., Talhan PP, Thakre S;Nanocapsules: Nano novel drug delivery system; PharmaTutor; 2017; 5(6); 14-16.

2.   Kothamasu, P.; Kanumur, H.; Ravur, N.; Maddu, C.; Parasuramrajam, R.; Thangavel, S., Nanocapsules: the weapons for novel drug delivery systems. *Bioimpacts* **2012,** *2* (2), 71-81.

3.   Poletto, F. S.; Beck, R. C. R.; Guterres, S. S.; Pohlmann, A. R., Polymeric Nanocapsules: Concepts and Applications. In *Nanocosmetics and Nanomedicines: New Approaches for Skin Care*, Beck, R.; Guterres, S.; Pohlmann, A., Eds. Springer Berlin Heidelberg: Berlin, Heidelberg, 2011; pp 49-68.

4.   De Jong, W. H.; Borm, P. J. A., Drug delivery and nanoparticles:applications and hazards. *Int J Nanomedicine* **2008,** *3* (2), 133-149.

5.   Tan, S. B. Z. Z. T. C. L. W. C. L. T. F. W., A Focus on Nanoparticles as a Drug Delivery System. *Nanomedicine* **2012,** *7(8):1253-1271.* .

6.   Poletto, F. S., Beck, R. C. R., Guterres, S. S., & Pohlmann, A. R. (2011). Polymeric Nanocapsules: Concepts and Applications. Nanocosmetics and Nanomedicines, 49–68.

7.   Mora-Huertas, C. E., Fessi, H., & Elaissari, A. (2010). Polymer-based nanocapsules for drug delivery. International Journal of Pharmaceutics, 385(1-2), 113–142. doi:10.1016/j.ijpharm.2009.10.018.

8.   Rong, X., Xie, Y., Hao, X., Chen, T., Wang, Y., & Liu, Y. (2011). Applications of Polymeric Nanocapsules in Field of Drug Delivery Systems. Current Drug Discovery Technologies, 8(3), 173–187. doi:10.2174/157016311796799008

9.   Siyuan Deng, M. R. G., Roberta Censi and Piera Di Martino Polymeric Nanocapsules as Nanotechnological

Alternative for Drug Delivery System: Current Status,

Challenges and Opportunities. *nanomaterials* **2020**.

10.   Akbarzadeh, A.; Rezaei-Sadabady, R.; Davaran, S.; Joo, S. W.; Zarghami, N.; Hanifehpour, Y.; Samiei, M.; Kouhi, M.; Nejati-Koshki, K., Liposome: classification, preparation, and applications. *Nanoscale Res Lett* **2013,** *8* (1), 102-102.

11.   Deb, P. K.; Al-Attraqchi, O.; Chandrasekaran, B.; Paradkar, A.; Tekade, R. K., Chapter 16 - Protein/Peptide Drug Delivery Systems: Practical Considerations in Pharmaceutical Product Development. In *Basic Fundamentals of Drug Delivery*, Tekade, R. K., Ed. Academic Press: 2019; pp 651-684.

12.   Rai, M.; Ingle, A. P.; Bansod, S.; Kon, K., Chapter 9 - Tackling the Problem of Tuberculosis by Nanotechnology: Disease Diagnosis and Drug Delivery. In *Nanotechnology in Diagnosis, Treatment and Prophylaxis of Infectious Diseases*, Rai, M.; Kon, K., Eds. Academic Press: Boston, 2015; pp 133-149.

13.   Nisini, R.; Poerio, N.; Mariotti, S.; De Santis, F.; Fraziano, M., The Multirole of Liposomes in Therapy and Prevention of Infectious Diseases. *Frontiers in Immunology* **2018,** *9* (155).

14.   Deb, P. K.; Abed, S. N.; Jaber, A. M. Y.; Tekade, R. K., Chapter 5 - Particulate Level Properties and its Implications on Product Performance and Processing. In *Dosage Form Design Parameters*, Tekade, R. K., Ed. Academic Press: 2018; pp 155-220.

15.   Daraee, H.; Etemadi, A.; Kouhi, M.; Alimirzalu, S.; Akbarzadeh, A., Application of liposomes in medicine and drug delivery. *Artificial Cells, Nanomedicine, and Biotechnology* **2016,** *44* (1), 381-391.

16.   Derman, S.; Katmıs, A.; Fide, S.; Karaismailoglu, S., Synthesis and characterization methods of polymeric nanoparticles. *Characterization and Application of Nanomaterials* **2018**.

17.   Rao, J. P.; Geckeler, K. E., Polymer nanoparticles: Preparation techniques and size-control parameters. *Progress in Polymer Science* **2011,** *36* (7), 887-913.

18.   Wang, Y.; Li, P.; Tran, T.; Zhang, J.; Kong, L., Manufacturing Techniques and Surface Engineering of Polymer Based Nanoparticles for Targeted Drug Delivery to Cancer. *Nanomaterials* **2016,** *6*, 26.

19.   Barreras-Urbina, C. G.; Ramírez-Wong, B.; López-Ahumada, G. A.; Burruel-Ibarra, S. E.; Martínez-Cruz, O.; Tapia-Hernández, J. A.; Rodríguez Félix, F., Nano- and Micro-Particles by Nanoprecipitation: Possible Application in the Food and Agricultural Industries. *International Journal of Food Properties* **2016,** *19* (9), 1912-1923.

20.   Nagavarma, B. V. N.; Yadav, H.; Ayaz, A.; Vasudha, L.; Shivakumar, H., Different techniques for preparation of polymeric nanoparticles- A review. *Asian Journal of Pharmaceutical and Clinical Research* **2012,** *5*, 16-23.

21.   Lim, K.; Hamid, Z. A. A., 10 - Polymer nanoparticle carriers in drug delivery systems: Research trend. In *Applications of Nanocomposite Materials in Drug Delivery*, Inamuddin; Asiri, A. M.; Mohammad, A., Eds. Woodhead Publishing: 2018; pp 217-237.

22.   Krishnamoorthy, K.; Mahalingam, M., Selection of a suitable method for the preparation of polymeric nanoparticles: multi-criteria decision making approach. *Adv Pharm Bull* **2015,** *5* (1), 57-67.

23.   VJ Mohanraj , Y. C., Nanoparticles – A Review *Tropical Journal of Pharmaceutical Research* **2006,** *5 (1): 561-573*.

24.   Reverchon, E.; Adami, R., Nanomaterials and supercritical fluids. *The Journal of Supercritical Fluids* **2006,** *37* (1), 1-22.

25.   Zahin, N.; Anwar, R.; Tewari, D.; Kabir, M. T.; Sajid, A.; Mathew, B.; Uddin, M. S.; Aleya, L.; Abdel-Daim, M. M., Nanoparticles and its biomedical applications in health and diseases: special focus on drug delivery. *Environmental Science and Pollution Research* **2020,** *27* (16), 19151-19168.

26.   Allen, T. M.; Cullis, P. R., Drug Delivery Systems: Entering the Mainstream. *Science* **2004,** *303* (5665), 1818.

27.   Doll, T. A. P. F.; Raman, S.; Dey, R.; Burkhard, P., Nanoscale assemblies and their biomedical applications. *Journal of The Royal Society Interface* **2013,** *10* (80), 20120740.

28.   Faraji, M.; Yamini, Y.; Rezaee, M., Magnetic nanoparticles: Synthesis, stabilization, functionalization, characterization, and applications. *Journal of the Iranian Chemical Society* **2010,** *7* (1), 1-37.

29.   Mayer, C., Nanocapsules as Drug Delivery Systems. *The International journal of artificial organs* **2005,** *28*, 1163-71.

30.   Holzinger, M.; Le Goff, A.; Cosnier, S., Nanomaterials for biosensing applications: a review. *Frontiers in Chemistry* **2014,** *2* (63).

31.   Liu, W.-T., Nanoparticles and their biological and environmental applications. *Journal of Bioscience and Bioengineering* **2006,** *102* (1), 1-7.

32.   Singh, S.; Kumar, V.; Romero, R.; Sharma, K.; Singh, J., Applications of Nanoparticles in Wastewater Treatment. In *Nanobiotechnology in Bioformulations*, Prasad, R.; Kumar, V.; Kumar, M.; Choudhary, D., Eds. Springer International Publishing: Cham, 2019; pp 395-418.

33.   Tasleem Arif, N. N., Syed Suhail Amin, Sheikh Shoib, Raheel Mushtaq and Muzafar Rashid Shawl, Therapeutic and Diagnostic Applications of Nanotechnology in Dermatology and Cosmetics. *Journal of Nanomedicine & nr uoJ Biotherapeutic Discovery* **2015**.

34.   Akram, M.; Afzal, A.; Khan, U.; Abdul, H.; Mohiuddin, E.; Asif, M., Curcuma longa and Curcumin: A review article. *Rom. J. Biol-Plant Biol.* **2010,** *55*, 65-70.

35.   Mohanty, C.; Das, M.; Sahoo, S. K., Emerging role of nanocarriers to increase the solubility and bioavailability of curcumin. *Expert Opin Drug Deliv* **2012,** *9* (11), 1347-64.

36.   Aggarwal, B. B.; Sundaram, C.; Malani, N.; Ichikawa, H., CURCUMIN: THE INDIAN SOLID GOLD. In *The Molecular Targets and Therapeutic Uses of Curcumin in Health and Disease*, Aggarwal, B. B.; Surh, Y.-J.; Shishodia, S., Eds. Springer US: Boston, MA, 2007; pp 1-75.

37.   Bhawana; Basniwal, R. K.; Buttar, H. S.; Jain, V. K.; Jain, N., Curcumin Nanoparticles: Preparation, Characterization, and Antimicrobial Study. *Journal of Agricultural and Food Chemistry* **2011,** *59* (5), 2056-2061.

38.   Raut, N. A.; Dhore, P. W.; Saoji, S. D.; Kokare, D. M., Chapter 9 - Selected Bioactive Natural Products for Diabetes Mellitus. In *Studies in Natural Products Chemistry*, Atta ur, R., Ed. Elsevier: 2016; Vol. 48, pp 287-322.

39.   Bhatia, N. K.; Kishor, S.; Katyal, N.; Gogoi, P.; Narang, P.; Deep, S., Effect of pH and temperature on conformational equilibria and aggregation behaviour of curcumin in aqueous binary mixtures of ethanol. *RSC Advances* **2016,** *6* (105), 103275-103288.

40.   Anand, P.; Kunnumakkara, A. B.; Newman, R. A.; Aggarwal, B. B., Bioavailability of Curcumin: Problems and Promises. *Molecular Pharmaceutics* **2007,** *4* (6), 807-818.

41.   Wing-Hin, L.; Ching-Yee, L.; Mary, B.; Frederick, L.; Rebecca, S. M.; Ramin, R., Curcumin and its Derivatives: Their Application in Neuropharmacology and Neuroscience in the 21st Century. *Current Neuropharmacology* **2013,** *11* (4), 338-378.

42.   Priyadarsini, K. I., Photophysics, photochemistry and photobiology of curcumin: Studies from organic solutions, bio-mimetics and living cells. *Journal of Photochemistry and Photobiology C: Photochemistry Reviews* **2009,** *10* (2), 81-95.

43.   Khopde, S. M.; Priyadarsini, K. I.; Palit, D. K.; Mukherjee, T., Effect of solvent on the excited-state photophysical properties of curcumin. *Photochemistry and photobiology* **2000,** *72* (5), 625-31.

44.   Barik, A.; Goel, N.; Priyadarsini, I.; Mohan, H., Effect of Deuterated Solvents on the Excited State Photophysical Properties of Curcumin. *J. Photosci.* **2004,** *11*.

45.   Wang, Y.-J.; Pan, M.-H.; Cheng, A.-L.; Lin, L.-I.; Ho, Y.-S.; Hsieh, C.-Y.; Lin, J.-K., Stability of curcumin in buffer solutions and characterization of its degradation products. *Journal of Pharmaceutical and Biomedical Analysis* **1997,** *15* (12), 1867-1876.

46.   Lestari, M. L. A. D.; Indrayanto, G., Chapter Three - Curcumin. In *Profiles of Drug Substances, Excipients and Related Methodology*, Brittain, H. G., Ed. Academic Press: 2014; Vol. 39, pp 113-204.

47.   Fugita, R. A.; Gálico, D. A.; Guerra, R.; Perpetuo, G.; Treu-Filho, O.; Galhiane, M. S.; Mendes, R. A.; Bannach, G., Thermal behaviour of curcumin. *Braz. J. Therm. Anal.* **2012,** *1*, 19-23.

48.   Wilken, R.; Veena, M. S.; Wang, M. B.; Srivatsan, E. S., Curcumin: A review of anti-cancer properties and therapeutic activity in head and neck squamous cell carcinoma. *Mol Cancer* **2011,** *10*, 12-12.

49.   Tomeh, M. A.; Hadianamrei, R.; Zhao, X., A Review of Curcumin and Its Derivatives as Anticancer Agents. *Int J Mol Sci* **2019,** *20* (5), 1033.

50.   Anand, P.; Sundaram, C.; Jhurani, S.; Kunnumakkara, A. B.; Aggarwal, B. B., Curcumin and cancer: An "old-age" disease with an "age-old" solution. *Cancer Letters* **2008,** *267* (1), 133-164.

51.   Manikandan, R.; Beulaja, M.; Arulvasu, C.; Sellamuthu, S.; Dinesh, D.; Prabhu, D.; Babu, G.; Vaseeharan, B.; Prabhu, N. M., Synergistic anticancer activity of curcumin and catechin: An in vitro study using human cancer cell lines. *Microscopy Research and Technique* **2012,** *75* (2), 112-116.

52.   Gunes, H.; Gulen, D.; Mutlu, R.; Gumus, A.; Tas, T.; Topkaya, A. E., Antibacterial effects of curcumin: An in vitro minimum inhibitory concentration study. *Toxicology and Industrial Health* **2013,** *32* (2), 246-250.

53.   Jennings, M. R.; Parks, R. J., Curcumin as an Antiviral Agent. *Viruses* **2020,** *12* (11), 1242.

54.   Sui, Z.; Salto, R.; Li, J.; Craik, C.; Ortiz de Montellano, P. R., Inhibition of the HIV-1 and HIV-2 proteases by curcumin and curcumin boron complexes. *Bioorganic & Medicinal Chemistry* **1993,** *1* (6), 415-422.

55.   Thimmulappa, R. K.; Mudnakudu-Nagaraju, K. K.; Shivamallu, C.; Subramaniam, K. J. T.; Radhakrishnan, A.; Bhojraj, S.; Kuppusamy, G., Antiviral and immunomodulatory activity of curcumin: A case for prophylactic therapy for COVID-19. *Heliyon* **2021,** *7* (2), e06350-e06350.

56.   Liu, Z.; Ying, Y., The Inhibitory Effect of Curcumin on Virus-Induced Cytokine Storm and Its Potential Use in the Associated Severe Pneumonia. *Frontiers in Cell and Developmental Biology* **2020,** *8* (479).

57.   Gülçin, İ., Antioxidant activity of food constituents: an overview. *Archives of Toxicology* **2012,** *86* (3), 345-391.

58.   Batinić-Haberle, I.; Rebouças, J. S.; Spasojević, I., Superoxide dismutase mimics: chemistry, pharmacology, and therapeutic potential. *Antioxid Redox Signal* **2010,** *13* (6), 877-918.

59.   Sökmen, M.; Akram Khan, M., The antioxidant activity of some curcuminoids and chalcones. *Inflammopharmacology* **2016,** *24* (2-3), 81-86.

60.   Cai, X.; Dou, J.; Yu, A.; Zhai, G., Bioavailability of Quercetin: Problems and Promises. *Current medicinal chemistry* **2013,** *20*.

61.   Lopresti, A. L., The Problem of Curcumin and Its Bioavailability: Could Its Gastrointestinal Influence Contribute to Its Overall Health-Enhancing Effects? *Advances in Nutrition* **2018,** *9* (1), 41-50.

62.   Bisht, S.; Feldmann, G.; Soni, S.; Ravi, R.; Karikar, C.; Maitra, A.; Maitra, A., Polymeric nanoparticle-encapsulated curcumin ("nano curcumin"): A novel strategy for human cancer therapy. *Journal of nanobiotechnology* **2007,** *5*, 3.

63.   Maiti, K.; Gantait, A.; Saha, B.; Mukherjee, P., Curcumin-phospholipid complex: Preparation, therapeutic evaluation and pharmacokinetic study in rats. *International journal of pharmaceutics* **2007,** *330*, 155-63.

64.   Safavy, A.; Raisch, K. P.; Mantena, S.; Sanford, L. L.; Sham, S. W.; Krishna, N. R.; Bonner, J. A., Design and Development of Water-Soluble Curcumin Conjugates as Potential Anticancer Agents. *Journal of Medicinal Chemistry* **2007,** *50* (24), 6284-6288.
65.   Wang, Z.; Leung, M. H. M.; Kee, T. W.; English, D. S., The Role of Charge in the Surfactant-Assisted Stabilization of the Natural Product Curcumin. *Langmuir* **2010,** *26* (8), 5520-5526.
66.   Tønnesen, H. H.; Másson, M.; Loftsson, T., Studies of curcumin and curcuminoids. XXVII. Cyclodextrin complexation: solubility, chemical and photochemical stability. *International Journal of Pharmaceutics* **2002,** *244* (1), 127-135.
67.   Makadia, H. K.; Siegel, S. J., Poly Lactic-co-Glycolic Acid (PLGA) as Biodegradable Controlled Drug Delivery Carrier. *Polymers* **2011,** *3* (3), 1377-1397.
68.   Sharma, S.; Parmar, A.; Kori, S.; Sandhir, R., PLGA-based nanoparticles: A new paradigm in biomedical applications. *TrAC Trends in Analytical Chemistry* **2016,** *80*, 30-40.
69.   Tabatabaei Mirakabad, F. S.; Nejati, K.; Akbarzadeh, A.; Rahmati, M.; Milani, M.; Zarghami, N.; Zeighamian, V.; Rahimzadeh, A.; Alimohammadi, S.; Hanifehpour, Y.; Joo, S., PLGA-Based Nanoparticles as Cancer Drug Delivery Systems. *Asian Pacific journal of cancer prevention : APJCP* **2014,** *15*, 517-535.
70.   Ochi, K.; Chen, G.; Ushida, T.; Gojo, S.; Segawa, K.; Tai, H.; Ueno, K.; Ohkawa, H.; Mori, T.; Yamaguchi, A.; Toyama, Y.; Hata, J.-i.; Umezawa, A., Use of isolated mature osteoblasts in abundance acts as desired-shaped bone regeneration in combination with a modified poly-DL-lactic-co-glycolic acid (PLGA)-collagen sponge. *Journal of Cellular Physiology* **2003,** *194* (1), 45-53.
71.   Virlan, M. J. R.; Miricescu, D.; Totan, A.; Greabu, M.; Tanase, C.; Sabliov, C. M.; Caruntu, C.; Calenic, B., Current Uses of Poly(lactic-co-glycolic acid) in the Dental Field: A Comprehensive Review. *Journal of Chemistry* **2015,** *2015*, 525832.
72.   Félix Lanao, R. P.; Jonker, A. M.; Wolke, J. G. C.; Jansen, J. A.; van Hest, J. C. M.; Leeuwenburgh, S. C. G., Physicochemical properties and applications of poly(lactic-co-glycolic acid) for use in bone regeneration. *Tissue Eng Part B Rev* **2013,** *19* (4), 380-390.
73.   Dawes, G. J. S.; Fratila-Apachitei, L. E.; Mulia, K.; Apachitei, I.; Witkamp, G. J.; Duszczyk, J., Size effect of PLGA spheres on drug loading efficiency and release profiles. *Journal of Materials Science: Materials in Medicine* **2009,** *20* (5), 1089-1094.
74.   Su, Y.; Zhang, B.; Sun, R.; Liu, W.; Zhu, Q.; Zhang, X.; Wang, R.; Chen, C., PLGA-based biodegradable microspheres in drug delivery: recent advances in research and application. *Drug Delivery* **2021,** *28* (1), 1397-1418.
75.   Lü, J.-M.; Wang, X.; Marin-Muller, C.; Wang, H.; Lin, P. H.; Yao, Q.; Chen, C., Current advances in research and clinical applications of PLGA-based nanotechnology. *Expert Rev Mol Diagn* **2009,** *9* (4), 325-341.
76.   Saxena, V.; Sadoqi, M.; Shao, J., Polymeric nanoparticulate delivery system for Indocyanine green: Biodistribution in healthy mice. *International Journal of Pharmaceutics* **2006,** *308* (1), 200-204.
77.   Phua, K. K. L.; Roberts, E. R. H.; Leong, K. W., 1.24 Degradable Polymers. In *Comprehensive Biomaterials II*, Ducheyne, P., Ed. Elsevier: Oxford, 2017; pp 516-553.
78.   Straub, J. A.; Chickering, D. E.; Church, C. C.; Shah, B.; Hanlon, T.; Bernstein, H., Porous PLGA microparticles: AI-700, an intravenously administered ultrasound

contrast agent for use in echocardiography. *Journal of Controlled Release* **2005,** *108* (1), 21-32.

79.   Chen, Z.; Weber, S. G., Determination of binding constants by affinity capillary electrophoresis, electrospray ionization mass spectrometry and phase-distribution methods. *Trends Analyt Chem* **2008,** *27* (9), 738-748.

80.   Pathare, B.; Tambe, V.; Patil, V., A review on various analytical methods used in determination of dissociation constant. *International Journal of Pharmacy and Pharmaceutical Sciences* **2014,** *6*, 26-34.

81.   Fielding, L., NMR Methods for the Determination of Protein- Ligand Dissociation Constants. *Current topics in medicinal chemistry* **2003,** *3*, 39-53.

82.   ZHANG Jian-Hua, L. Q., CHEN Yu-Miao, LIU Zhao-Qing, XU Chang-Wei, Determination of Acid Dissociation Constant of Methyl Red by Multi-Peaks Gaussian Fitting Method Based on UV-Visible Absorption Spectrum. *Acta Phys. -Chim. Sin.* **2012,** *28* (05), 1030-1036.

83.   Prystay, L.; Gosselin, M.; Banks, P., Determination of Equilibrium Dissociation Constants in Fluorescence Polarization. *Journal of Biomolecular Screening* **2001,** *6* (3), 141-150.

84.   Vogel, M.; Suess, B., Label-Free Determination of the Dissociation Constant of Small Molecule-Aptamer Interaction by Isothermal Titration Calorimetry. *Methods Mol Biol* **2016,** *1380*, 113-125.

85.   Bakar, K. A.; Feroz, S. R., A critical view on the analysis of fluorescence quenching data for determining ligand–protein binding affinity. *Spectrochimica Acta Part A: Molecular and Biomolecular Spectroscopy* **2019,** *223*, 117337.

86.   leilabadi-asl, A.; Divsalar, A.; Saboury, A.; Parivar, K., Comparing the Interactions and Structural Changes in Milk Carrier Protein of (- Lactoglobulin upon Binding of 5-Fluorouracil and Oxali-palladium. **2018**, 28-34.

87.   Alam, M. F.; Varshney, S.; Khan, M.; Laskar, A.; Younus, H., In vitro DNA binding studies of therapeutic and prophylactic drug citral. *International Journal of Biological Macromolecules* **2018,** *113*.

88.   Kabiri, M.; Amiri Tehranizadeh, Z.; Baratian, A.; Saberi, M.-R.; Chamani, J., Use of Spectroscopic, Zeta Potential and Molecular Dynamic Techniques to Study the Interaction between Human Holo-Transferrin and Two Antagonist Drugs:Comparison of Binary and Ternary Systems. *Molecules (Basel, Switzerland)* **2012,** *17*, 3114-47.

89.   Lu, G. W.; Gao, P., CHAPTER 3 - Emulsions and Microemulsions for Topical and Transdermal Drug Delivery. In *Handbook of Non-Invasive Drug Delivery Systems*, Kulkarni, V. S., Ed. William Andrew Publishing: Boston, 2010; pp 59-94.

90.   Meesaragandla, B.; García, I.; Biedenweg, D.; Toro-Mendoza, J.; Coluzza, I.; Liz-Marzán, L. M.; Delcea, M., H-Bonding-mediated binding and charge reorganization of proteins on gold nanoparticles. *Physical Chemistry Chemical Physics* **2020,** *22* (8), 4490-4500.

91.   Kumar, D.; Hidayathulla, S.; Rub, M., Association behavior of a mixed system of the antidepressant drug imipramine hydrochloride and dioctyl sulfosuccinate sodium salt: Effect of temperature and salt. *Journal of Molecular Liquids* **2018,** *271*.

92.   Kumar, D.; Rub, M. A., Interaction of ninhydrin with chromium-glycylglycine complex in the presence of dimeric gemini surfactants. *Journal of Molecular Liquids* **2018,** *250*, 329-334.

93.   Voutsas, E. C.; Flores, M. V.; Spiliotis, N.; Bell, G.; Halling, P. J.; Tassios, D. P., Prediction of Critical Micelle Concentrations of Nonionic Surfactants in Aqueous

and Nonaqueous Solvents with UNIFAC. *Industrial & Engineering Chemistry Research* **2001,** *40* (10), 2362-2366.

94. Zheng, L.; Guo, C.; Liang, X.; Bahadur, P.; Chen, S.; Ma, J.; Liu, H., Micellization of Pluronic L64 in salt solution by FTIR spectroscopy. *Vibrational Spectroscopy* **2005,** *39*, 157-162.

95. Desai, M.; Jain, N. J.; Sharma, R.; Bahadur, P., Temperature and salt-induced micellization of some block copolymers in aqueous solution. *Journal of Surfactants and Detergents* **2000,** *3* (2), 193-199.

96. Alexandridis, P.; Holzwarth, J. F.; Hatton, T. A., Micellization of Poly(ethylene oxide)-Poly(propylene oxide)-Poly(ethylene oxide) Triblock Copolymers in Aqueous Solutions: Thermodynamics of Copolymer Association. *Macromolecules* **1994,** *27* (9), 2414-2425.

97. Karimi, M. A.; Mozaheb, M. A.; Hatefi-Mehrjardi, A.; Tavallali, H.; Attaran, A. M.; Shamsi, R., A new simple method for determining the critical micelle concentration of surfactants using surface plasmon resonance of silver nanoparticles. *Journal of Analytical Science and Technology* **2015,** *6* (1), 35.

98. Chattopadhyay, A.; Harikumar, K. G., Dependence of critical micelle concentration of a zwitterionic detergent on ionic strength: implications in receptor solubilization. *FEBS letters* **1996,** *391* (1-2), 199-202.

99. Oliveira, M.; Ribeiro, A.; Guilhermino, L., Effects of short-term exposure to microplastics and pyrene on Pomatoschistus microps (Teleostei, Gobiidae). *Comparative Biochemistry and Physiology a-Molecular & Integrative Physiology* **2012,** *163*, S20-S20.

100. Bechnak, L.; Patra, D., Salt and bile salt accelerate self-assembly behavior of poly(ethylene oxide)-block-poly(propylene oxide)-block-poly(ethylene oxide) probed by curcumin fluorescence. *Colloids and Surfaces A: Physicochemical and Engineering Aspects* **2019,** *583*, 123955.

101. Zhu, C.; Pang, S.; Xu, J.; Jia, L.; Xu, F.; Mei, J.; Qin, A.; Sun, J.; Ji, J.; Tang, B., Aggregation-induced emission of tetraphenylethene derivative as a fluorescence method for probing the assembling/disassembling of amphiphilic molecules. *The Analyst* **2011,** *136*, 3343-8.

102. Palit, D. K.; Sapre, A. V.; Mittal, J. P., Picosecond studies on the electron transfer from pyrene and perylene excited singlet states to N-hexadecyl pyridinium chloride. *Chemical Physics Letters* **1997,** *269*, 286-292.

103. Sujatha, J.; Mishra, A. K., Phase Transitions in Phospholipid Vesicles: Excited State Prototropism of 1-Naphthol as a Novel Probe Concept. *Langmuir* **1998,** *14* (9), 2256-2262.

104. Moussa, Z.; Chebl, M.; Patra, D., Fluorescence of tautomeric forms of curcumin in different pH and biosurfactant rhamnolipids systems: Application towards on-off ratiometric fluorescence temperature sensing. *Journal of Photochemistry and Photobiology B: Biology* **2017,** *173*.

105. Barry, J.; Fritz, M.; Brender, J. R.; Smith, P. E. S.; Lee, D.-K.; Ramamoorthy, A., Determining the Effects of Lipophilic Drugs on Membrane Structure by Solid-State NMR Spectroscopy: The Case of the Antioxidant Curcumin. *Journal of the American Chemical Society* **2009,** *131* (12), 4490-4498.

106. Pérez-Lara, A.; Ausili, A.; Aranda, F. J.; de Godos, A.; Torrecillas, A.; Corbalán-García, S.; Gómez-Fernández, J. C., Curcumin Disorders 1,2-Dipalmitoyl-sn-glycero-3-phosphocholine Membranes and Favors the Formation of Nonlamellar

Structures by 1,2-Dielaidoyl-sn-glycero-3-phosphoethanolamine. *The Journal of Physical Chemistry B* **2010,** *114* (30), 9778-9786.

107.   Othman, A. K.; El Kurdi, R.; Patra, D., Outstanding Enhancement of Curcumin Fluorescence in PDDA and Silica Nanoparticles Coated DMPC Liposomes Based Nanocapsules: Application for Selective Estimation of ATP**. *ChemistrySelect* **2021,** *6* (25), 6324-6332.

108.   Bechnak, L.; El Kurdi, R.; Patra, D., Fluorescence Sensing of Nucleic Acid by Curcumin Encapsulated Poly(Ethylene Oxide)-Block-Poly(Propylene Oxide)-Block-Poly(Ethylene Oxide) Based Nanocapsules. *Journal of Fluorescence* **2020,** *30* (3), 547-556.

109.   Luz, P.; Magalhaes, L.; Pereira, A.; Cunha, W.; Rodrigues, V.; Silva, M., Curcumin-loaded into PLGA nanoparticles. *Parasitology research* **2011,** *110*, 593-8.

110.   Verderio, P.; Bonetti, P.; Colombo, M.; Pandolfi, L.; Prosperi, D., Intracellular Drug Release from Curcumin-Loaded PLGA Nanoparticles Induces G2/M Block in Breast Cancer Cells. *Biomacromolecules* **2013,** *14* (3), 672-682.

111.   Liu, M.; Teng, C. P.; Win, K. Y.; Chen, Y.; Zhang, X.; Yang, D.-P.; Li, Z.; Ye, E., Polymeric Encapsulation of Turmeric Extract for Bioimaging and Antimicrobial Applications. *Macromolecular Rapid Communications* **2019,** *40* (5), 1800216.

112.   Asad Khan, M.; Ahmad, S.; Ahmad, I.; Rizvi, M. M. A., Anti-Proliferative Activity of Curcumin Loaded PLGA Nanoparticles for Prostate Cancer. In *Nanotechnology Applied To Pharmaceutical Technology*, Rai, M.; Alves dos Santos, C., Eds. Springer International Publishing: Cham, 2017; pp 267-278.

113.   Manbohi, A.; Ahmadi, S. H., Sensitive and selective detection of dopamine using electrochemical microfluidic paper-based analytical nanosensor. *Sensing and Bio-Sensing Research* **2019,** *23*, 100270.

114.   Qasem, M.; El Kurdi, R.; Patra, D., Preparation of Curcubit[6]uril functionalized CuO Nanoparticles: A New Nanosensing Scheme Based on Fluorescence recovery after FRET for the Label Free Determination of Dopamine. *ChemistrySelect* **2020,** *5* (15), 4642-4649.

115.   Liu, X.; Liu, J., Biosensors and sensors for dopamine detection. *VIEW* **2021,** *2* (1), 20200102.

116.   Zhang, Y.; Qi, S.; Liu, Z.; Shi, Y.; Yue, W.; Yi, C., Rapid determination of dopamine in human plasma using a gold nanoparticle-based dual-mode sensing system. *Materials Science and Engineering: C* **2016,** *61*, 207-213.

117.   Sawant, A.; Kamath, S.; Kg, H.; Kulyadi, G. P., Solid-in-Oil-in-Water Emulsion: An Innovative Paradigm to Improve Drug Stability and Biological Activity. *AAPS PharmSciTech* **2021,** *22* (5), 199.

118.   Slika, L.; Moubarak, A.; Borjac, J.; Baydoun, E.; Patra, D., Preparation of curcumin-poly (allyl amine) hydrochloride based nanocapsules: Piperine in nanocapsules accelerates encapsulation and release of curcumin and effectiveness against colon cancer cells. *Materials Science and Engineering: C* **2020,** *109*, 110550.

119.   Su, S.; Wu, W.; Gao, J.; Lu, J.; Fan, C., Nanomaterials-based sensors for applications in environmental monitoring. *Journal of Materials Chemistry* **2012,** *22* (35), 18101-18110.

120.   Qasem, M.; el kurdi, R.; Patra, D., Preparation of Curcubit[6]uril functionalized CuO Nanoparticles: A New Nanosensing Scheme Based on Fluorescence recovery after FRET for the Label Free Determination of Dopamine. *ChemistrySelect* **2020,** *5*, 4642-4649.

121.   Li, N.; Zhang, H.; Zhang, F.; Su, X., A simple and convenient fluorescent strategy for the highly sensitive detection of dopamine and ascorbic acid based on graphene quantum dots. *Talanta* **2018,** *189*.

122.   Liu, C.; Gomez, F.; Miao, Y.; Cui, P.; Lee, W., A colorimetric assay system for dopamine using microfluidic paper-based analytical devices. *Talanta* **2018,** *194*.

123.   Loutfy, S.; Elberry, M.; Farroh, K.; Mohamed, H.; Mohamed, A.; Mohamed, E.; Faraag, A.; Faraag, I.; Mousa, S., Antiviral Activity of Chitosan Nanoparticles Encapsulating Curcumin Against Hepatitis C Virus Genotype 4a in Human Hepatoma Cell Lines. *Int J Nanomedicine* **2020,** *Volume 15*.

124.   Rabiee, N.; Deljoo, S.; Rabiee, M., Curcumin-hybrid Nanoparticles in Drug Delivery System. **2018,** *2*, 66-91.

125.   Farjadian, F.; Moghoofei, M.; Mirkiani, S.; Ghasemi, A.; Rabiee, N.; Hadifar, S.; Beyzavi, A.; Karimi, M.; Hamblin, M. R., Bacterial components as naturally inspired nano-carriers for drug/gene delivery and immunization: Set the bugs to work? *Biotechnology Advances* **2018,** *36* (4), 968-985.

126.   Audi, A.; Soudani, N.; Dbaibo, G.; Zaraket, H., Depletion of Host and Viral Sphingomyelin Impairs Influenza Virus Infection. *Front Microbiol* **2020,** *11*, 612-612.

127.   Palanikumar, L.; Choi, E. S.; Oh, J. Y.; Park, S. A.; Choi, H.; Kim, K.; Kim, C.; Ryu, J.-H., Importance of Encapsulation Stability of Nanocarriers with High Drug Loading Capacity for Increasing in Vivo Therapeutic Efficacy. *Biomacromolecules* **2018,** *19* (7), 3030-3039.

128.   Mukerjee, A.; Vishwanatha, J., Formulation, Characterization and Evaluation of Curcumin-loaded PLGA Nanospheres for Cancer Therapy. *Anticancer research* **2009,** *29*, 3867-75.

129.   Umerska, A.; Gaucher, C.; Oyarzun-Ampuero, F.; Fries, I.; Colin, F.; Villamizar-Sarmiento, M.; Maincent, P.; Sapin-Minet, A., Polymeric Nanoparticles for Increasing Oral Bioavailability of Curcumin. *Antioxidants* **2018,** *7*, 46.

130.   Kita, K.; Dittrich, C., Drug delivery vehicles with improved encapsulation efficiency: taking advantage of specific drug–carrier interactions. *Expert Opinion on Drug Delivery* **2011,** *8* (3), 329-342.

131.   Kuete, V.; Karaosmanoğlu, O.; Sivas, H., Chapter 10 - Anticancer Activities of African Medicinal Spices and Vegetables. In *Medicinal Spices and Vegetables from Africa*, Kuete, V., Ed. Academic Press: 2017; pp 271-297.

132.   Chiamenti, L.; Silva, F.; Schallemberger, K.; Demoliner, M.; Rigotto, C.; Fleck, J., Cytotoxicity and antiviral activity evaluation of Cymbopogon spp hydroethanolic extracts. *Brazilian Journal of Pharmaceutical Sciences* **2019,** *55*.

133.   Gao, M.; Long, X.; Du, J.; Teng, M.; Zhang, W.; Wang, Y.; Wang, X.; Wang, Z.; Zhang, P.; Li, J., Enhanced curcumin solubility and antibacterial activity by encapsulation in PLGA oily core nanocapsules. *Food & Function* **2020,** *11* (1), 448-455.

134.   Parveen, S.; Misra, R.; Sahoo, S. K., Nanoparticles: a boon to drug delivery, therapeutics, diagnostics and imaging. *Nanomedicine: Nanotechnology, Biology and Medicine* **2012,** *8* (2), 147-166.

135.   Nazlı, E.; Safiye, A.; Erem, B., Nanocapsules for Drug Delivery: An Updated Review of the Last Decade. *Recent Patents on Drug Delivery & Formulation* **2018,** *12* (4), 252-266.

136.   Klippstein, R.; Wang, J. T.-W.; El-Gogary, R. I.; Bai, J.; Mustafa, F.; Rubio, N.; Bansal, S.; Al-Jamal, W. T.; Al-Jamal, K. T., Passively Targeted Curcumin-Loaded

PEGylated PLGA Nanocapsules for Colon Cancer Therapy In Vivo. *Small* **2015,** *11* (36), 4704-4722.

137. Thomas, M.; Radhakrishnan, K.; Gnanadhas, D. P.; Chakravortty, D.; Raichur, A., Intracellular delivery of doxorubicin encapsulated in novel pH-responsive chitosan/heparin nanocapsules. *Int J Nanomedicine* **2013,** *8*, 267-73.

138. Deng, S.; Gigliobianco, M. R.; Censi, R.; Di Martino, P., Polymeric Nanocapsules as Nanotechnological Alternative for Drug Delivery System: Current Status, Challenges and Opportunities. *Nanomaterials (Basel)* **2020,** *10* (5), 847.

139. Behdarvand, N.; Bikhof, M.; Shaabanzadeh, M., Tamoxifen-loaded PLA/DPPE-PEG lipid-polymeric nanocapsules for inhibiting the growth of estrogen-positive human breast cancer cells through cell cycle arrest. *Journal of Nanoparticle Research* **2020,** *22*.

140. Allison, S., Effect Of Structural Relaxation On The Preparation And Drug Release Behavior Of Poly(lactic-co-glycolic)acid Microparticle Drug Delivery Systems. *Journal of pharmaceutical sciences* **2008,** *97*, 2022-35.

141. Sankar, P.; Telang, A. G.; Suresh, S.; Kesavan, M.; Kannan, K.; Kalaivanan, R.; Sarkar, S. N., Immunomodulatory effects of nanocurcumin in arsenic-exposed rats. *International Immunopharmacology* **2013,** *17* (1), 65-70.

142. El Kurdi, R.; Patra, D., Capping of supramolecular curcubit[7]uril facilitates formation of Au nanorods during pre-reduction by curcumin. *Colloids and Surfaces A: Physicochemical and Engineering Aspects* **2018,** *553*, 97-104.

143. Bechnak, L.; Khalil, C.; El Kurdi, R.; Khnayzer, R. S.; Patra, D., Curcumin encapsulated colloidal amphiphilic block co-polymeric nanocapsules: colloidal nanocapsules enhance photodynamic and anticancer activities of curcumin. *Photochemical & Photobiological Sciences* **2020,** *19* (8), 1088-1098.

144. Moussa, Z.; Chebl, M.; Patra, D., Fluorescence of tautomeric forms of curcumin in different pH and biosurfactant rhamnolipids systems: Application towards on-off ratiometric fluorescence temperature sensing. *Journal of Photochemistry and Photobiology B: Biology* **2017,** *173*, 307-317.

145. Patra, D.; Ahmadieh, D.; Al Aridi, R., Study on interaction of bile salts with curcumin and curcumin embedded in dipalmitoyl-sn-glycero-3-phosphocholine liposome. *Colloids and surfaces. B, Biointerfaces* **2013,** *110C*, 296-304.

146. El Kurdi, R.; Patra, D., The role of OH− in the formation of highly selective gold nanowires at extreme pH: multi-fold enhancement in the rate of the catalytic reduction reaction by gold nanowires. *Physical Chemistry Chemical Physics* **2017,** *19* (7), 5077-5090.

147. Gao, M.; Long, X.; Du, J.; Teng, M.; Zhang, W.; Wang, Y.; Wang, X.; Wang, Z.; Zhang, P.; Li, J., Enhanced curcumin solubility and antibacterial activity by encapsulation in PLGA oily core nanocapsules. *Food & Function* **2019,** *11*.

148. Honary, S.; Zahir, F., Effect of Zeta Potential on the Properties of Nano-Drug Delivery Systems - A Review (Part 1). *Tropical Journal of Pharmaceutical Research* **2013,** *12*.

149. Shutava, T. G.; Pattekari, P. P.; Arapov, K. A.; Torchilin, V. P.; Lvov, Y. M., Architectural layer-by-layer assembly of drug nanocapsules with PEGylated polyelectrolytes. *Soft Matter* **2012,** *8* (36), 9418-9427.

150. Priya, P.; Mohan Raj, R.; Vasanthakumar, V.; Raj, V., Curcumin-loaded layer-by-layer folic acid and casein coated carboxymethyl cellulose/casein nanogels for treatment of skin cancer. *Arabian Journal of Chemistry* **2020,** *13* (1), 694-708.